Noble-metal free catalysts for ammonia dehydrogenation within permeation membrane reactors for improved conversion

Christopher J. Koch[a], Daniel Clairmonte[a], Jennifer Naglic[a], Houston Smith[a], Logan T. Kearney[b], Jose D. Arregui-Mena[c], Harry M. Meyer III[b], Sarah Stofik[d], Victoria Rogers[d], John T. Kelly[a], William Gilbraith[a], Jochen Lauterbach[d], Lucas Angelette[a], Tyler Guin[a,*]

Contents

Catalyst Optimization

The optimization on the catalyst was done with nickel, ytterbium, and potassium to determine the metal loading of the catalyst and was performed with γ-Al_2O_3 powder instead of pellets. This leads to slightly higher conversions with the powder when compared to the pellets due to the increased surface area of the powder-based catalysts. Figure S1 shows the conversion with different promoted catalysts at various temperatures. The 3%Ni/Al_2O_3, the unpromoted nickel-catalyst, demonstrated the lowest conversions. With the addition of ytterbium and potassium, the performance increases slightly. However, upon further increasing the metal loadings of nickel and ytterbium, the performance of the catalyst greatly improves. The 12%Ni/4%Yb/12%K/Al_2O_3 catalyst had significantly improved performance at lower temperatures (<500°C) and was then utilized as the metal loadings for the other catalysts tested.

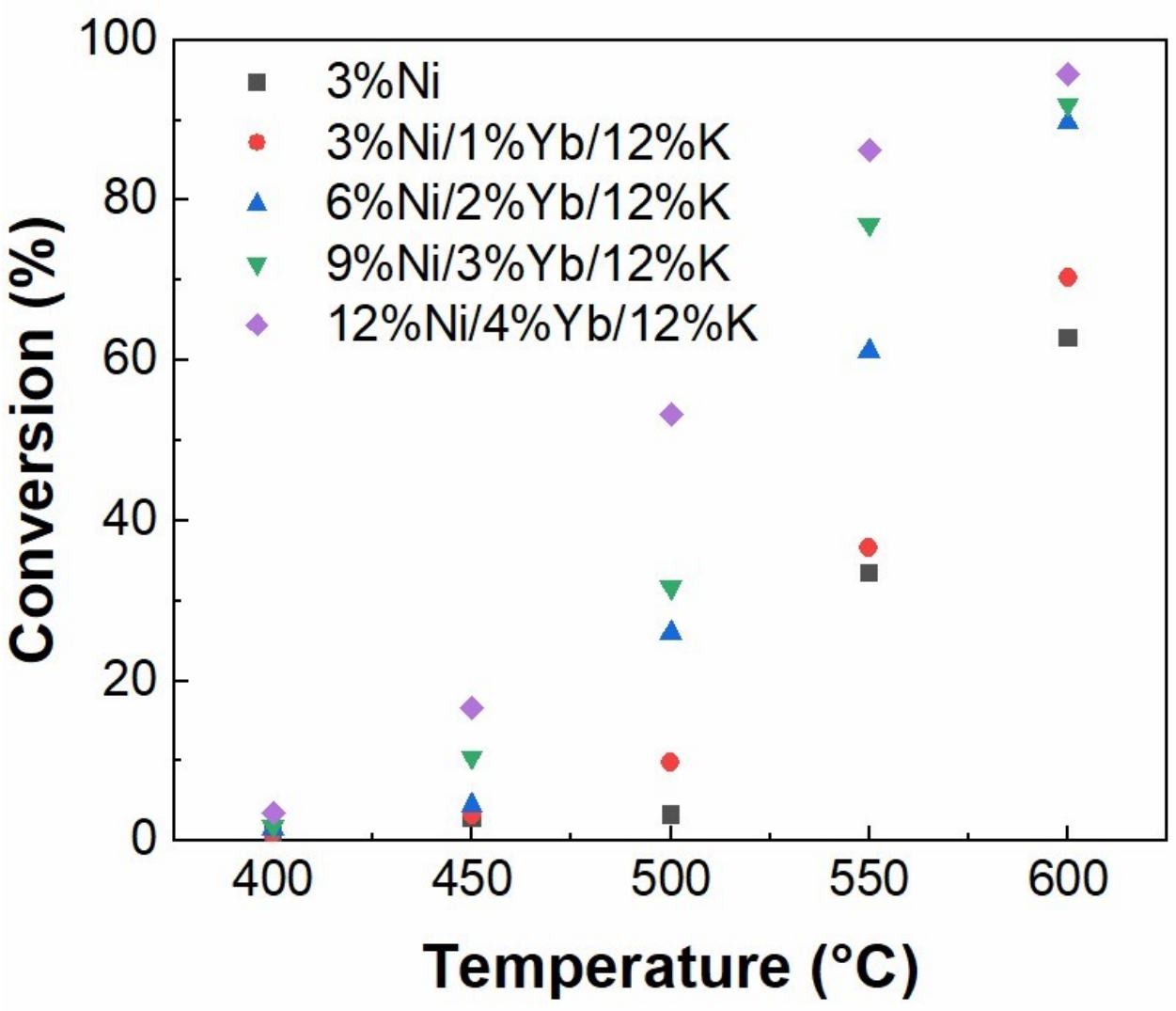

Figure S1. Comparison of ammonia cracking of five catalysts with varying metal loading on γ-Al_2O_3.

Figure S2 shows the overlayed Arrhenius plots for the catalysts synthesized in the metal loading optimization studies. The rate constants for the temperatures below 500°C were highest with the 12%Ni/4%Yb/12%K/Al_2O_3 catalysts, indicating that the higher metal loadings would be more useful in permeation membrane reactor conditions (300-500°C). Expansions of the Arrhenius plots for each catalyst tested in the metal loading optimization are shown in Figure S3-Figure S7.

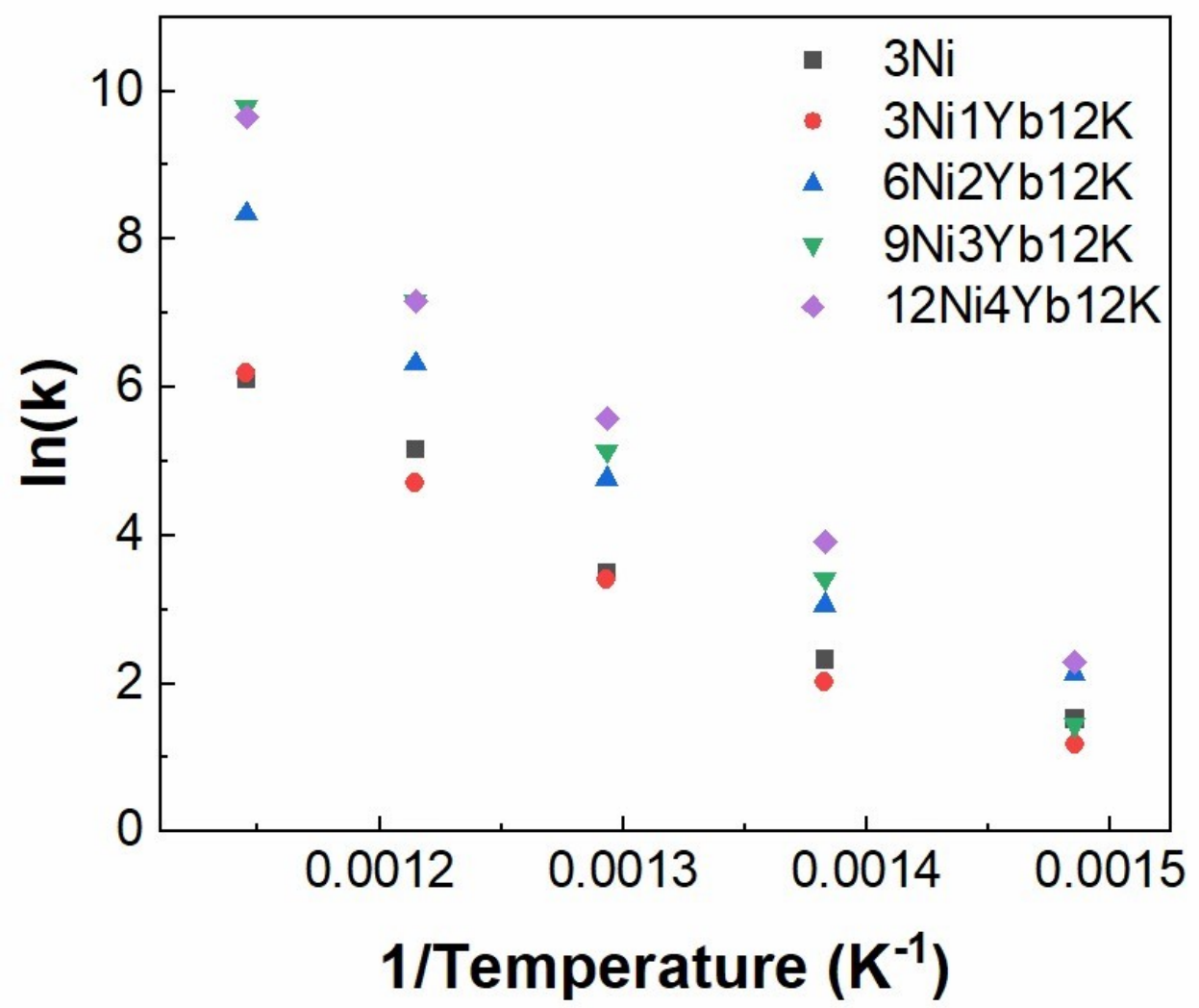

Figure S2. The Arrhenius plots of the 5 catalysts tested with varying metal loadings on γ-Al_2O_3.

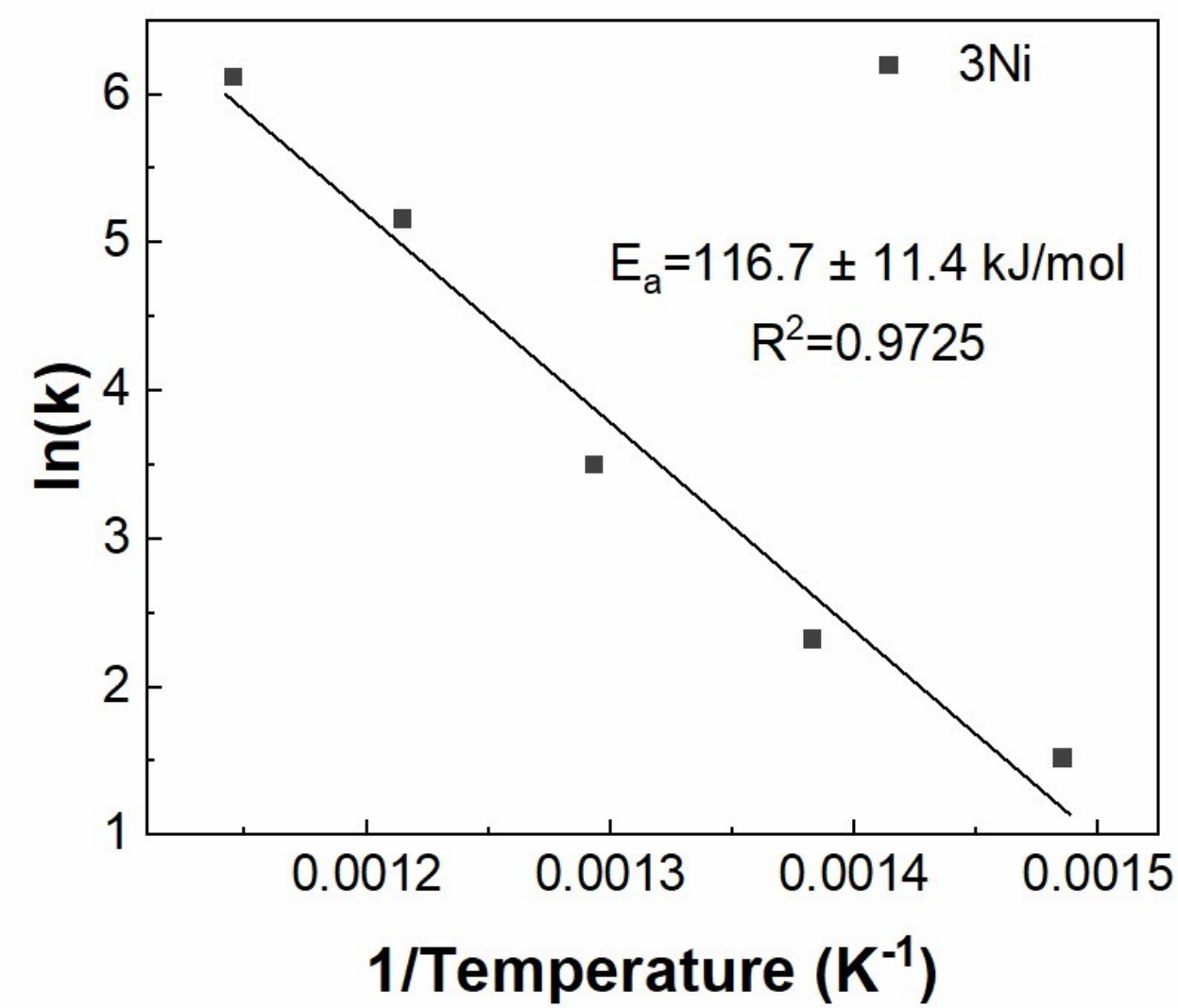

Figure S3. Arrhenius plot of the 3%Ni/γ-Al_2O_3.

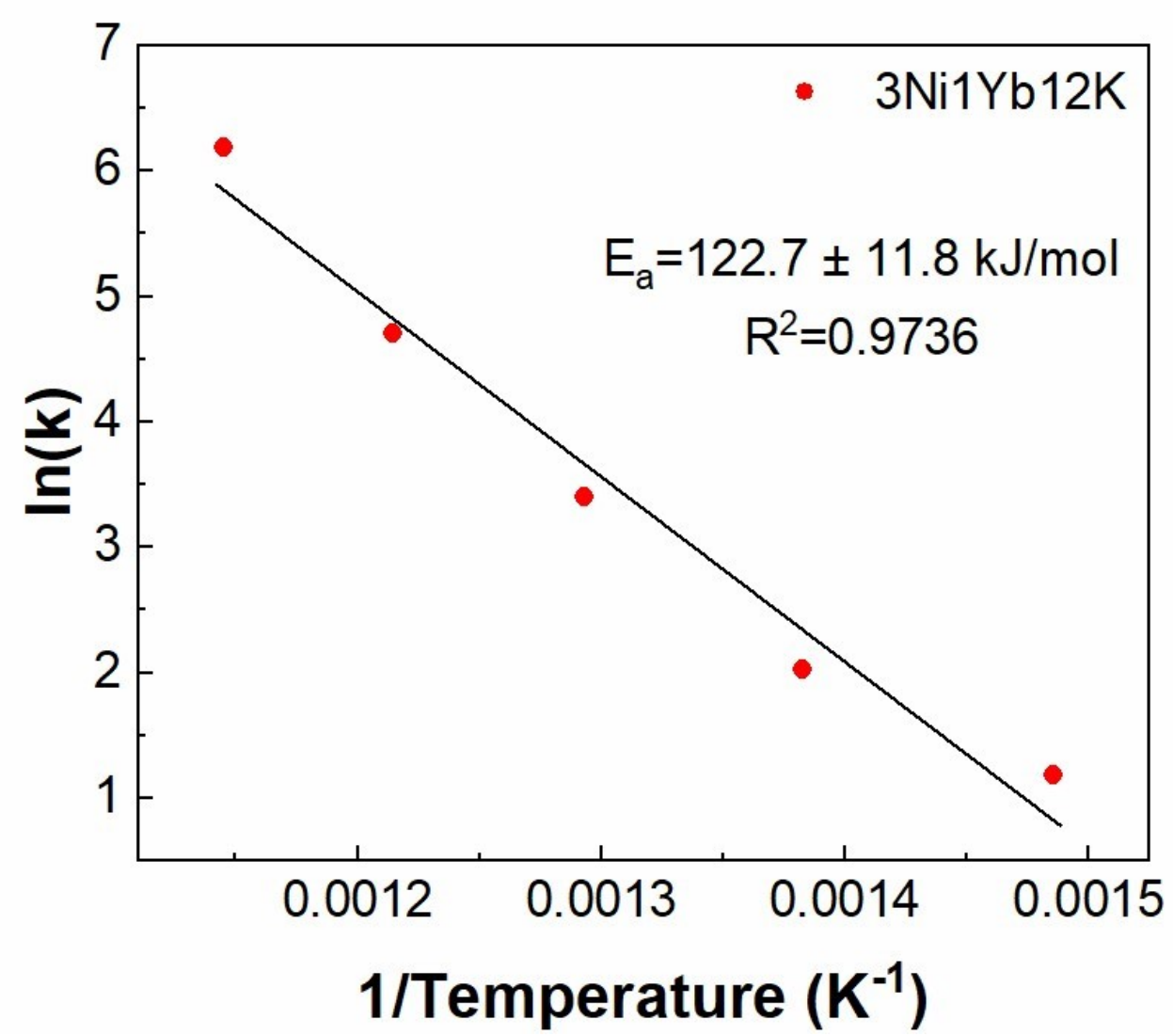

Figure S4. Arrhenius plot of the 3%Ni/1%Yb/12%K/γ-Al_2O_3.

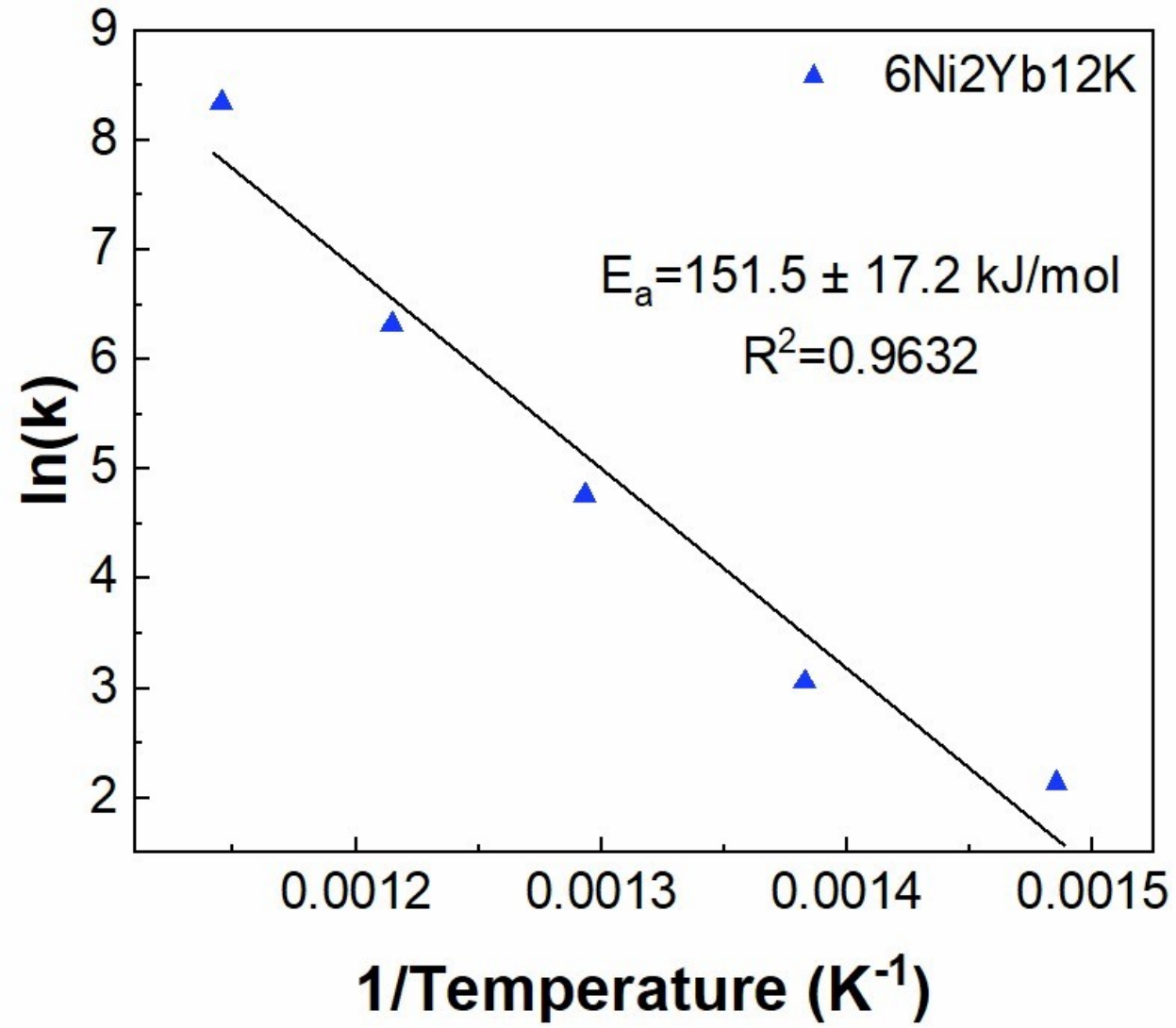

Figure S5. Arrhenius plot of the 6%Ni/2%Yb/12%K/γ-Al_2O_3.

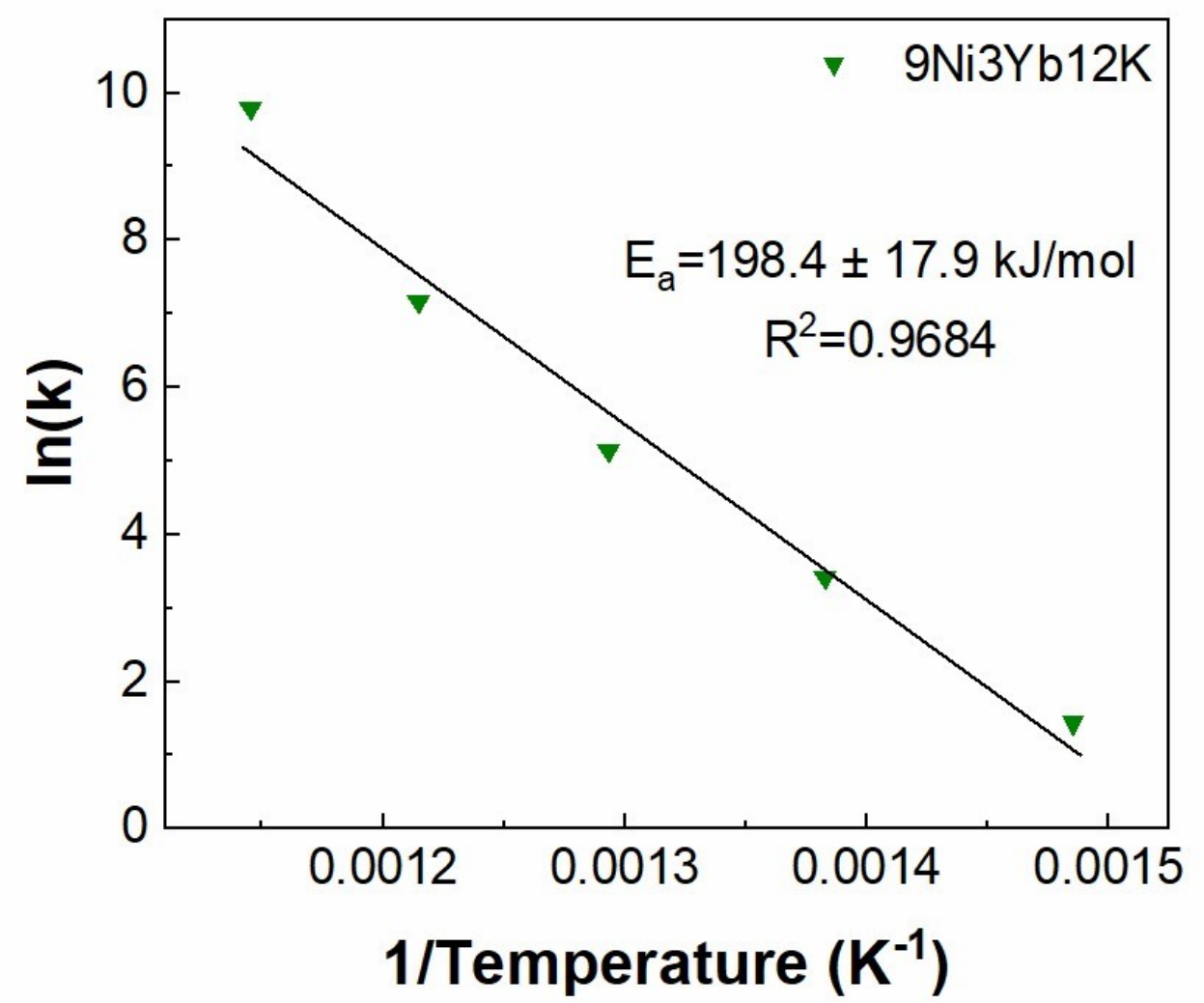

Figure S6. Arrhenius plot of the 9%Ni/3%Yb/12%K/γ-Al_2O_3.

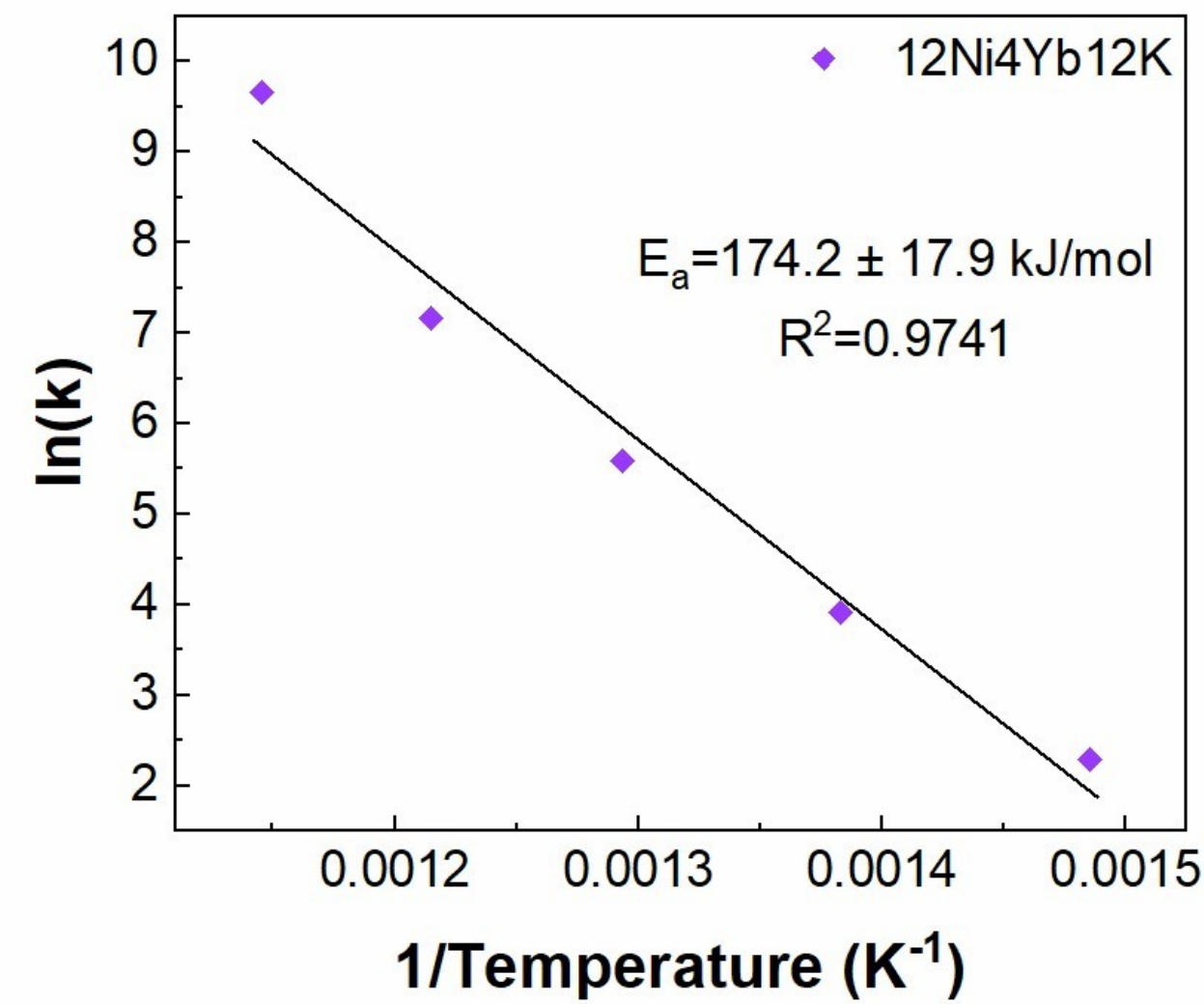

Figure S7. Arrhenius plot of the 12%Ni/4%Yb/12%K/γ-Al_2O_3.

Additional Catalyst Data

Figure S8-Figure S14 shows the conversion of ammonia to nitrogen and hydrogen over the course of a 200°C temperature range (400-600°C) and a variety of flow rates (30-70mL/min).

The turnover frequency (TOF) and the hydrogen production for each of the catalysts are also reported in Table S1 through Table S14. The turnover frequency was calculated by utilizing the total moles of metal added onto the alumina as the mole of catalyst in the calculation.

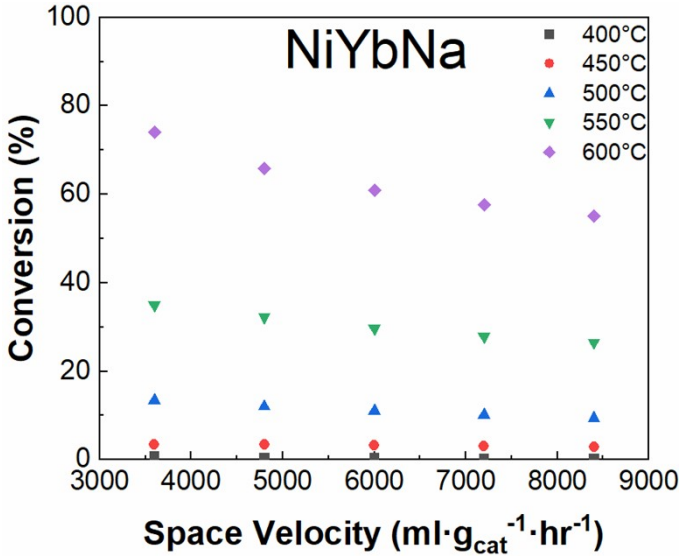

Figure S8. Conversion of the 12%Ni/4%Yb/12%Na/Al_2O_3 catalyst over the temperature range and flow rates that construct the Arrhenius plot.

Table S1. Turnover frequency of the 12%Ni/4%Yb/12%Na/Al_2O_3 catalyst reflecting the results in Figure S8.

Ammonia Space Velocity (mL·g_{cat}^{-1}·hr^{-1})	TOF (s^{-1})				
	400°C	450°C	500°C	550°C	600°C
3600	0.003	0.01	0.05	0.13	0.26
4800	0.002	0.02	0.06	0.15	0.31
6000	0.002	0.02	0.07	0.18	0.36
7200	0.002	0.02	0.07	0.20	0.41
8400	0.002	0.02	0.08	0.22	0.52

Table S2. H_2 productivity of the 12%Ni/4%Yb/12%Na/Al_2O_3 catalyst reflecting the results in Figure S8.

Ammonia Space Velocity ($mL \cdot g_{cat}^{-1} \cdot hr^{-1}$)	H_2 productivity ($mmol_{H2} \cdot g_{cat}^{-1} \cdot hr^{-1}$)				
	400°C	450°C	500°C	550°C	600°C
3600	0.002	0.008	0.03	0.08	0.18
4800	0.002	0.01	0.03	0.10	0.21
6000	0.002	0.01	0.04	0.12	0.24
7200	0.001	0.01	0.05	0.13	0.28
8400	0.001	0.02	0.05	0.15	0.35

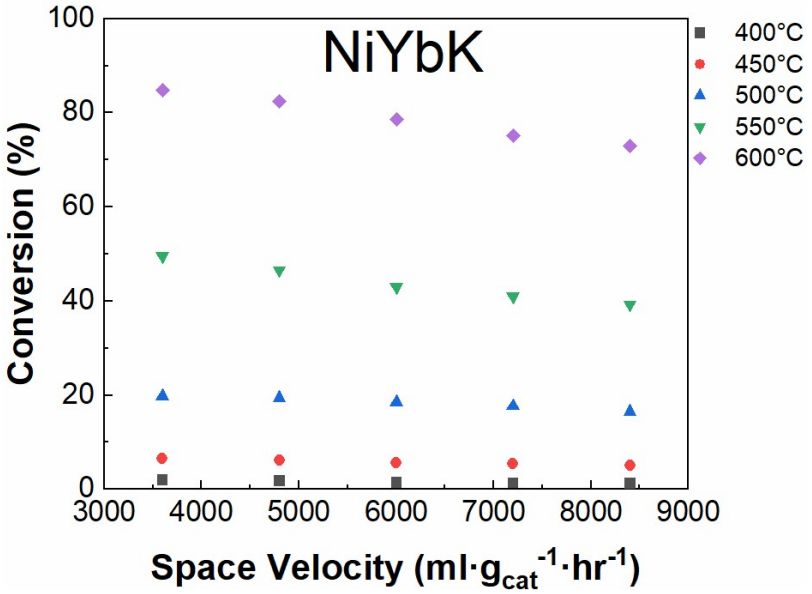

Figure S9. Conversion of the 12%Ni/4%Yb/12%K/Al_2O_3 catalyst over the temperature range and flow rates that construct the Arrhenius plot.

Table S3. Turnover frequency of the 12%Ni/4%Yb/12%K/Al_2O_3 catalyst reflecting the results in Figure S9.

Ammonia Space Velocity ($mL \cdot g_{cat}^{-1} \cdot hr^{-1}$)	TOF (s^{-1})				
	400°C	450°C	500°C	550°C	600°C
3600	0.01	0.03	0.10	0.26	0.44
4800	0.01	0.04	0.13	0.32	0.57
6000	0.01	0.05	0.16	0.37	0.68
7200	0.01	0.06	0.18	0.42	0.78
8400	0.02	0.06	0.20	0.47	0.88

Table S4. H_2 productivity of the 12%Ni/4%Yb/12%K/Al_2O_3 catalyst reflecting the results in Figure S9.

Ammonia Space Velocity ($mL \cdot g_{cat}^{-1} \cdot hr^{-1}$)	H_2 productivity ($mmol_{H2} \cdot g_{cat}^{-1} \cdot hr^{-1}$)				
	400°C	450°C	500°C	550°C	600°C
3600	0.005	0.02	0.05	0.12	0.20
4800	0.006	0.02	0.06	0.15	0.27
6000	0.006	0.02	0.07	0.17	0.32
7200	0.007	0.03	0.09	0.20	0.36
8400	0.007	0.03	0.09	0.22	0.41

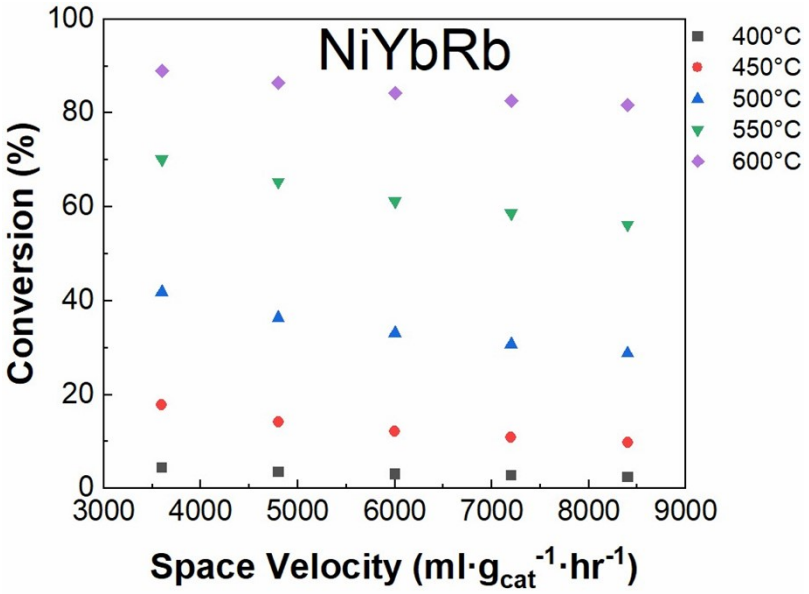

Figure S10. Conversion of the 12%Ni/4%Yb/12%Rb/Al_2O_3 catalyst over the temperature range and flow rates that construct the Arrhenius plot.

Table S5. Turnover frequency of the 12%Ni/4%Yb/12%Rb/Al_2O_3 catalyst reflecting the results in Figure S10.

Ammonia Space Velocity ($mL \cdot g_{cat}^{-1} \cdot hr^{-1}$)	TOF (s^{-1})				
	400°C	450°C	500°C	550°C	600°C
3600	0.03	0.14	0.32	0.54	0.68
4800	0.04	0.14	0.37	0.66	0.88
6000	0.04	0.15	0.42	0.78	1.07
7200	0.04	0.17	0.47	0.90	1.26

8400	0.05	0.17	0.51	1.00	1.46

Table S6. H_2 productivity of the 12%Ni/4%Yb/12%Rb/Al_2O_3 catalyst reflecting the results in Figure S10.

Ammonia Space Velocity ($mL \cdot g_{cat}^{-1} \cdot hr^{-1}$)	H_2 productivity ($mmol_{H2} \cdot g_{cat}^{-1} \cdot s^{-1}$)				
	400°C	450°C	500°C	550°C	600°C
3600	0.01	0.04	0.10	0.17	0.22
4800	0.01	0.05	0.12	0.21	0.28
6000	0.01	0.05	0.13	0.25	0.34
7200	0.01	0.05	0.15	0.28	0.40
8400	0.01	0.06	0.16	0.32	0.46

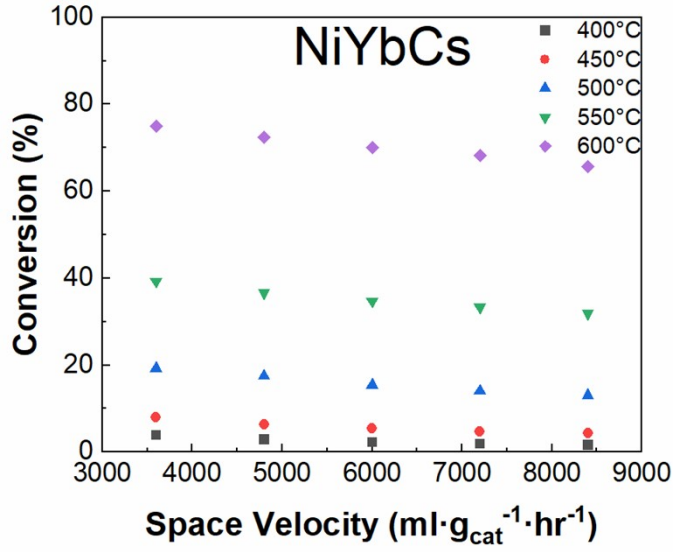

Figure S11. Conversion of the 12%Ni/4%Yb/12%Cs/Al_2O_3 catalyst over the temperature range and flow rates that construct the Arrhenius plot.

Table S7. Turnover frequency of the 12%Ni/4%Yb/12%Cs/Al_2O_3 catalyst reflecting the results in Figure S11.

Ammonia Space Velocity ($mL \cdot g_{cat}^{-1} \cdot hr^{-1}$)	TOF (s^{-1})				
	400°C	450°C	500°C	550°C	600°C
3600	0.03	0.07	0.17	0.35	0.67
4800	0.03	0.07	0.21	0.43	0.86
6000	0.03	0.08	0.23	0.51	1.04

7200	0.03	0.08	0.25	0.59	1.21
8400	0.03	0.09	0.27	0.66	1.36

Table S8. H_2 productivity of the 12%Ni/4%Yb/12%Cs/Al_2O_3 catalyst reflecting the results in Figure S11.

Ammonia Space Velocity ($mL \cdot g_{cat}^{-1} \cdot hr^{-1}$)	H_2 productivity ($mmol_{H2} \cdot g_{cat}^{-1} \cdot hr^{-1}$)				
	400°C	450°C	500°C	550°C	600°C
3600	0.009	0.02	0.05	0.09	0.18
4800	0.009	0.02	0.6	0.12	0.23
6000	0.009	0.02	0.6	0.14	0.28
7200	0.009	0.02	0.7	0.16	0.33
8400	0.009	0.02	0.7	0.18	0.37

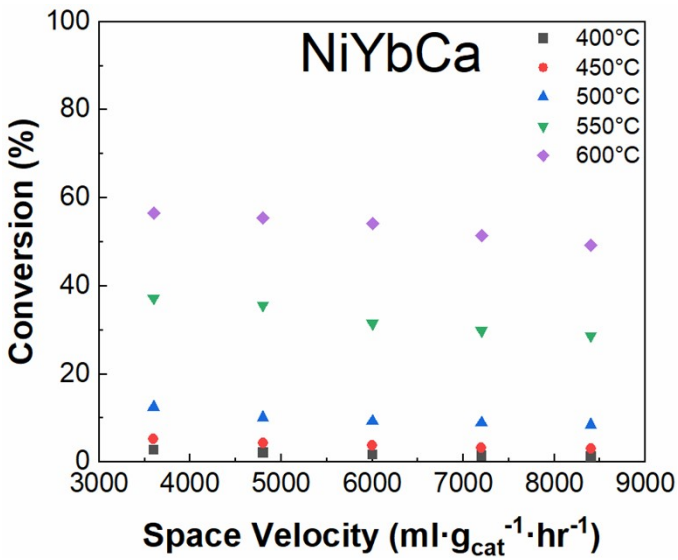

Figure S12. Conversion of the 12%Ni/4%Yb/12%Ca/Al_2O_3 catalyst over the temperature range and flow rates that construct the Arrhenius plot.

Table S9. Turnover frequency of the 12%Ni/4%Yb/12%Ca/Al_2O_3 catalyst reflecting the results in Figure S12.

Ammonia Space Velocity ($mL \cdot g_{cat}^{-1} \cdot hr^{-}$	TOF (s^{-1})				
	400°C	450°C	500°C	550°C	600°C

^{1})					
3600	0.02	0.03	0.07	0.20	0.30
4800	0.02	0.03	0.07	0.25	0.39
6000	0.02	0.03	0.08	0.28	0.47
7200	0.02	0.03	0.09	0.31	0.54
8400	0.02	0.04	0.10	0.35	0.60

Table S10. H_2 productivity of the 12%Ni/4%Yb/12%Ca/Al_2O_3 catalyst reflecting the results in Figure S12.

Ammonia Space Velocity ($mL \cdot g_{cat}^{-1} \cdot hr^{-1}$)	H_2 productivity ($mmol_{H2} \cdot g_{cat}^{-1} \cdot hr^{-1}$)				
	400°C	450°C	500°C	550°C	600°C
3600	0.007	0.01	0.03	0.09	0.14
4800	0.007	0.01	0.03	0.11	0.18
6000	0.007	0.02	0.04	0.12	0.22
7200	0.007	0.02	0.04	0.14	0.25
8400	0.007	0.02	0.05	0.16	0.28

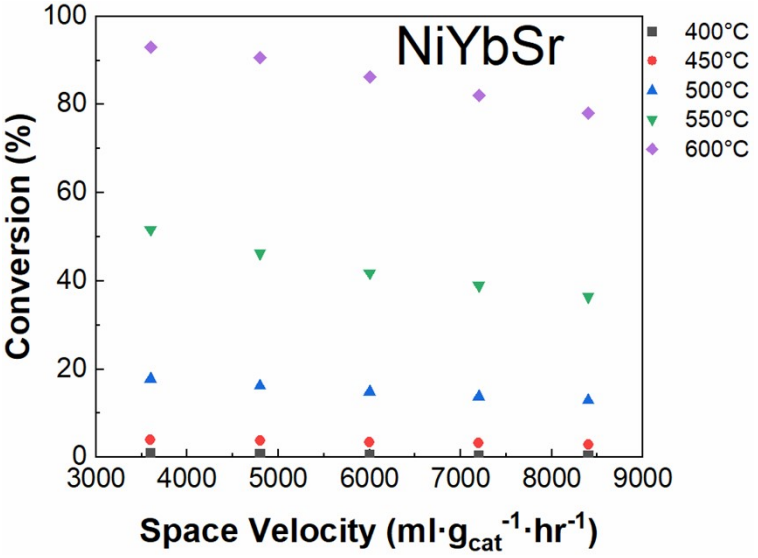

Figure S13. Conversion of the 12%Ni/4%Yb/12%Sr/Al_2O_3 catalyst over the temperature range and flow rates that construct the Arrhenius plot.

Table S11. Turnover frequency of the 12%Ni/4%Yb/12%Sr/Al_2O_3 catalyst reflecting the results in Figure S13.

Ammonia Space Velocity ($mL \cdot g_{cat}^{-1} \cdot hr^{-1}$)	TOF (s^{-1})				
	400°C	450°C	500°C	550°C	600°C
3600	0.01	0.03	0.14	0.40	0.72
4800	0.01	0.04	0.17	0.48	0.93
6000	0.01	0.04	0.19	0.54	1.11
7200	0.01	0.05	0.21	0.60	1.26
8400	0.01	0.05	0.23	0.66	1.40

Table S12. H_2 productivity of the 12%Ni/4%Yb/12%Sr/Al_2O_3 catalyst reflecting the results in Figure S13.

Ammonia Space Velocity ($mL \cdot g_{cat}^{-1} \cdot hr^{-1}$)	H_2 productivity ($mmol_{H2} \cdot g_{cat}^{-1} \cdot hr^{-1}$)				
	400°C	450°C	500°C	550°C	600°C
3600	0.002	0.01	0.04	0.13	0.22
4800	0.002	0.01	0.05	0.15	0.29
6000	0.002	0.01	0.06	0.17	0.35
7200	0.003	0.02	0.07	0.19	0.40
8400	0.003	0.02	0.07	0.21	0.44

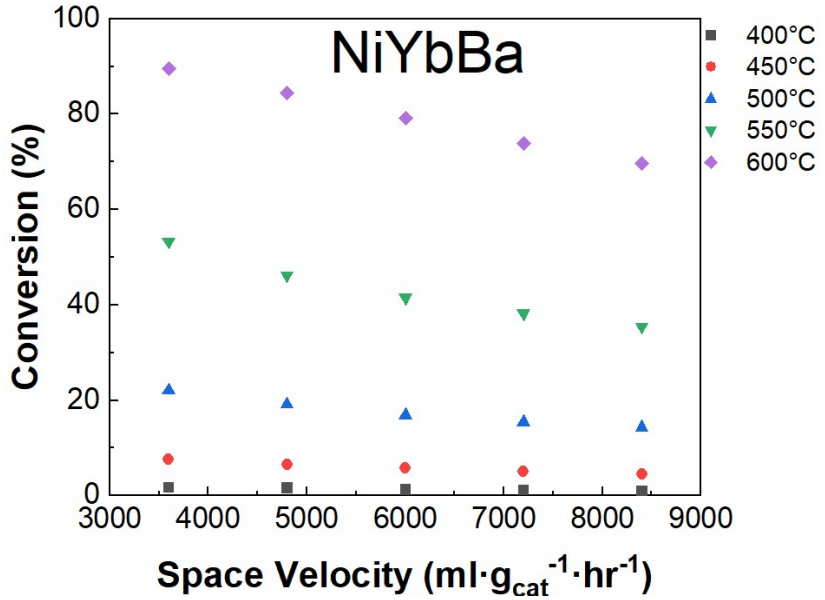

Figure S14. Conversion of the 12%Ni/4%Yb/12%Ba/Al_2O_3 catalyst over the temperature range and flow rates that construct the Arrhenius plot.

Table S13. Turnover frequency of the 12%Ni/4%Yb/12%Ba/Al_2O_3 catalyst reflecting the results in Figure S14.

Ammonia Space Velocity ($mL \cdot g_{cat}^{-1} \cdot hr^{-1}$)	TOF (s^{-1})				
	400°C	450°C	500°C	550°C	600°C
3600	0.02	0.07	0.20	0.48	0.80
4800	0.02	0.08	0.23	0.55	1.02
6000	0.02	0.09	0.25	0.62	1.19
7200	0.02	0.09	0.28	0.69	1.33
8400	0.02	0.09	0.30	0.74	1.46

Table S14. H_2 productivity of the 12%Ni/4%Yb/12%Ba/Al_2O_3 catalyst reflecting the results in Figure S14.

Ammonia Space Velocity ($mL \cdot g_{cat}^{-1} \cdot hr^{-1}$)	H_2 productivity ($mmol_{H2} \cdot g_{cat}^{-1} \cdot hr^{-1}$)				
	400°C	450°C	500°C	550°C	600°C
3600	0.004	0.02	0.05	0.13	0.22
4800	0.005	0.02	0.06	0.15	0.27
6000	0.005	0.02	0.07	0.17	0.32
7200	0.006	0.02	0.07	0.19	0.36
8400	0.005	0.03	0.08	0.20	0.39

Arrhenius Plots

The Arrhenius plots of the various NiYbM are shown in Figure S15 and expansions are shown in Figure S16-Figure S22.

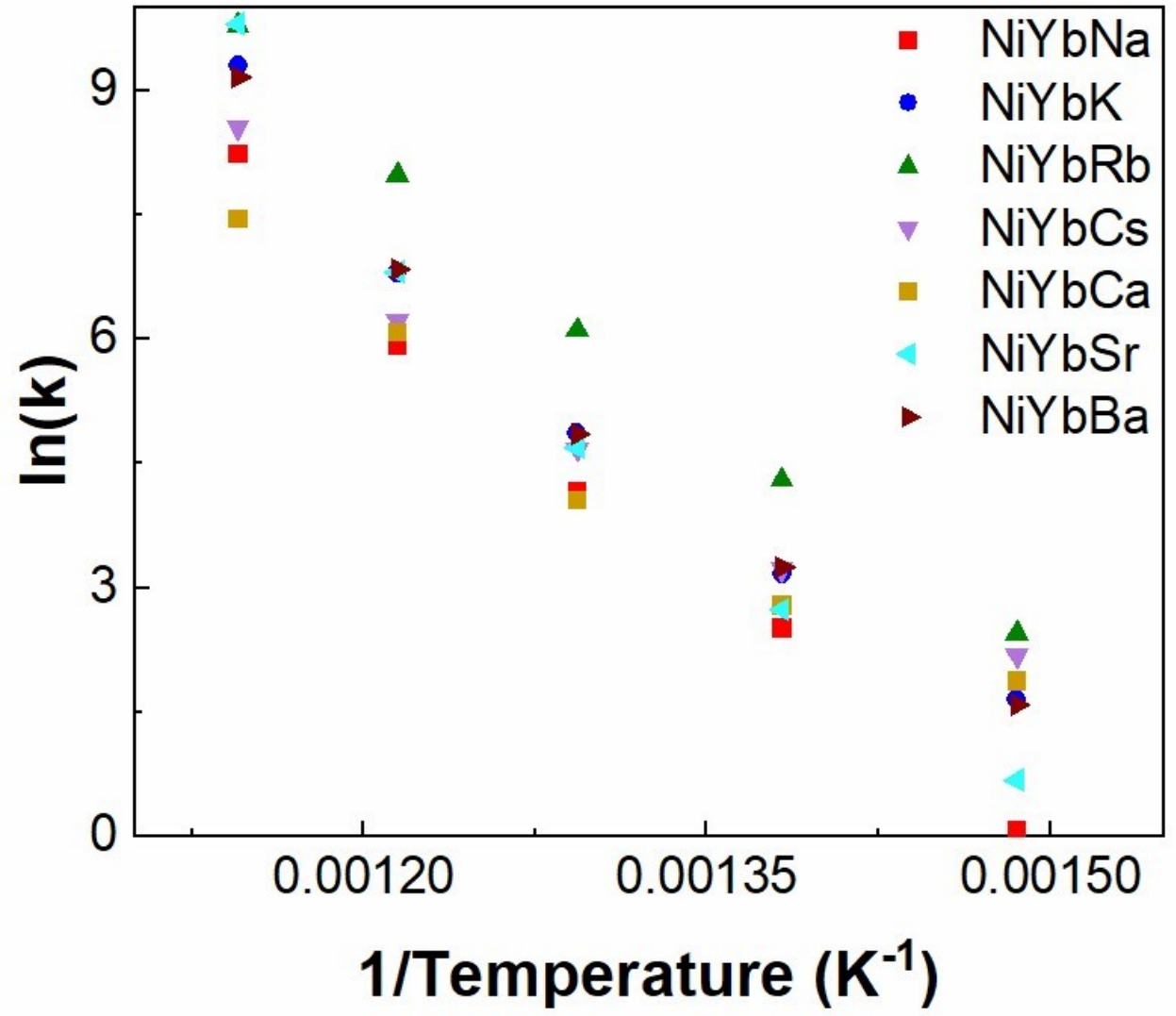

Figure S15. Overlay of the Arrhenius plots for the NiYbM catalysts, where M is the alkali or alkaline earth metal utilized in the catalyst.

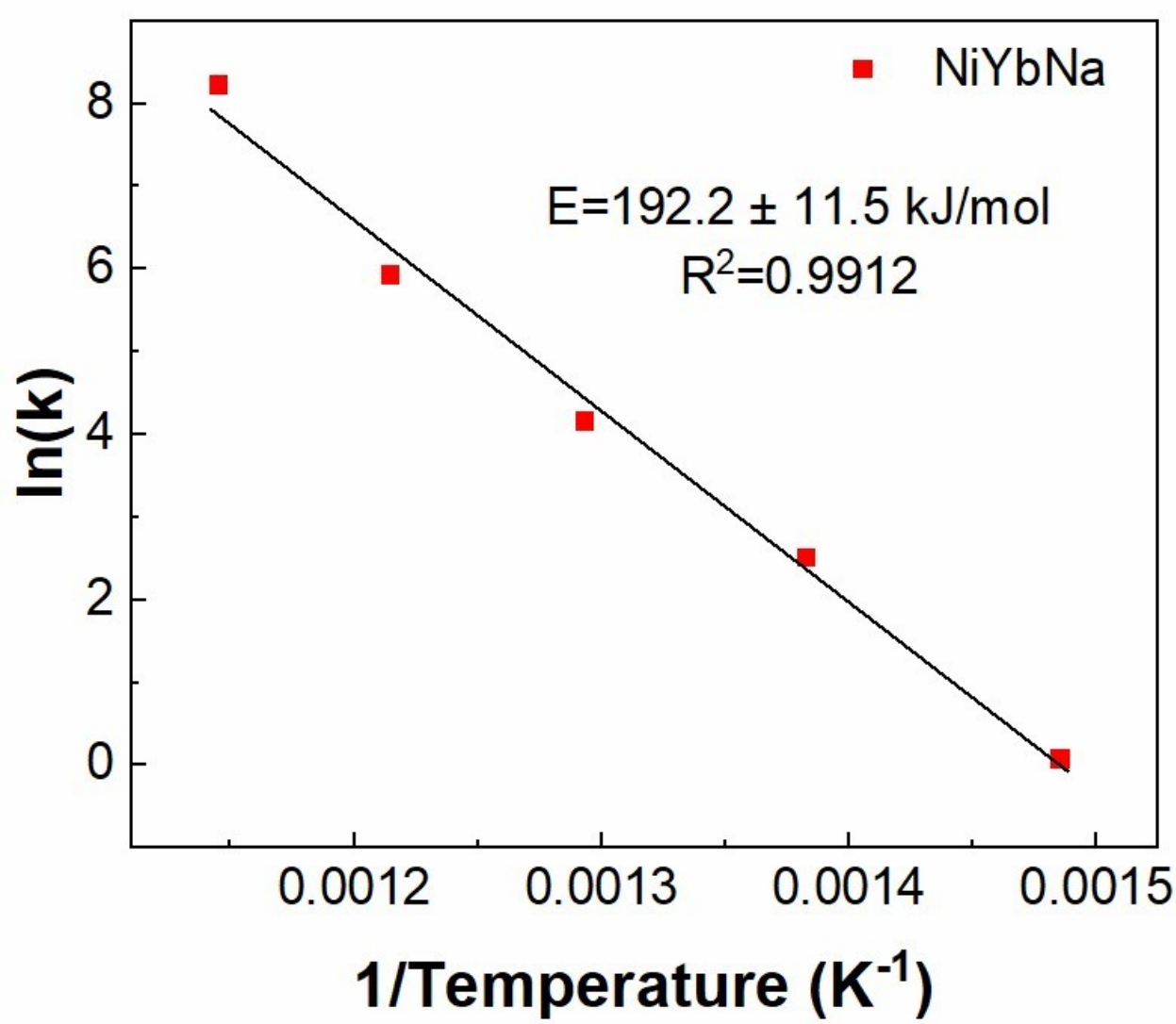

Figure S16. Arrhenius plot of the 12%Ni/4%Yb/12%Na/γ-Al_2O_3.

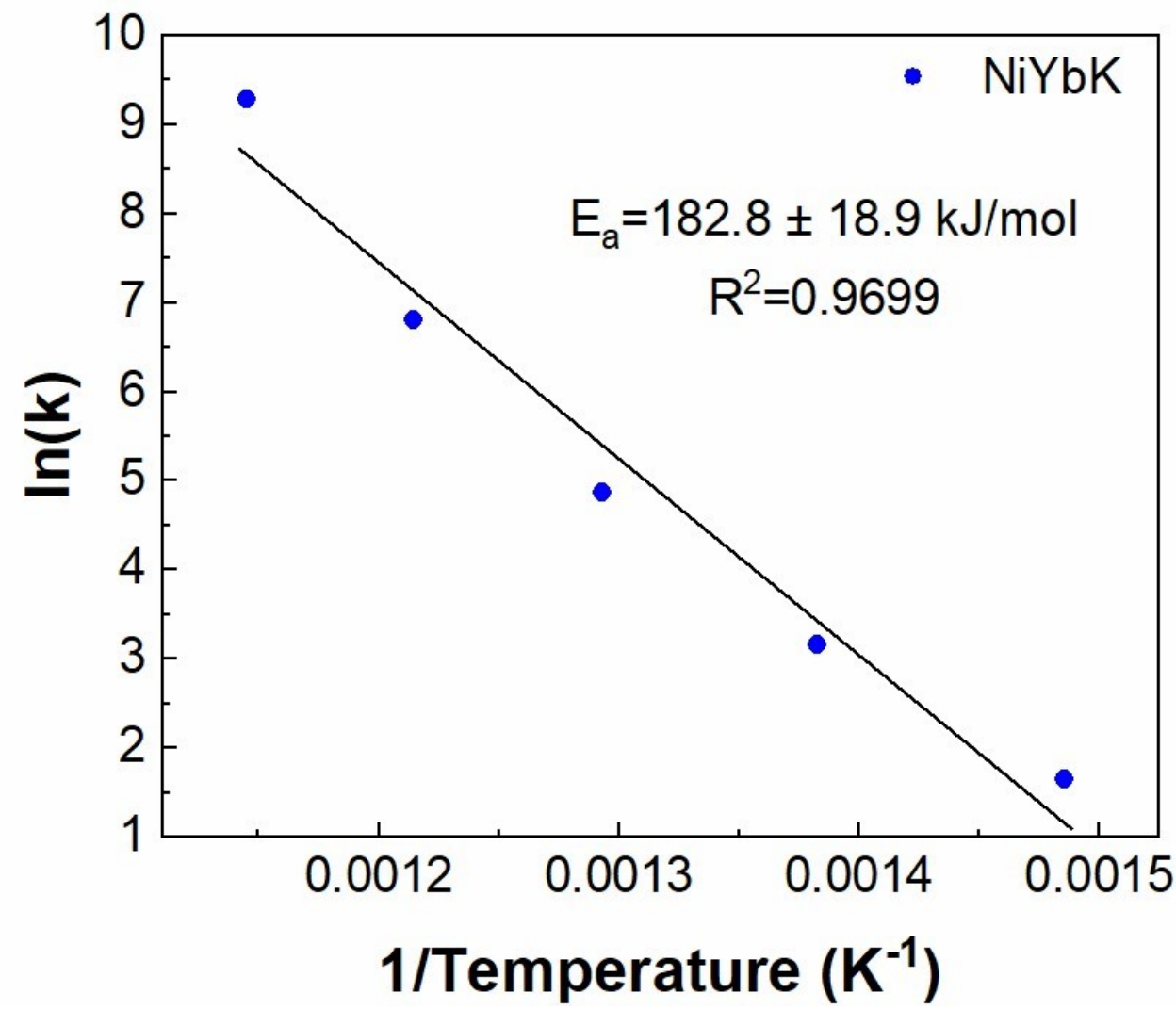

Figure S17. Arrhenius plot of the 12%Ni/4%Yb/12%K/γ-Al_2O_3.

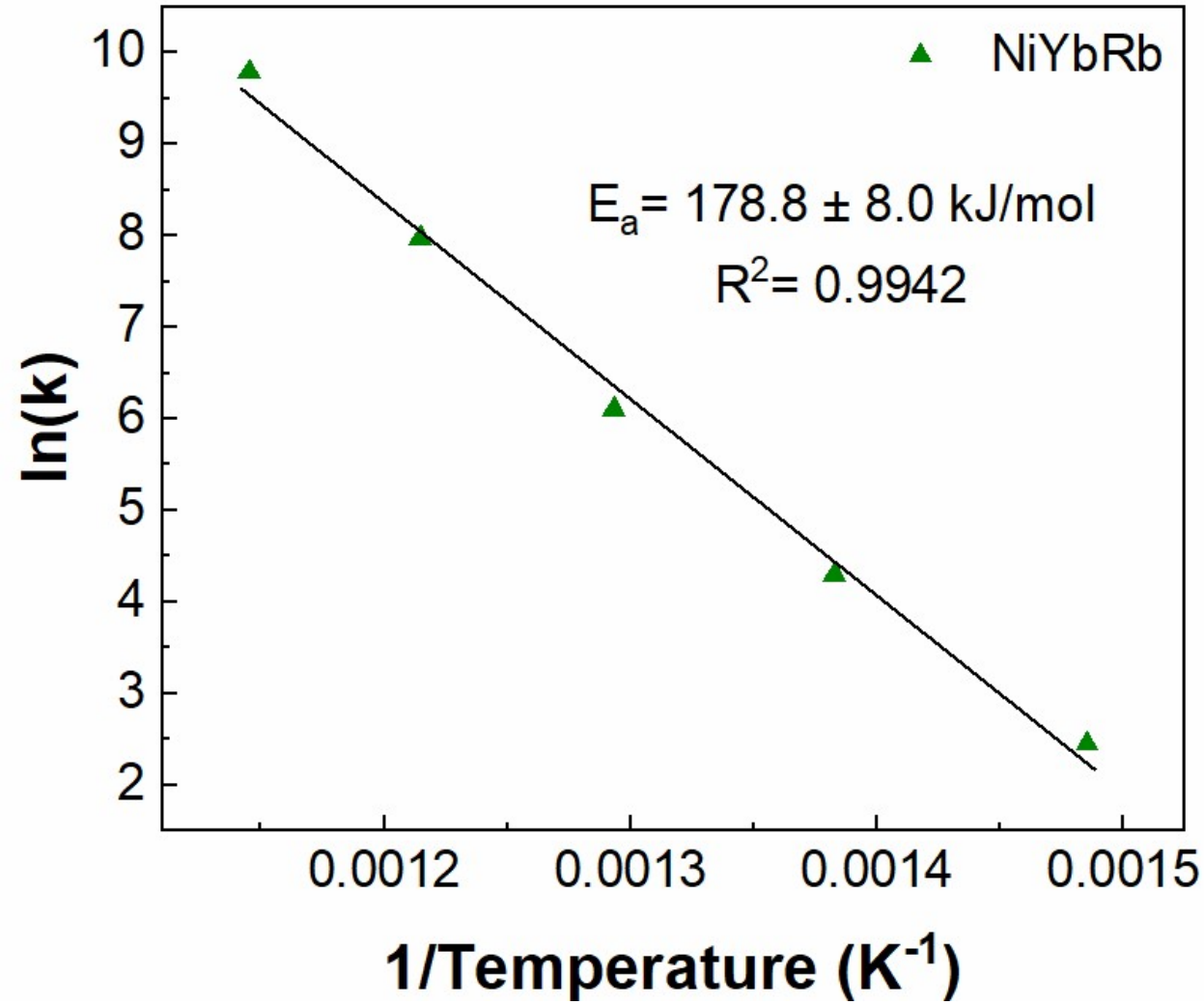

Figure S18. Arrhenius plot of the 12%Ni/4%Yb/12%Rb/γ-Al_2O_3.

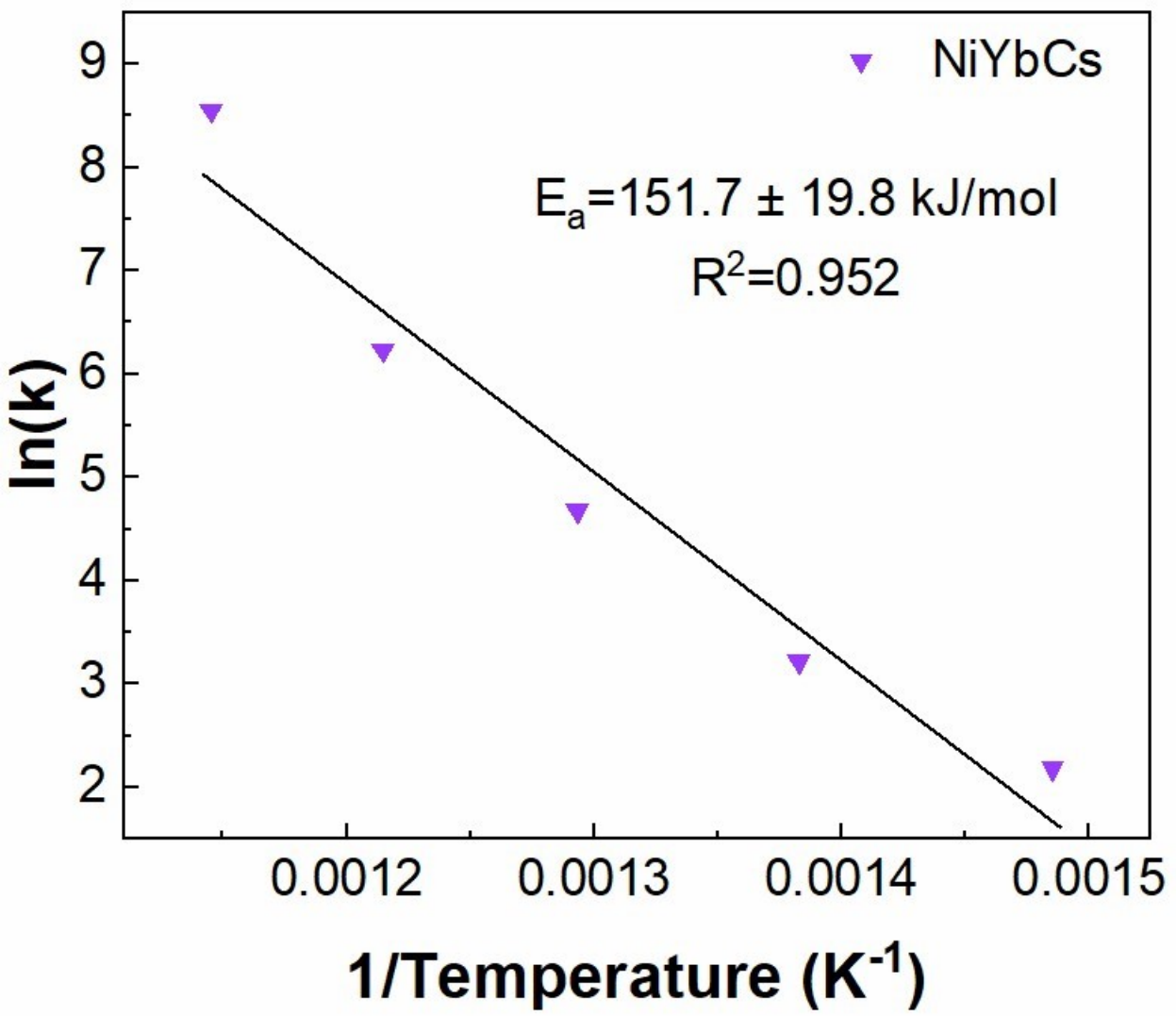

Figure S19. Arrhenius plot of the 12%Ni/4%Yb/12%Cs/γ-Al_2O_3.

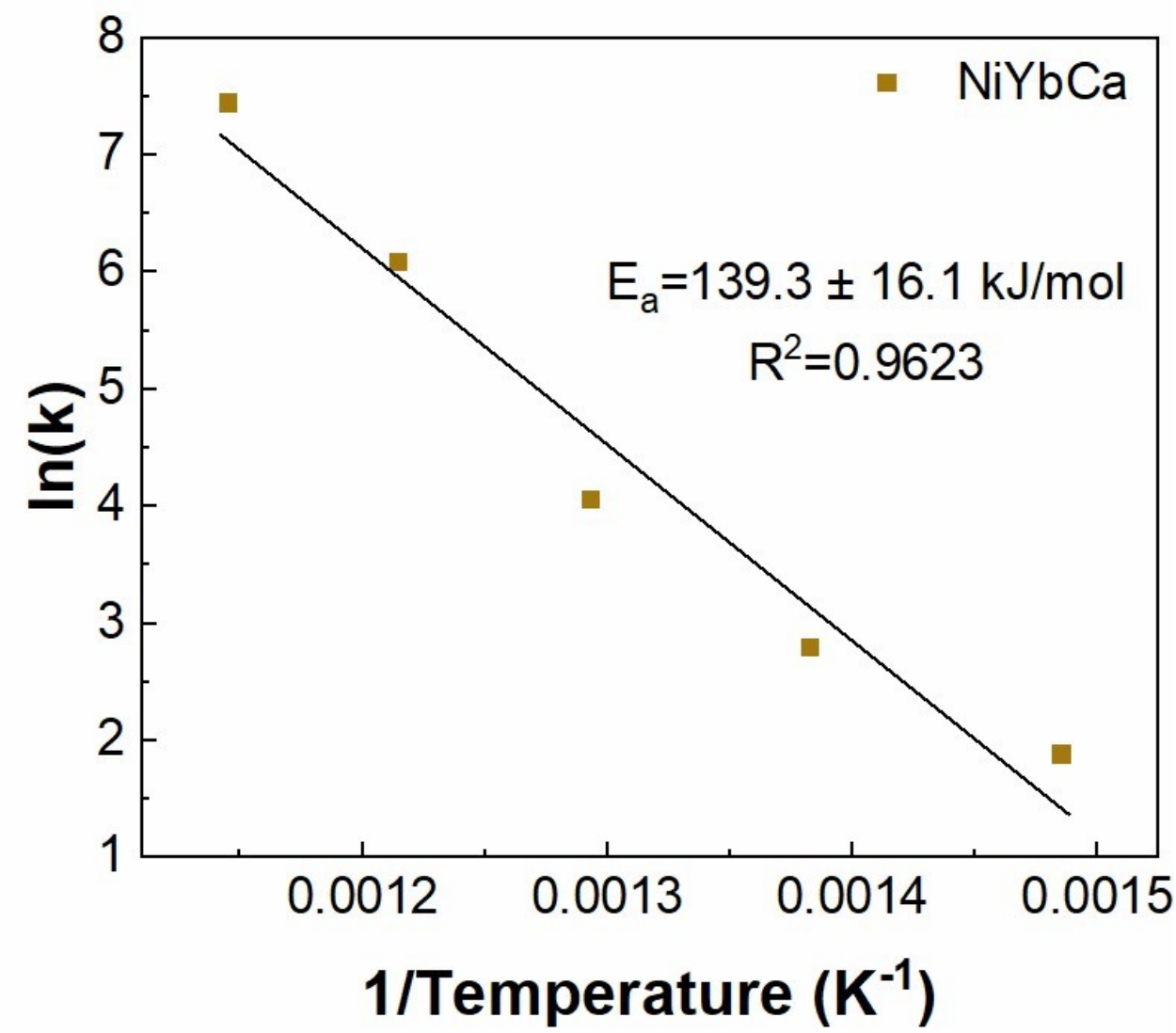

Figure S20. Arrhenius plot of the 12%Ni/4%Yb/12%Ca/γ-Al_2O_3.

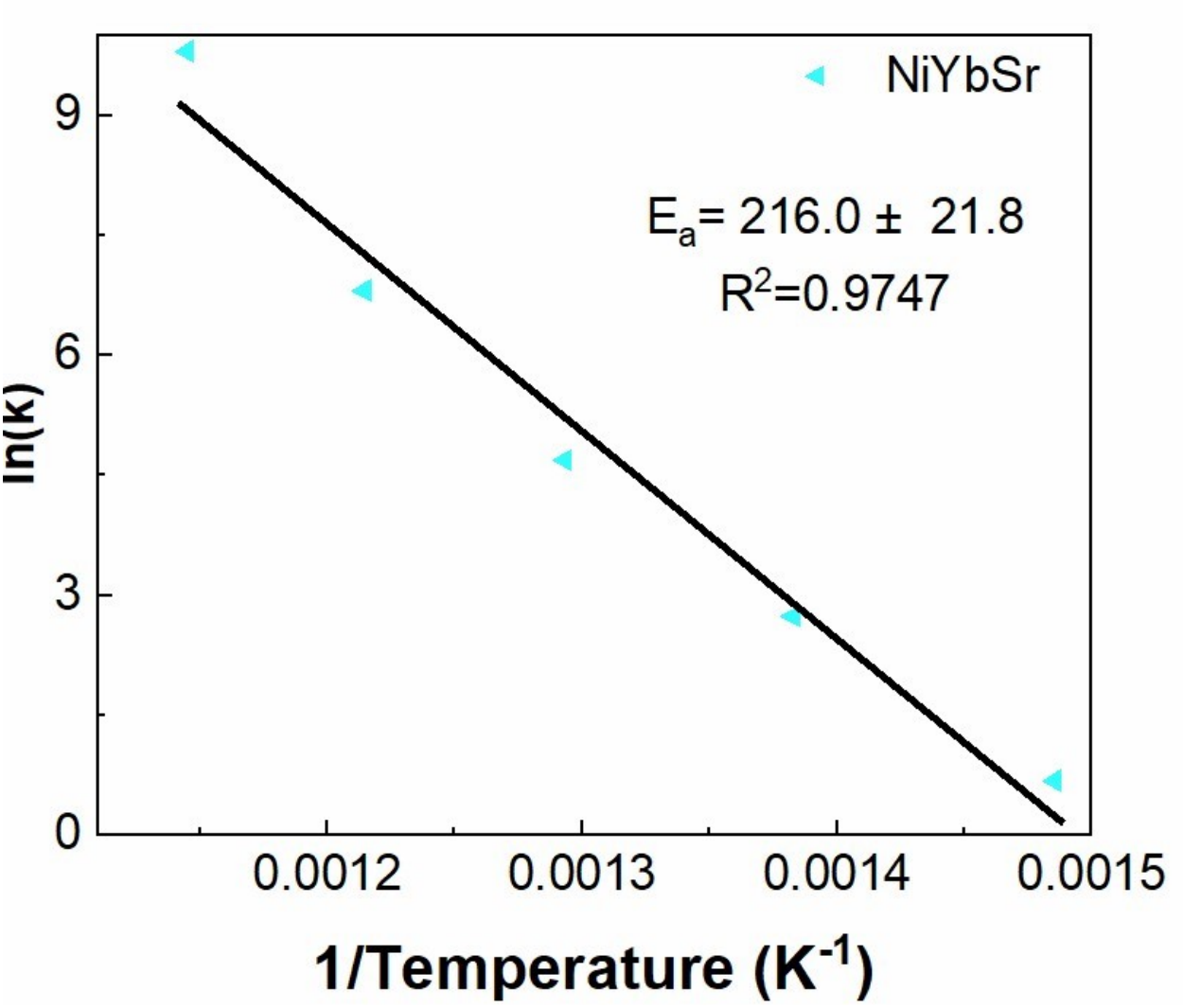

Figure S21. Arrhenius plot of the 12%Ni/4%Yb/12%Sr/γ-Al_2O_3.

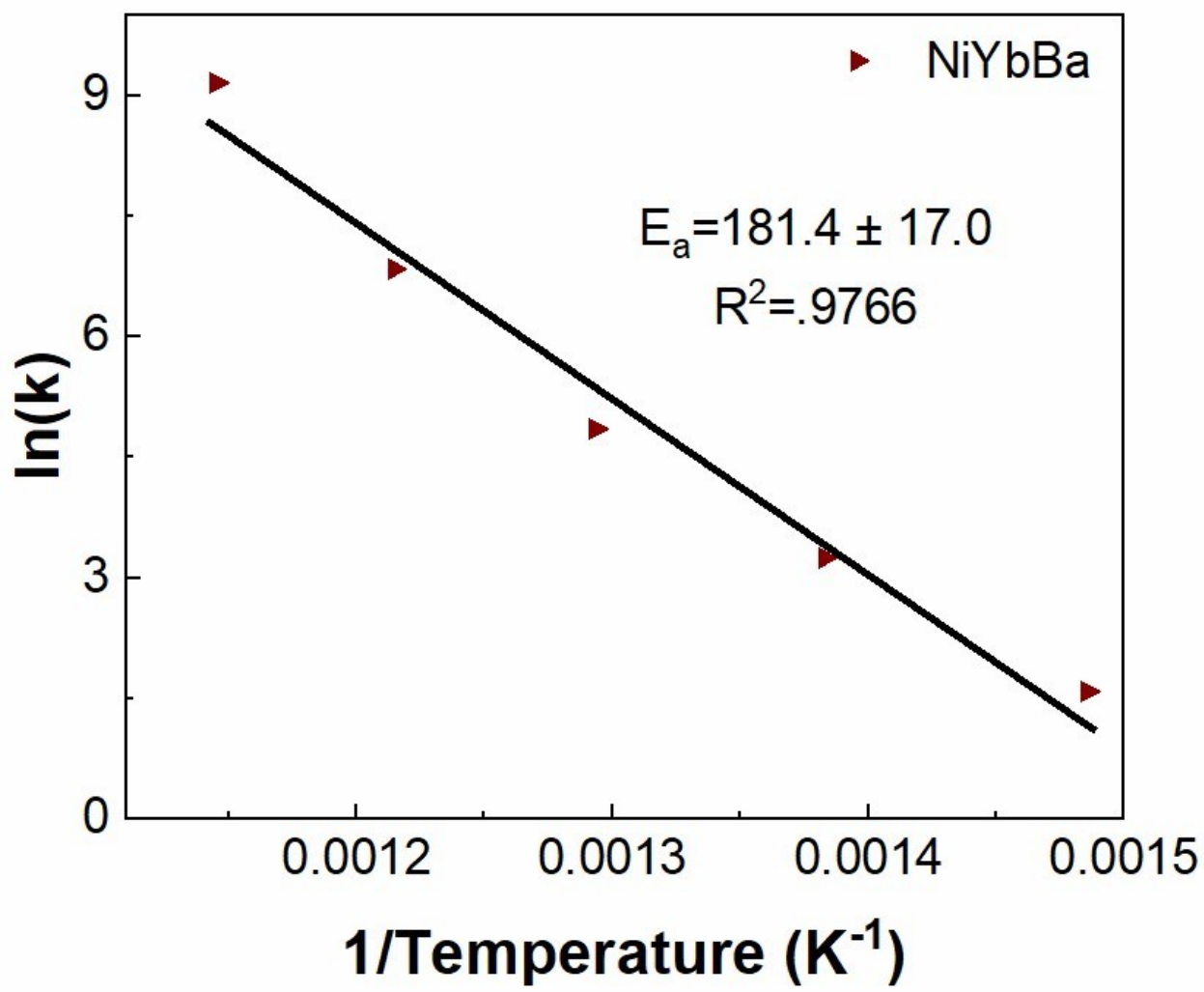

Figure S22. Arrhenius plot of the 12%Ni/4%Yb/12%Ba/γ-Al_2O_3.

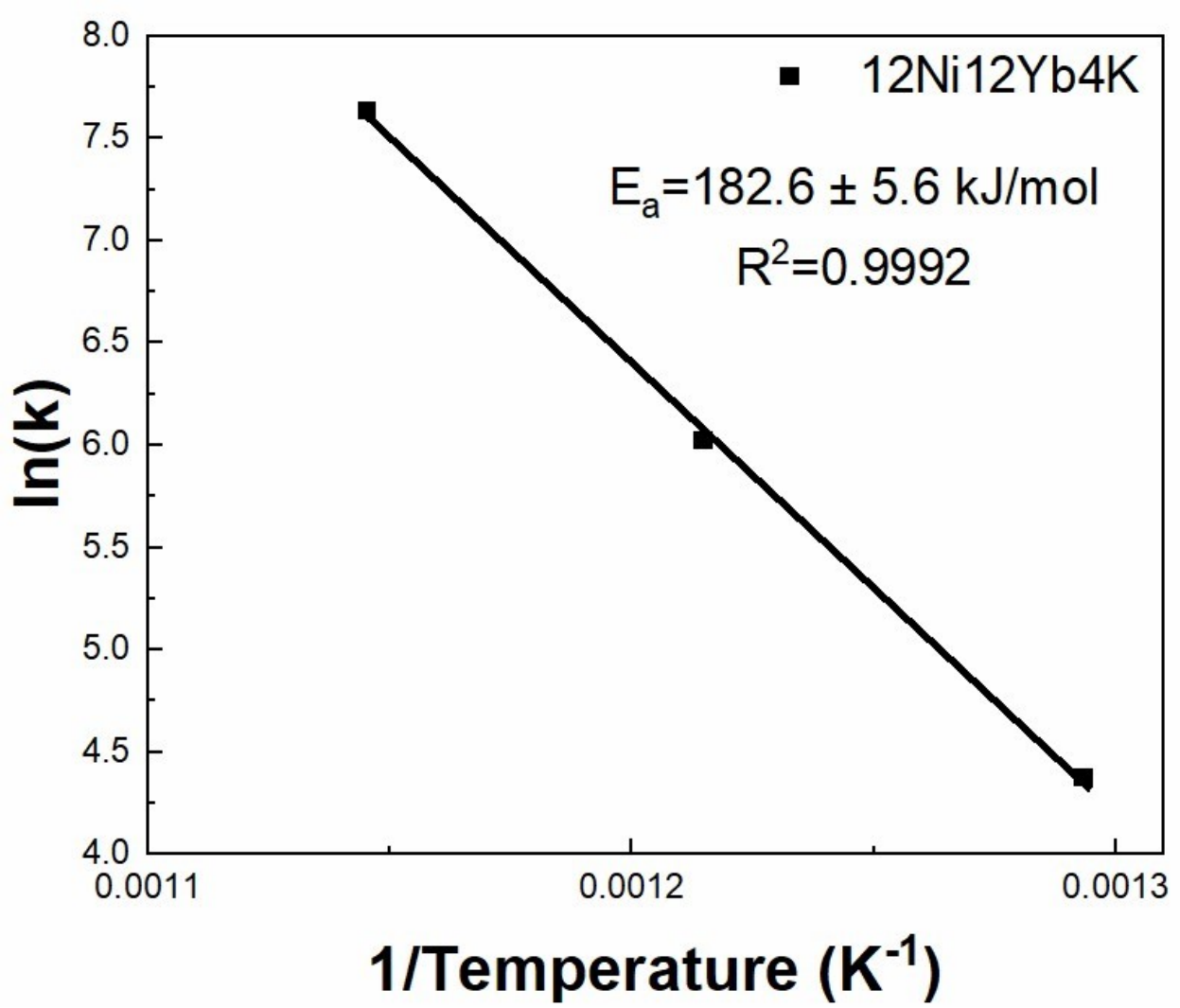

Figure S23. Arrhenius plot of the 12%Ni/12%Yb/4%K/γ-Al_2O_3.

Stability Data

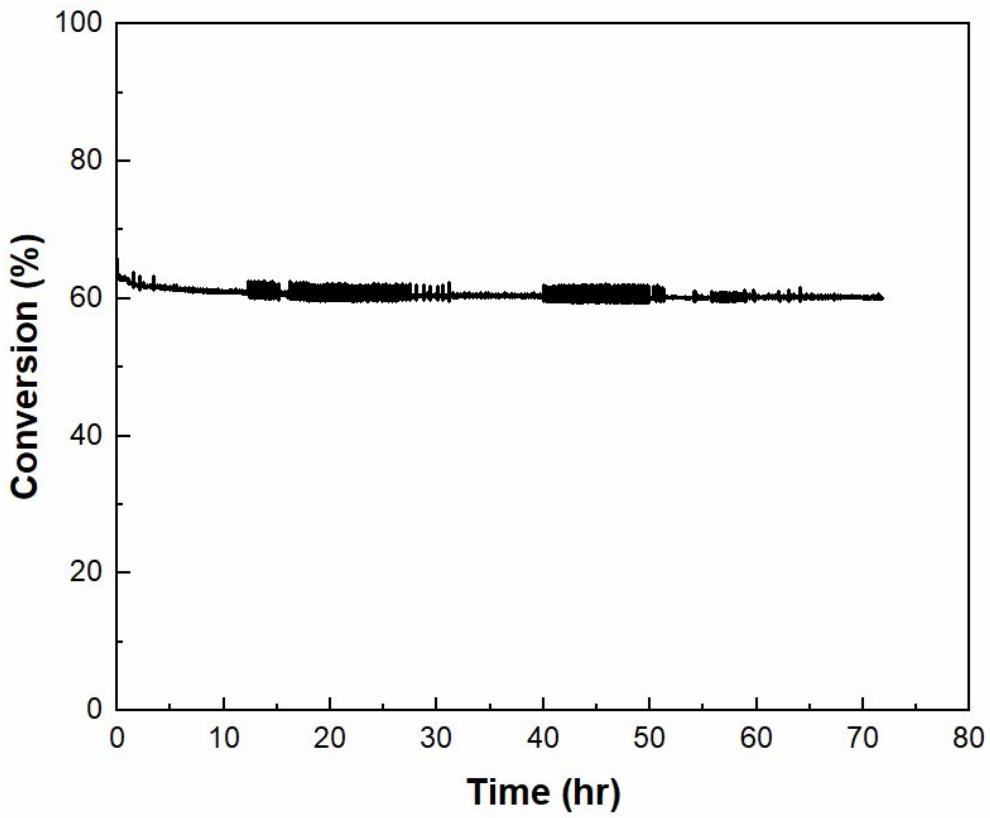

Figure S24. Stability of the 12%Ni/4%Yb/12%Rb/Al_2O_3 catalyst over 72 hours.

Additional Permeation Membrane Data

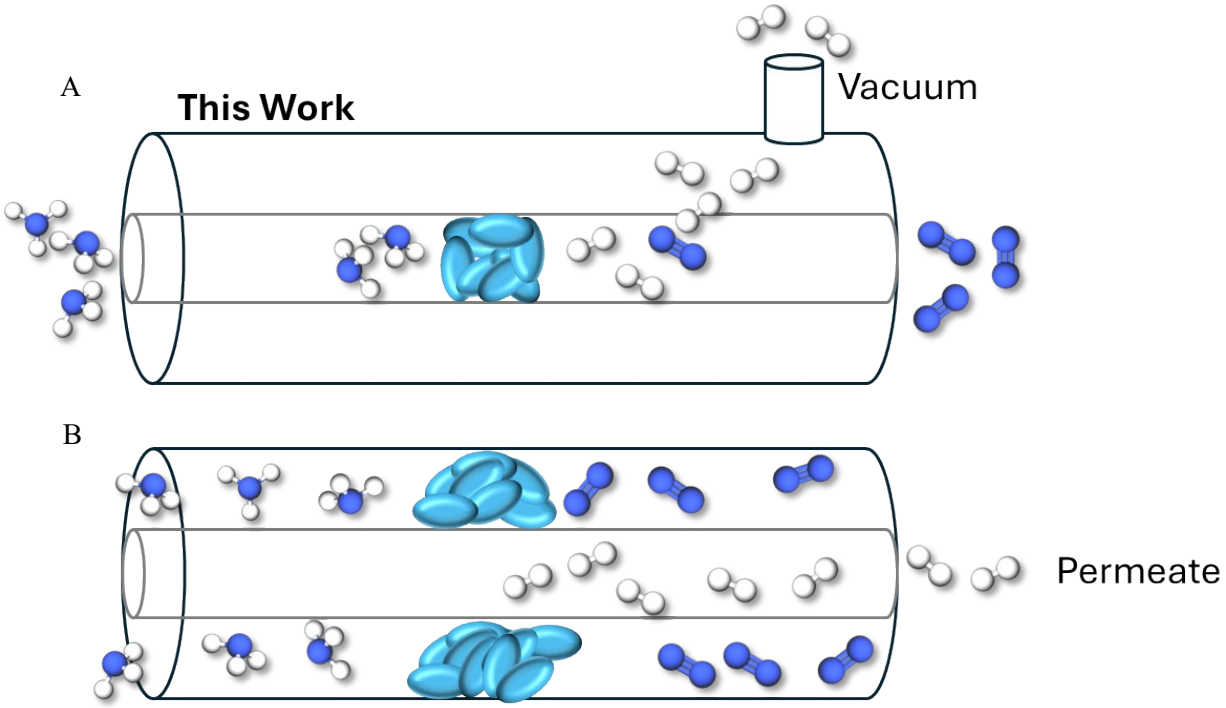

Figure S25. Example of the [B] typical pressure-based permeation membrane reactor and the [A] vacuum-based permeation membrane reactor utilized in this study.

Figure S25 shows two examples of potential designs for PdAg permeation membrane reactors. Figure S25B is an example of traditional design of a permeation membrane reactor where the reactor has an over pressure on one side of the membrane, which creates a pressure differential. This drives the hydrogen to permeate through the membrane to the side has lower pressures. Figure S25A shows the design of the permeation membrane used in this study. Instead of there being an initial over pressure on one side of the reactor, a vacuum is applied to one side to create the pressure differential. As the reaction occurs the hydrogen permeates through the membrane to the lower pressure.

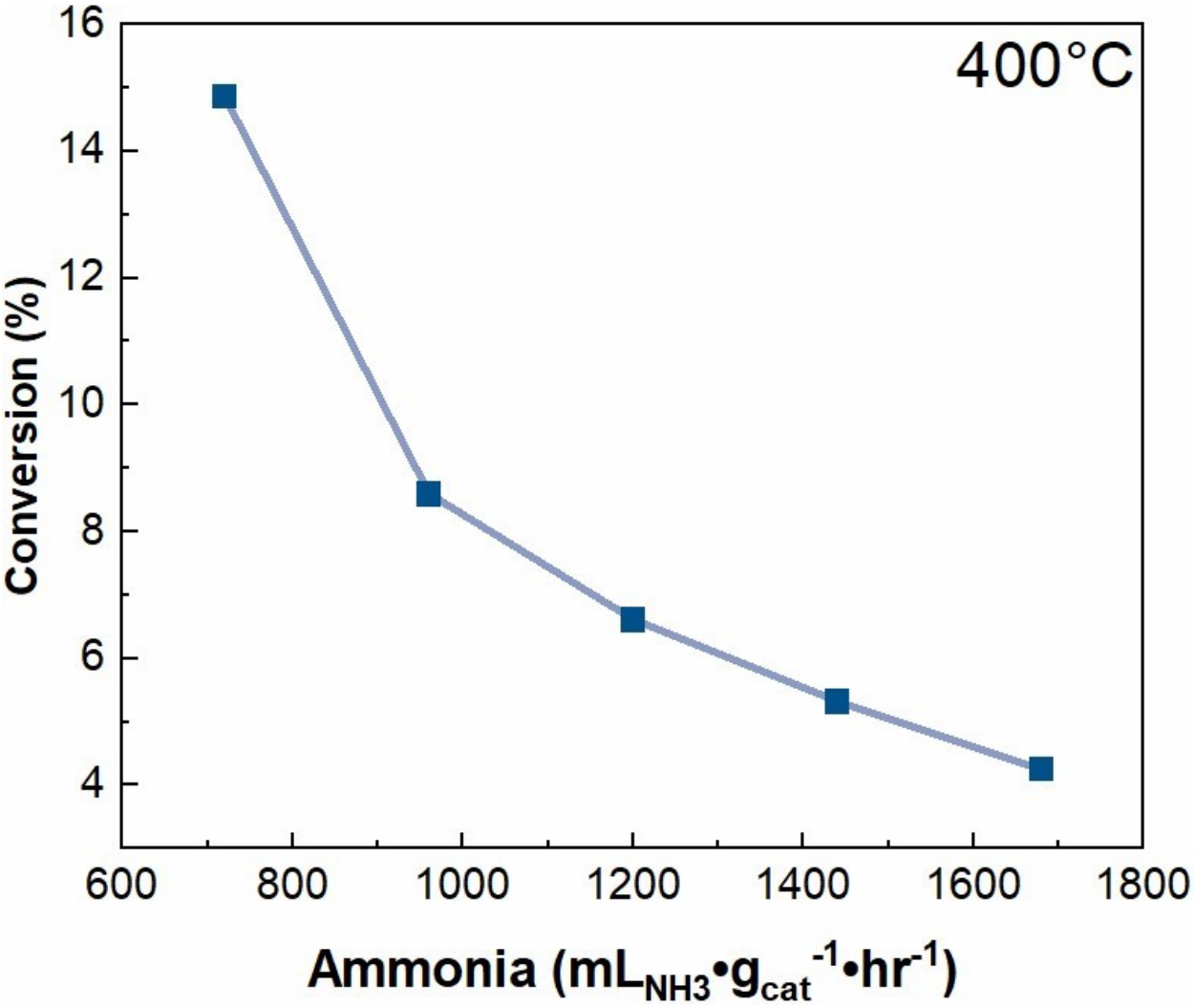

Figure S26. 12%Ni/4%Yb/12%Rb/Al2O3 packed PdAg permeation membrane for ammonia dehydrogenation at 400°C.

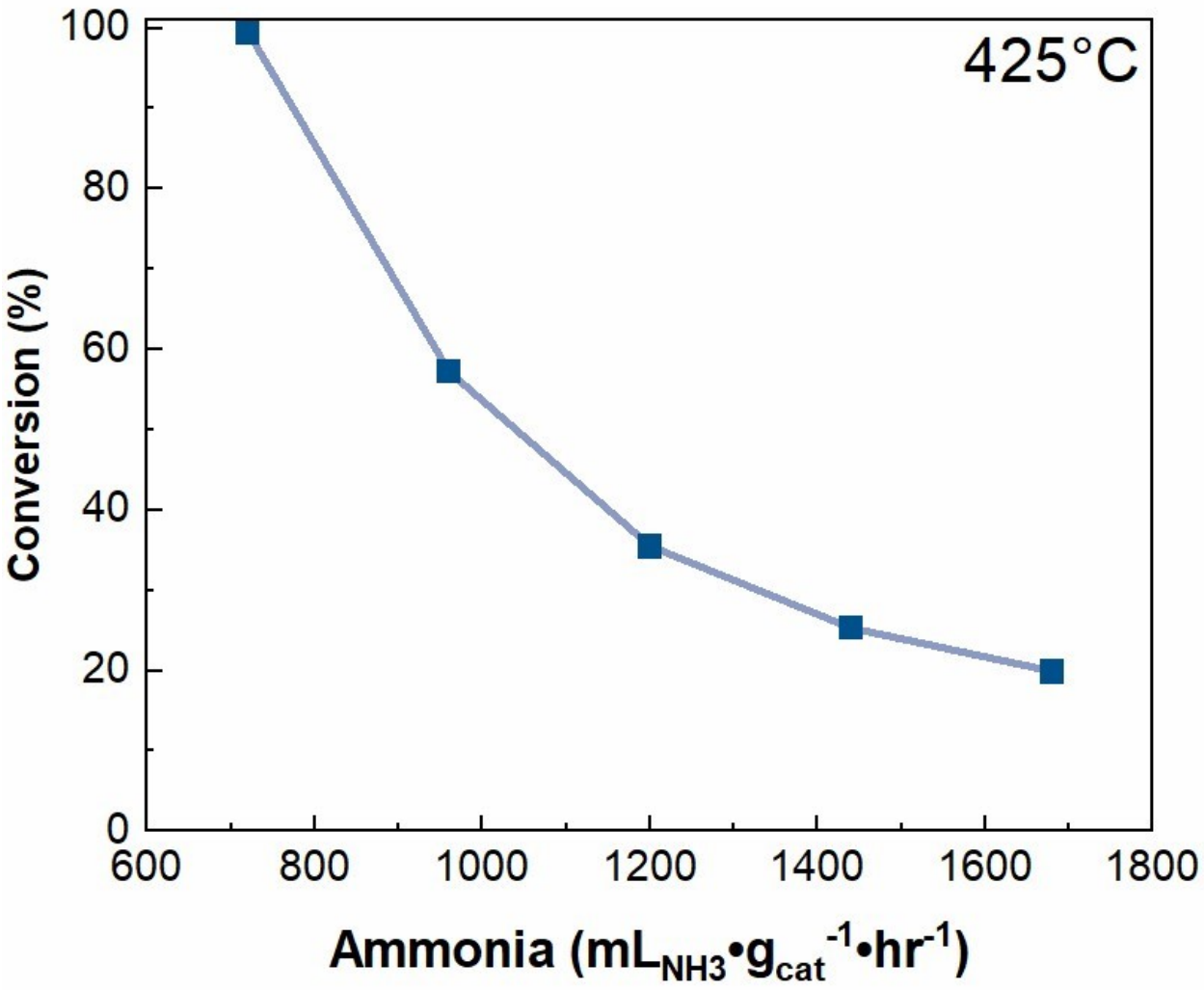

Figure S27. 12%Ni/4%Yb/12%Rb/Al_2O_3 packed PdAg permeation membrane for ammonia dehydrogenation at 425°C.

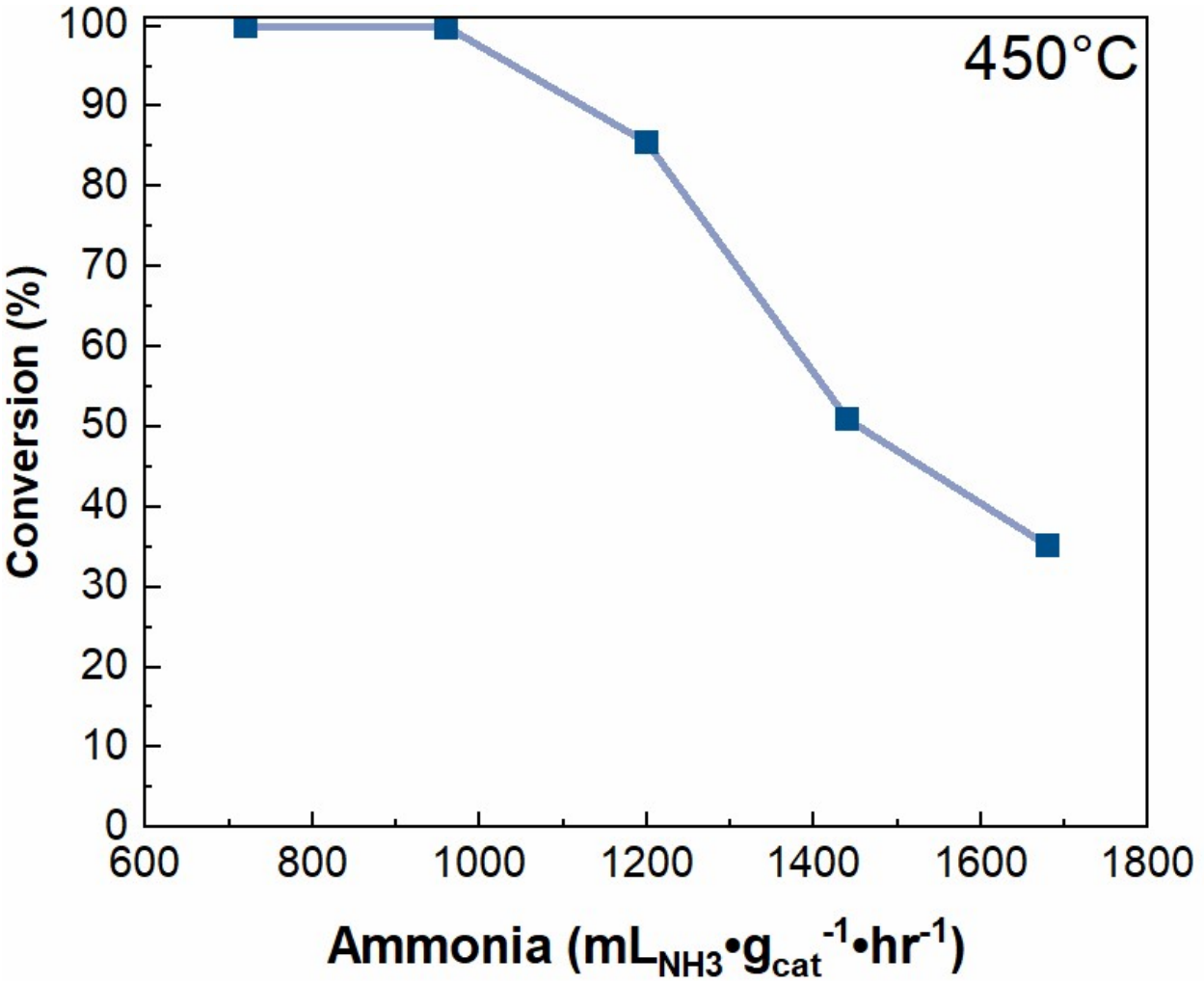

Figure S28. 12%Ni/4%Yb/12%Rb/Al_2O_3 packed PdAg permeation membrane for ammonia dehydrogenation at 450°C.

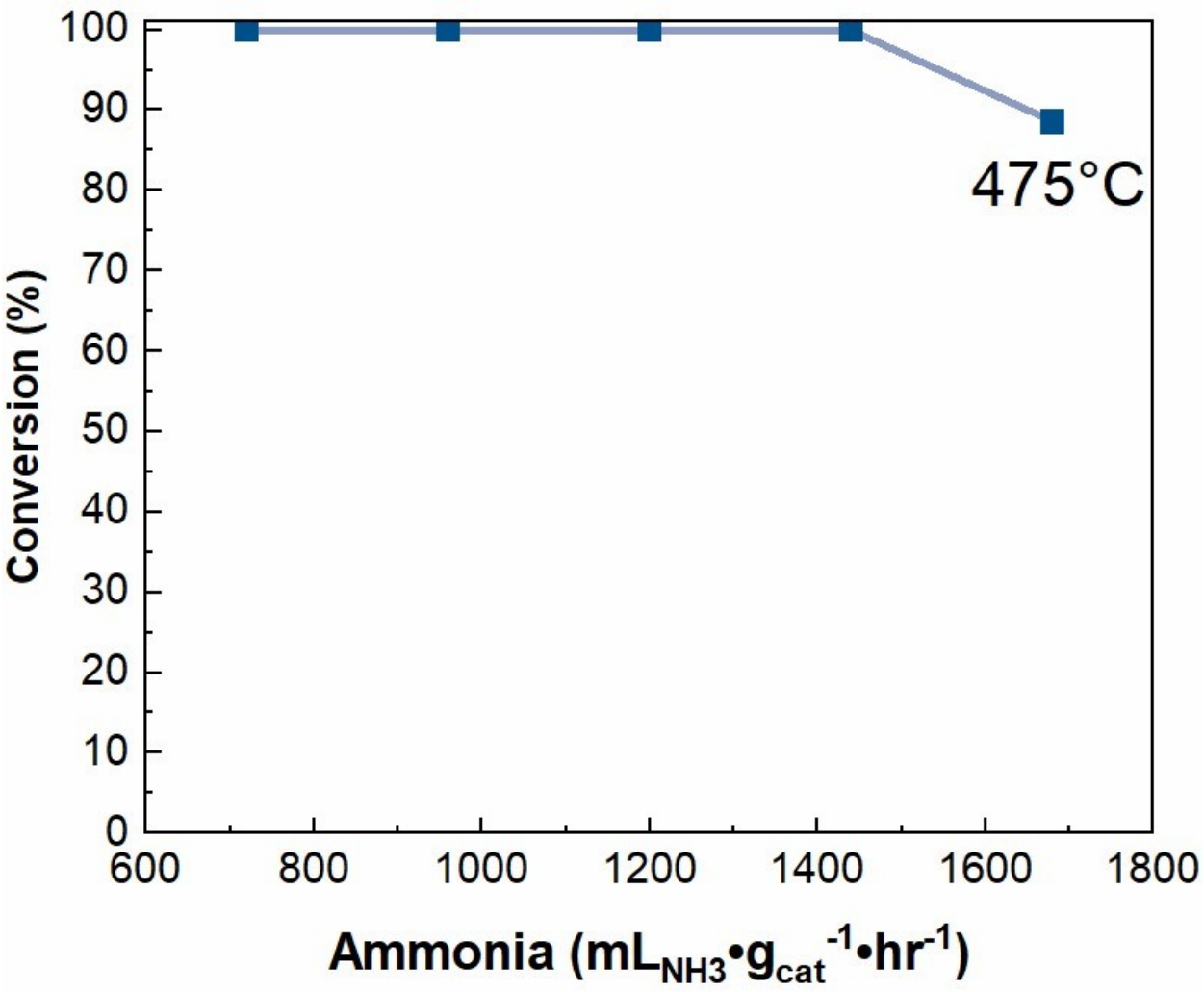

Figure S29. 12%Ni/4%Yb/12%Rb/Al2O3 packed PdAg permeation membrane for ammonia dehydrogenation at 475°C.

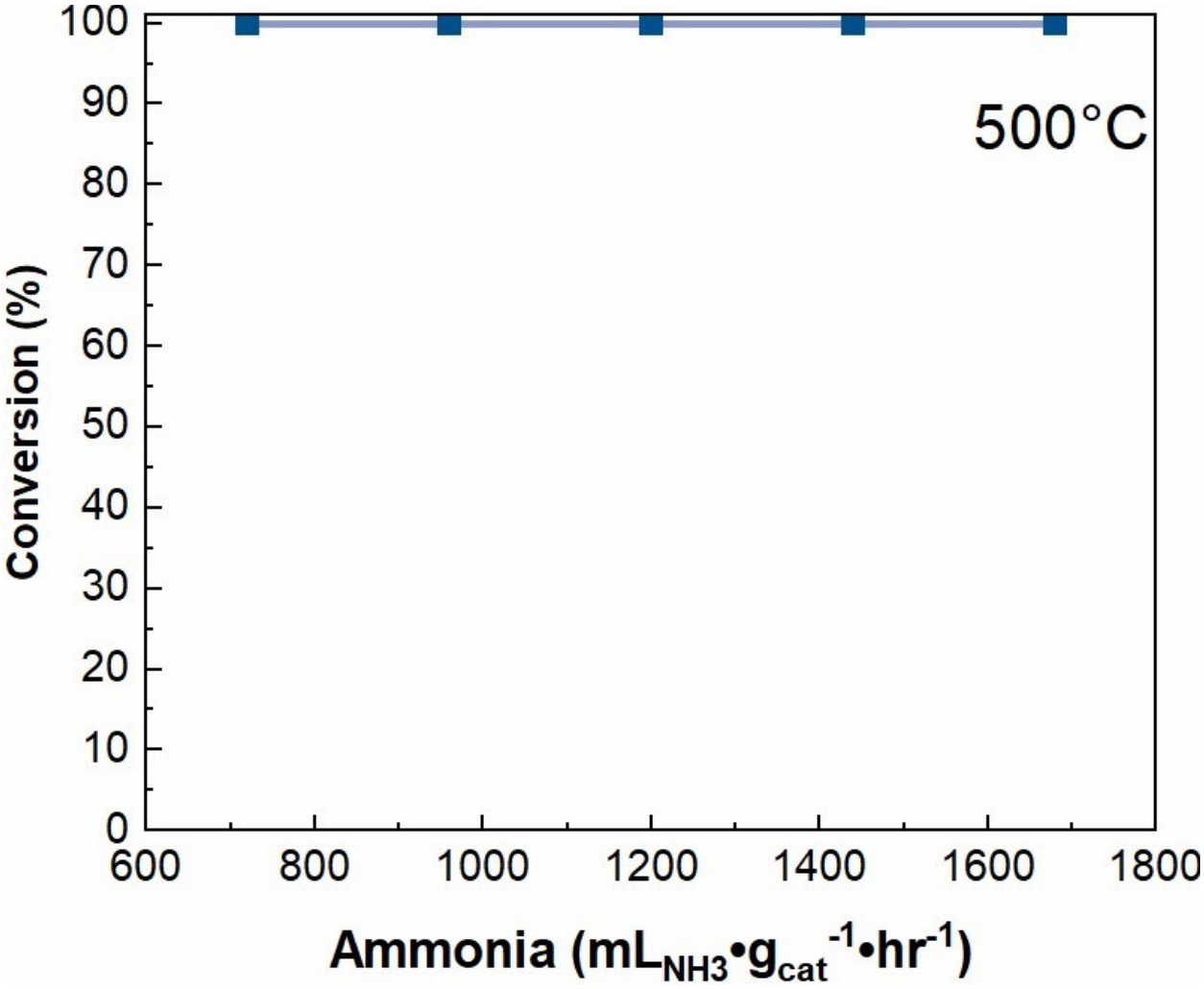

Figure S30. 12%Ni/4%Yb/12%Rb/Al2O3 packed PdAg permeation membrane for ammonia dehydrogenation at 500°C.

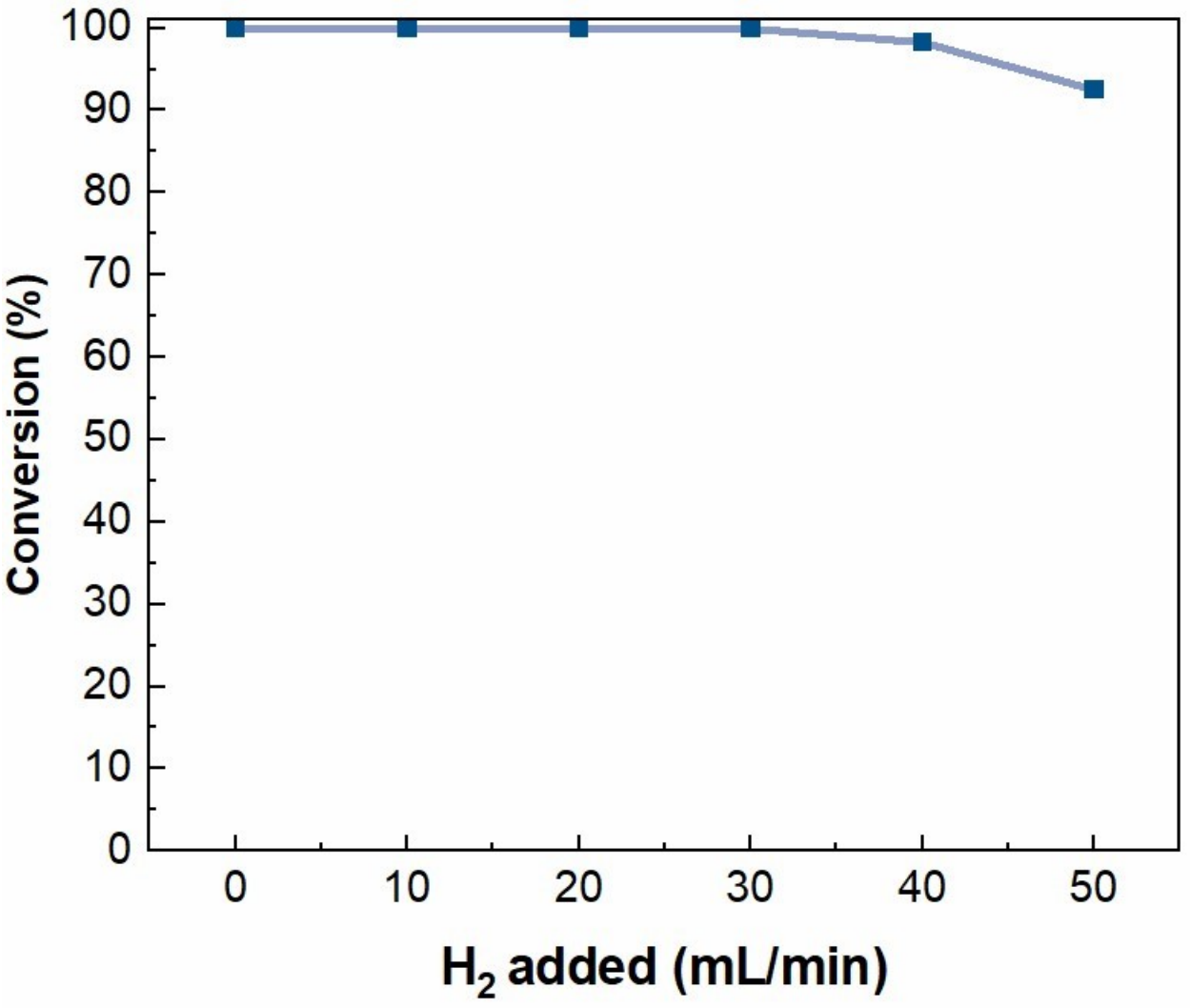

Figure S31. 12%Ni/4%Yb/12%Rb/Al2O3 packed PdAg permeation membrane for ammonia dehydrogenation at 500°C with H_2 added into the reagent gas of 50mL/min NH_3 (or 1200 $mL_{NH3} \bullet g_{cat}^{-1} \bullet hr^{-1}$).

H_2 Temperature Programmed Reduction

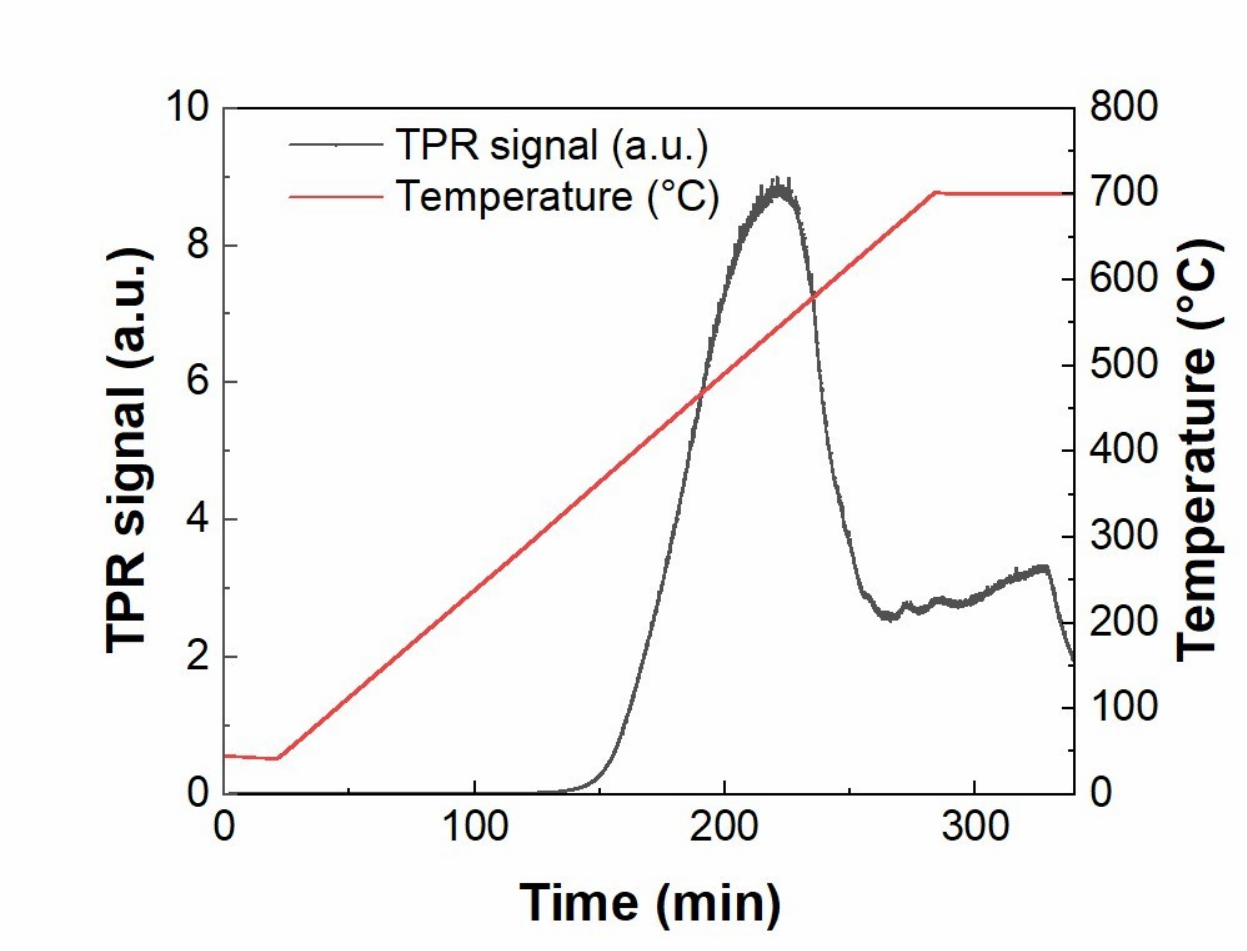

Figure S32. Temperature programmed reduction of the 12%Ni/4%Yb/12%Na/Al_2O_3 catalyst.

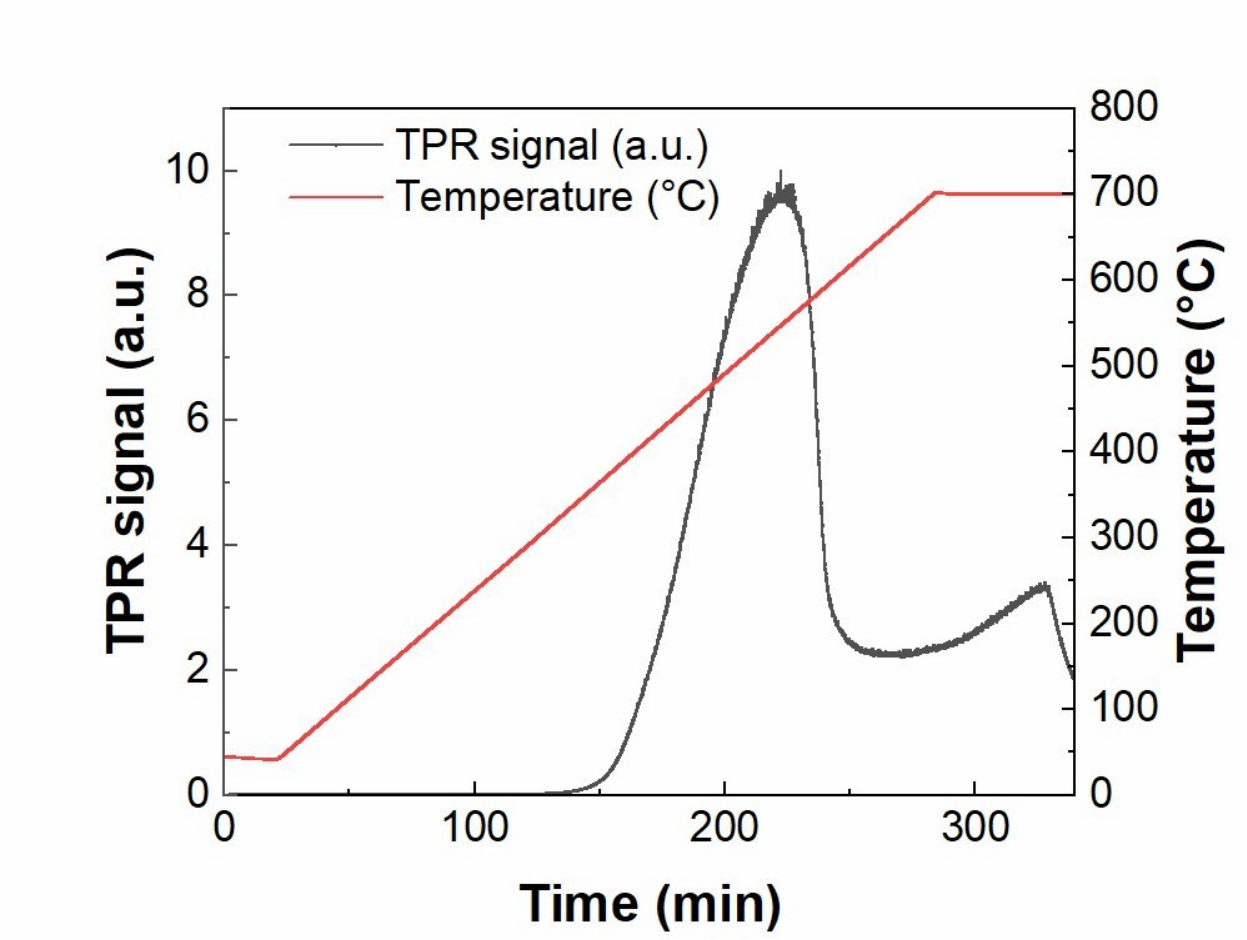

Figure S33. Temperature programmed reduction of the 12%Ni/4%Yb/12%K/Al_2O_3 catalyst.

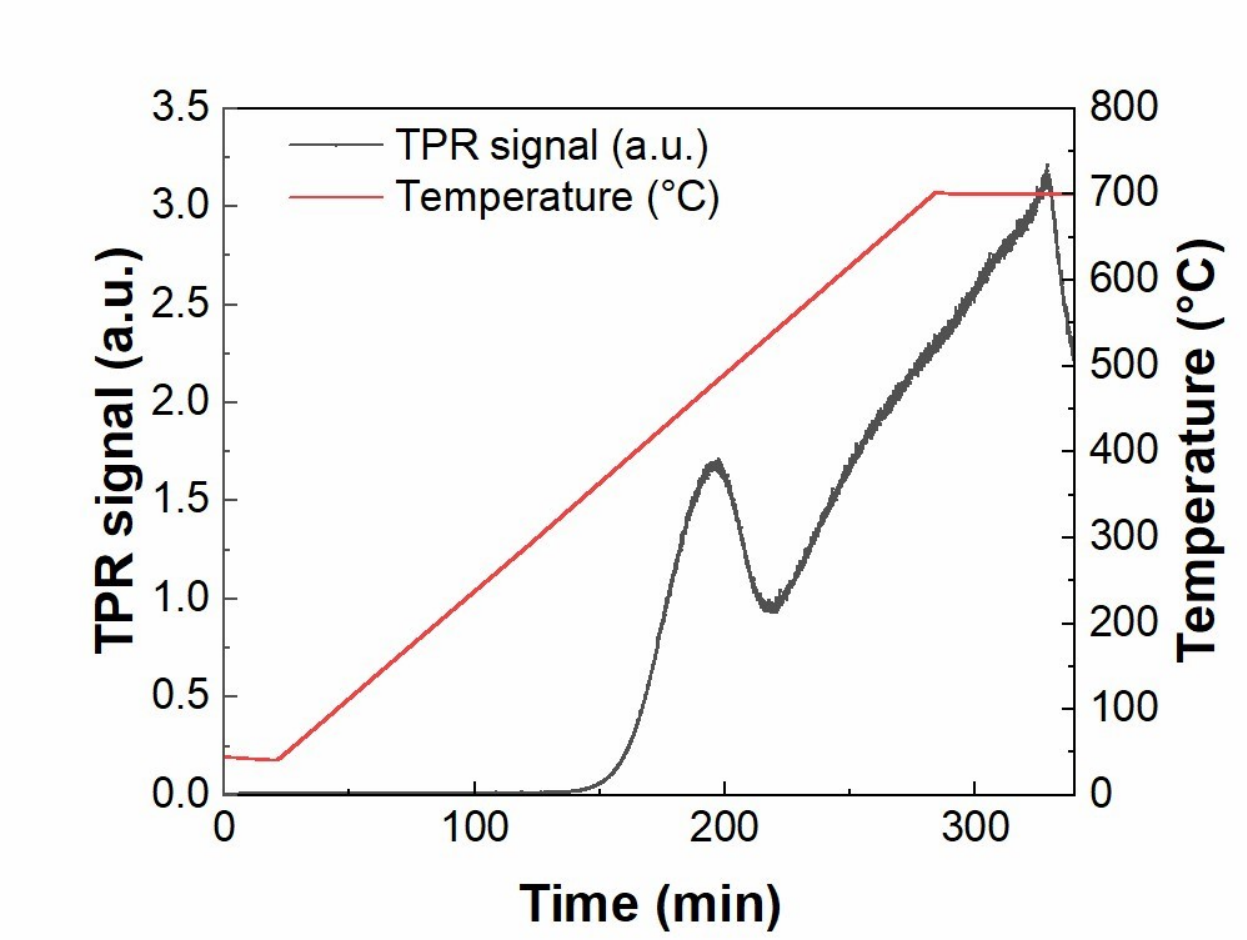

Figure S34. Temperature programmed reduction of the 12%Ni/4%Yb/12%Rb/Al_2O_3 catalyst.

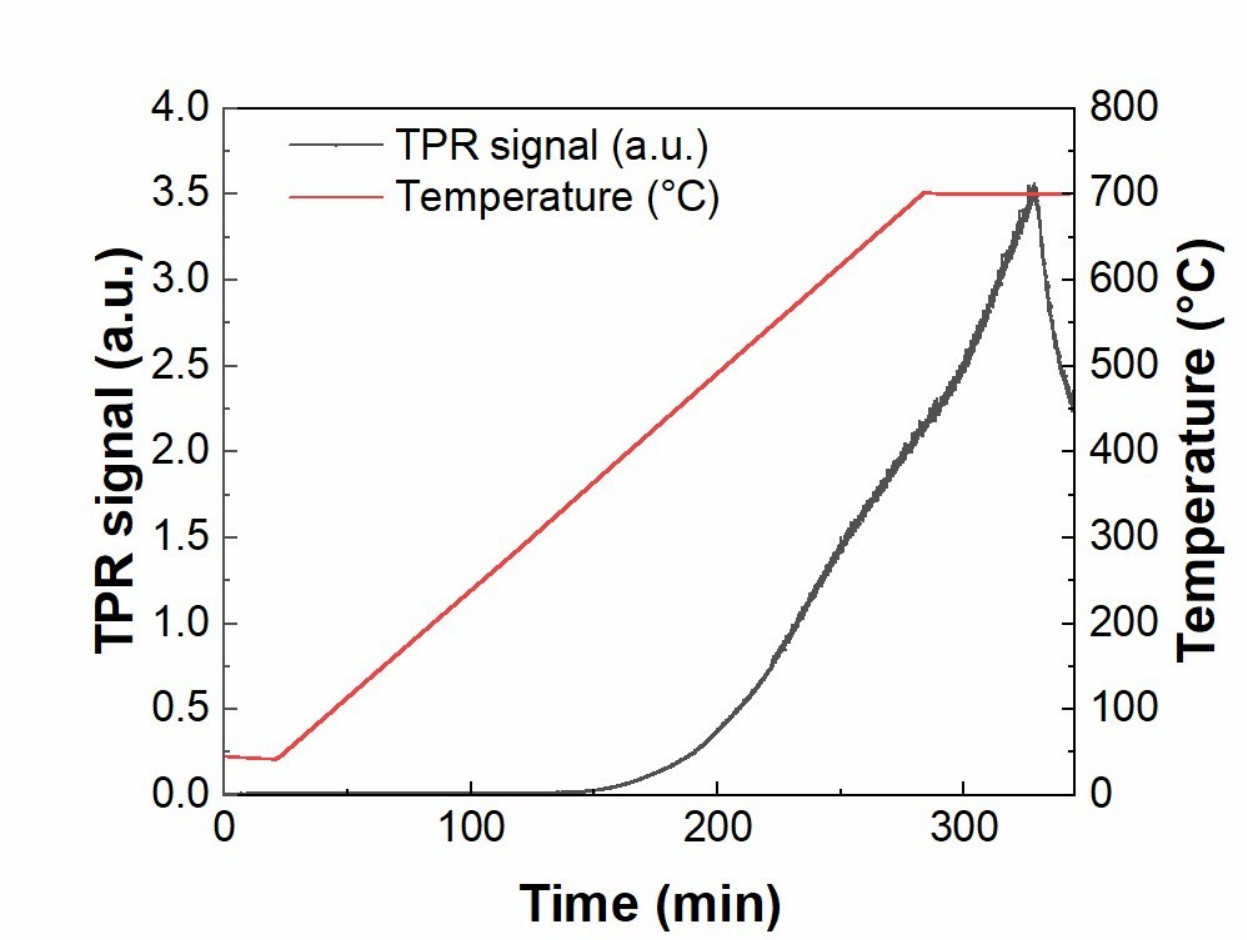

Figure S35. Temperature programmed reduction of the 12%Ni/4%Yb/12%Cs/Al_2O_3 catalyst.

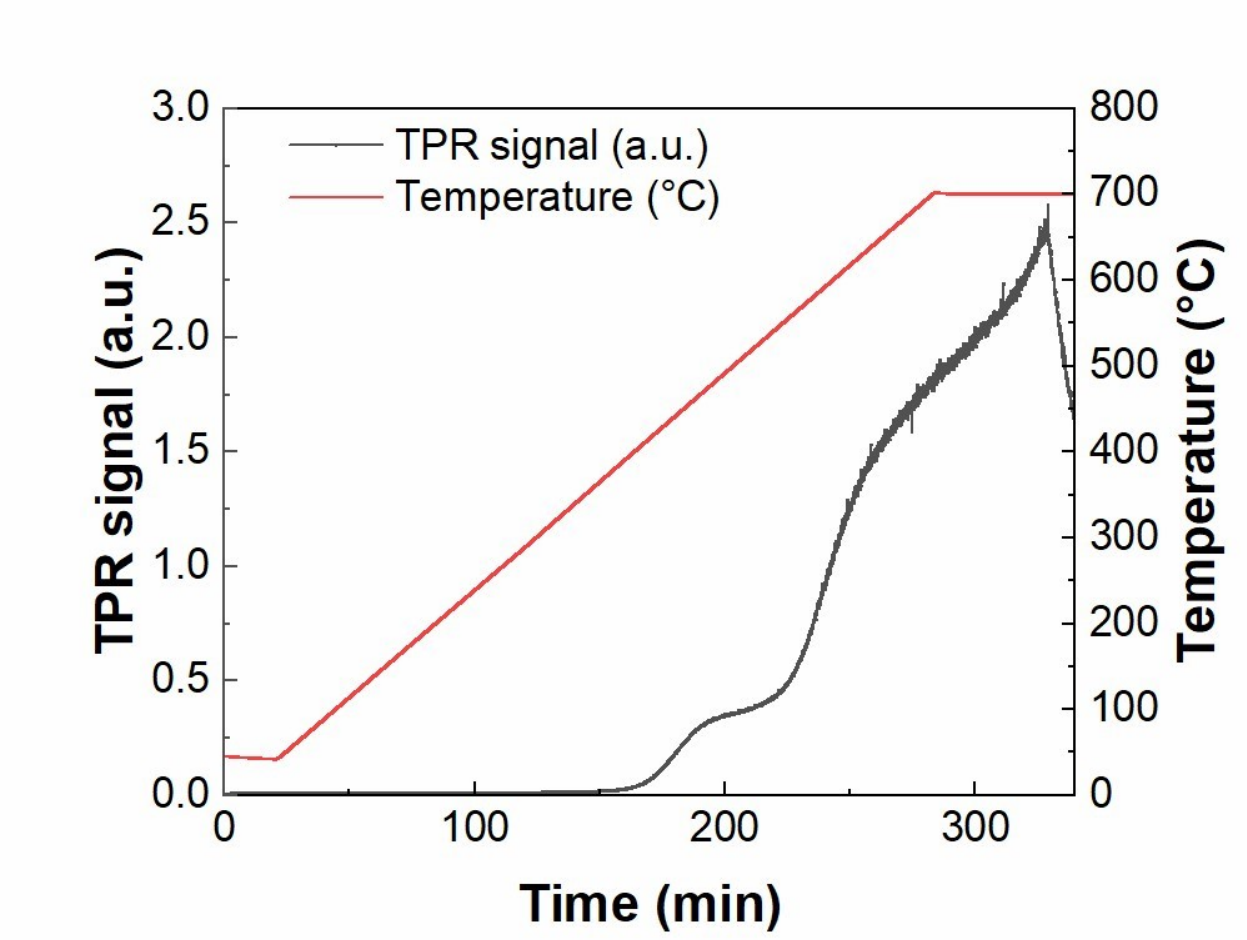

Figure S36. Temperature programmed reduction of the 12%Ni/4%Yb/12%Ca/Al_2O_3 catalyst.

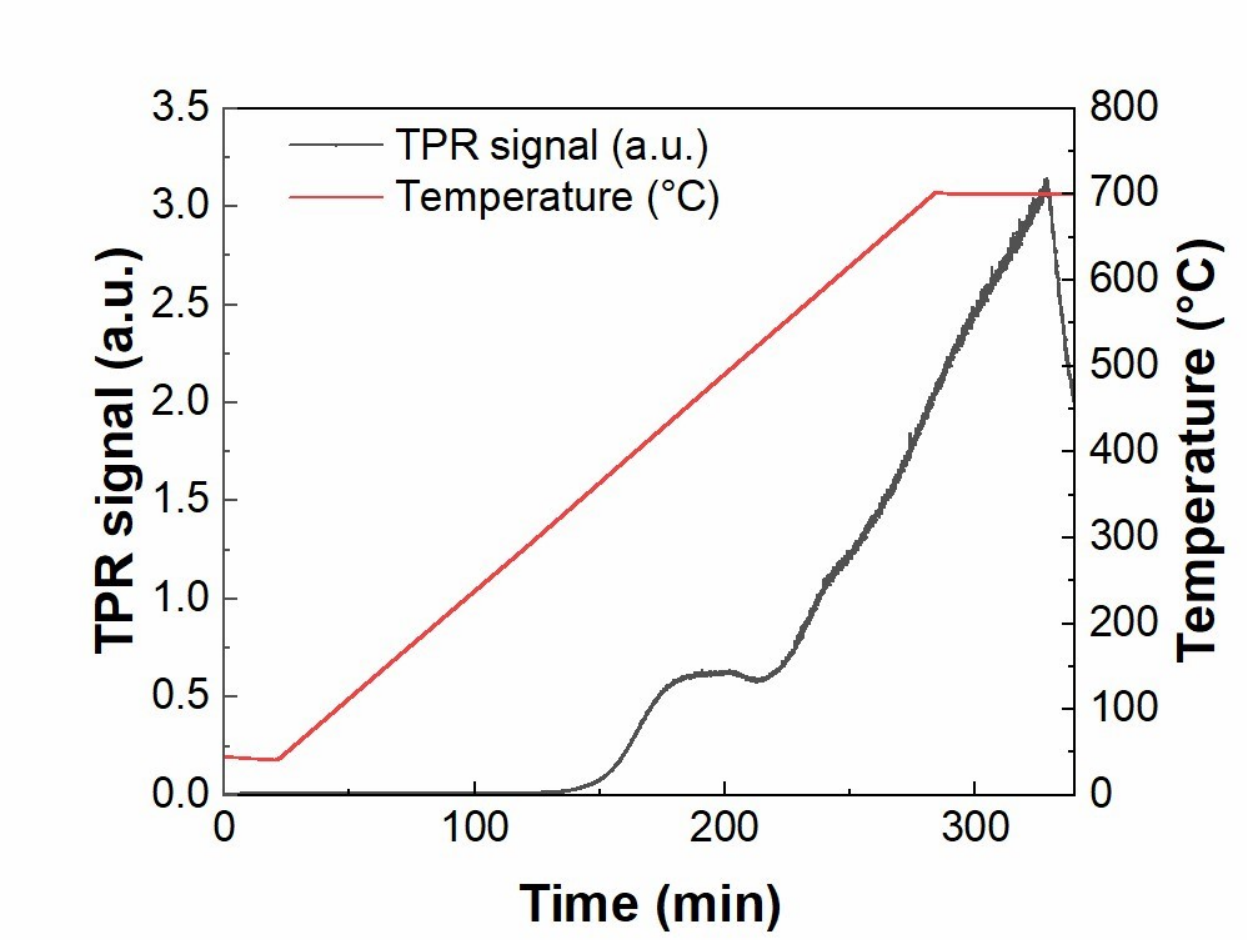

Figure S37. Temperature programmed reduction of the 12%Ni/4%Yb/12%Sr/Al_2O_3 catalyst.

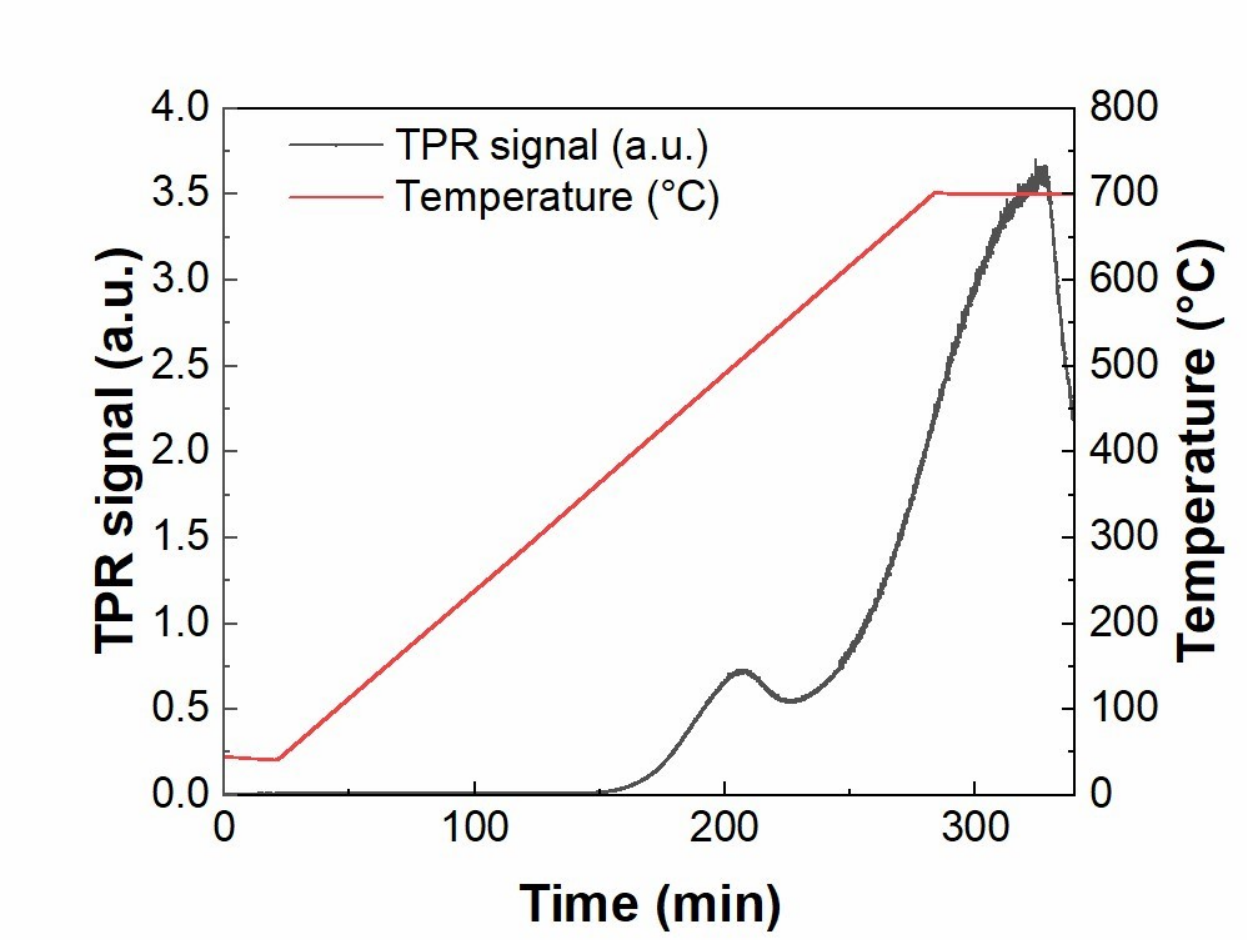

Figure S38. Temperature programmed reduction of the 12%Ni/4%Yb/12%Ba/Al_2O_3 catalyst.

Ammonia Temperature Programmed Desorption

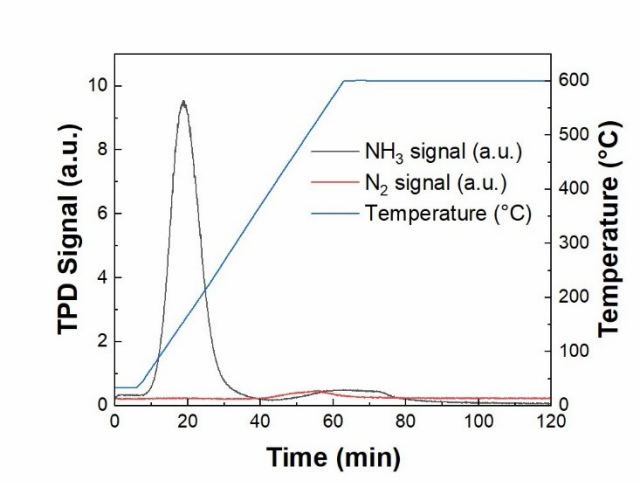

Figure S39. NH_3 programmed desorption of the 12%Ni/4%Yb/12%Na/Al_2O_3 catalyst.

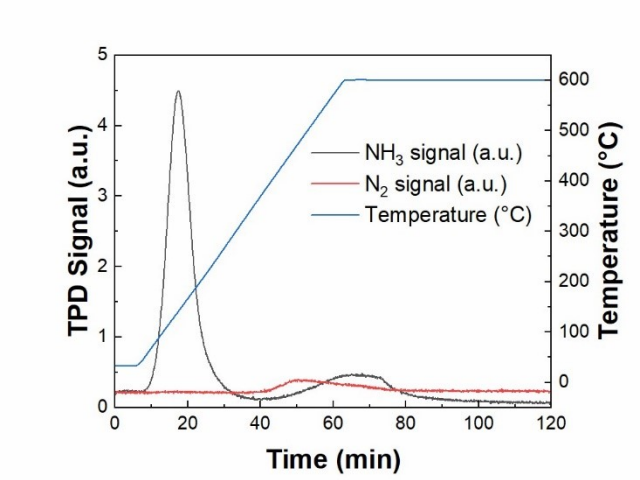

Figure S40. NH_3 programmed desorption of the 12%Ni/4%Yb/12%K/Al_2O_3 catalyst.

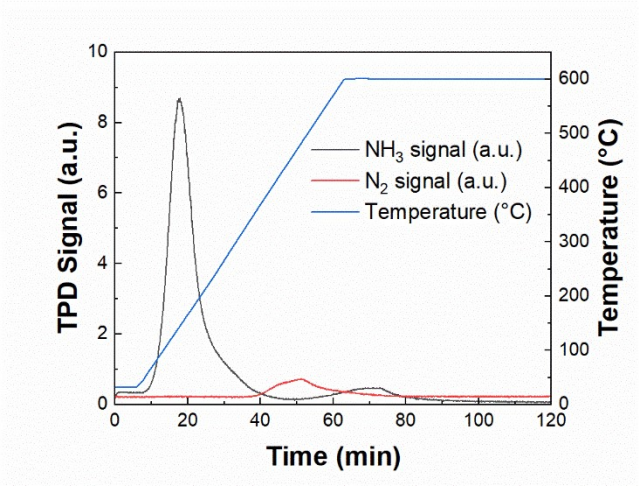

Figure S41. NH_3 programmed desorption of the 12%Ni/4%Yb/12%Rb/Al_2O_3 catalyst.

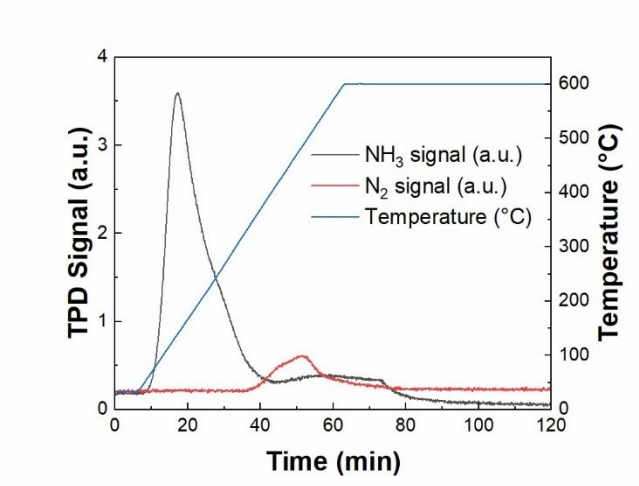

Figure S42. NH_3 programmed desorption of the 12%Ni/4%Yb/12%Cs/Al_2O_3 catalyst.

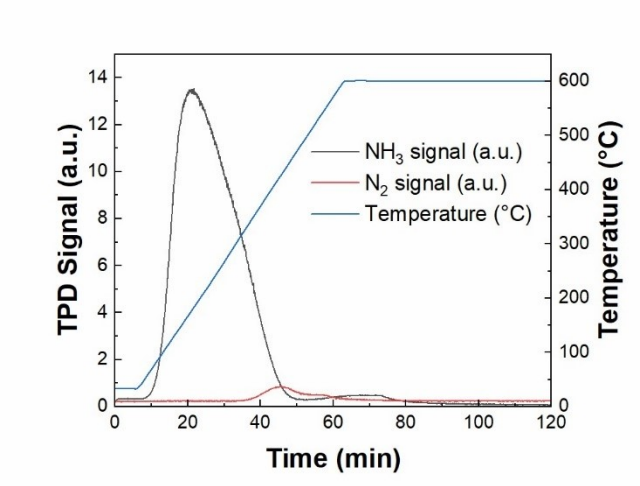

Figure S43. NH_3 programmed desorption of the 12%Ni/4%Yb/12%Ca/Al_2O_3 catalyst.

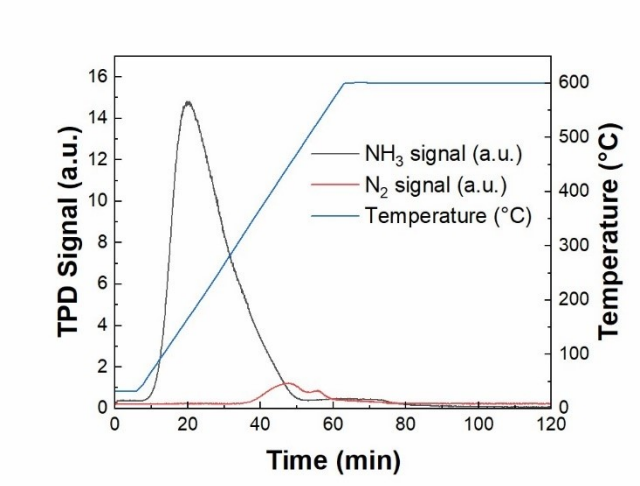

Figure S44. NH_3 programmed desorption of the 12%Ni/4%Yb/12%Sr/Al_2O_3 catalyst.

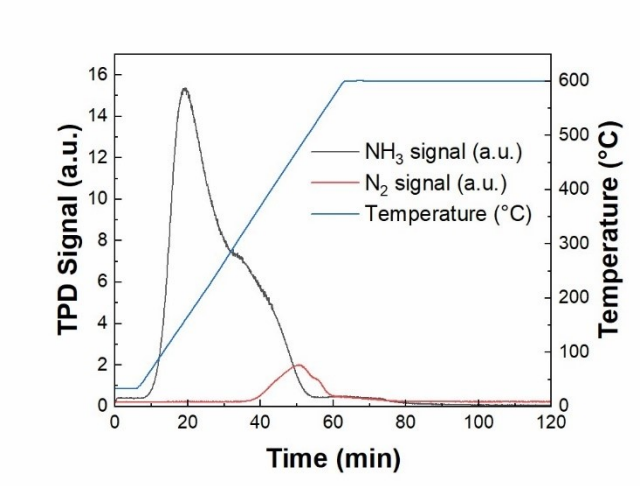

Figure S45. NH_3 programmed desorption of the 12%Ni/4%Yb/12%Ba/Al_2O_3 catalyst.

N_2 Physisorption

Nitrogen physisorption was conducted to determine the difference in pore size and volume in the pores for each of the catalysts.

Table S15. Median pore size and volume in pores calculated from N_2 physisorption.

Sample	Median Pore Size (A)	Total Volume in Pores (cm^3/g)
12%Ni/4%Yb/12%Na/Al_2O_3	9.004	0.32402
12%Ni/4%Yb/12%K/Al_2O_3	8.773	0.41865
12%Ni/4%Yb/12%Rb/Al_2O_3	9.340	0.42221
12%Ni/4%Yb/12%Cs/Al_2O_3	10.124	0.47062
12%Ni/4%Yb/12%Ca/Al_2O_3	9.688	0.52131
12%Ni/4%Yb/12%Sr/Al_2O_3	8.525	0.42712
12%Ni/4%Yb/12%Ba/Al_2O_3	9.048	0.78070

N_2 Chemisorption

The catalysts were subjected to N_2 chemisorption at both 25 and 450°C to determine how the N_2 product could be binding to the catalyst at both room temperature and at reaction temperatures. The majority of the catalysts tested at 450°C showed no uptake of N_2 with the exception of the NiYbBa

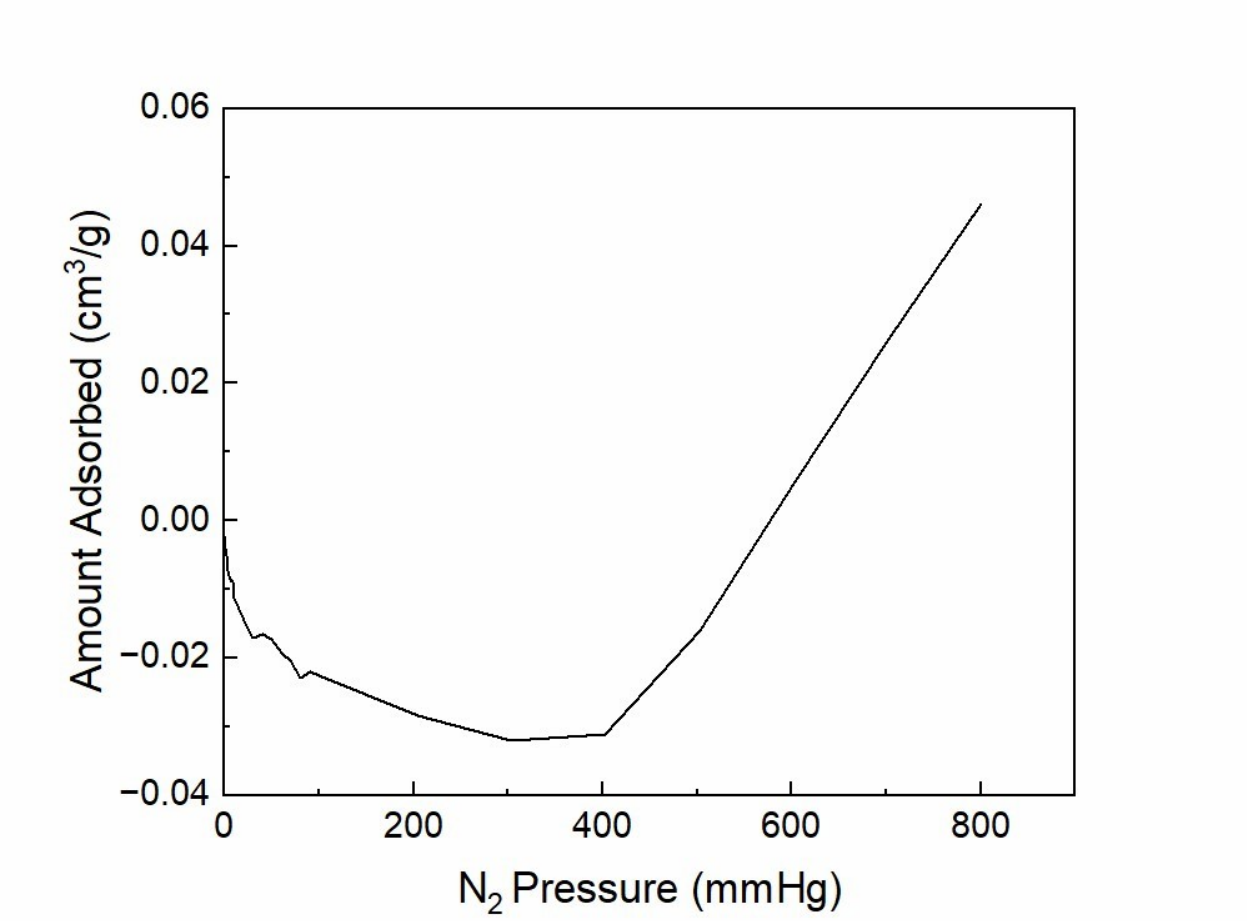

Figure S46. 12%Ni/4%Yb/12%Na/Al_2O_3 N_2 chemisorption at 25°C.

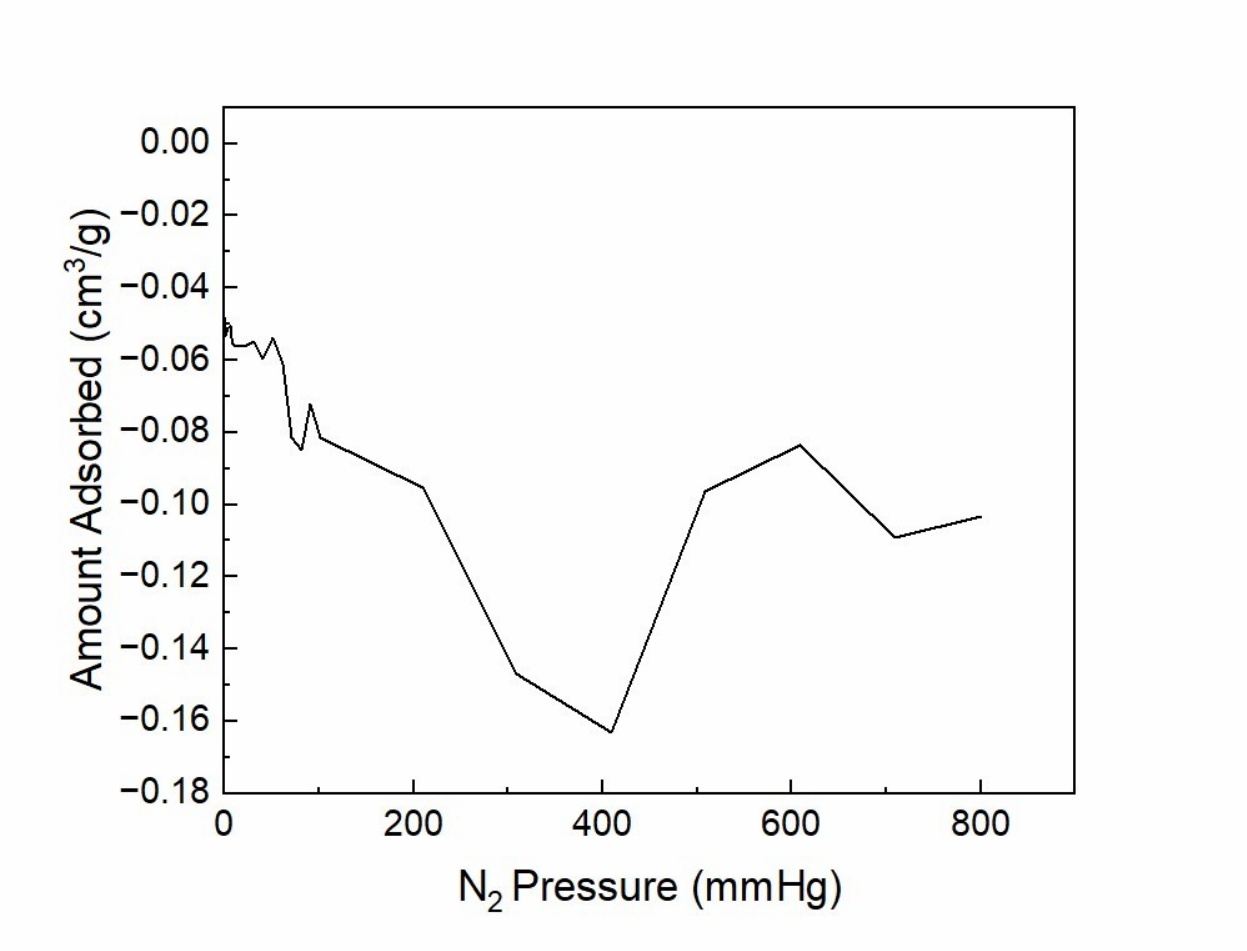

Figure S47. 12%Ni/4%Yb/12%Na/Al_2O_3 N_2 chemisorption at 450°C.

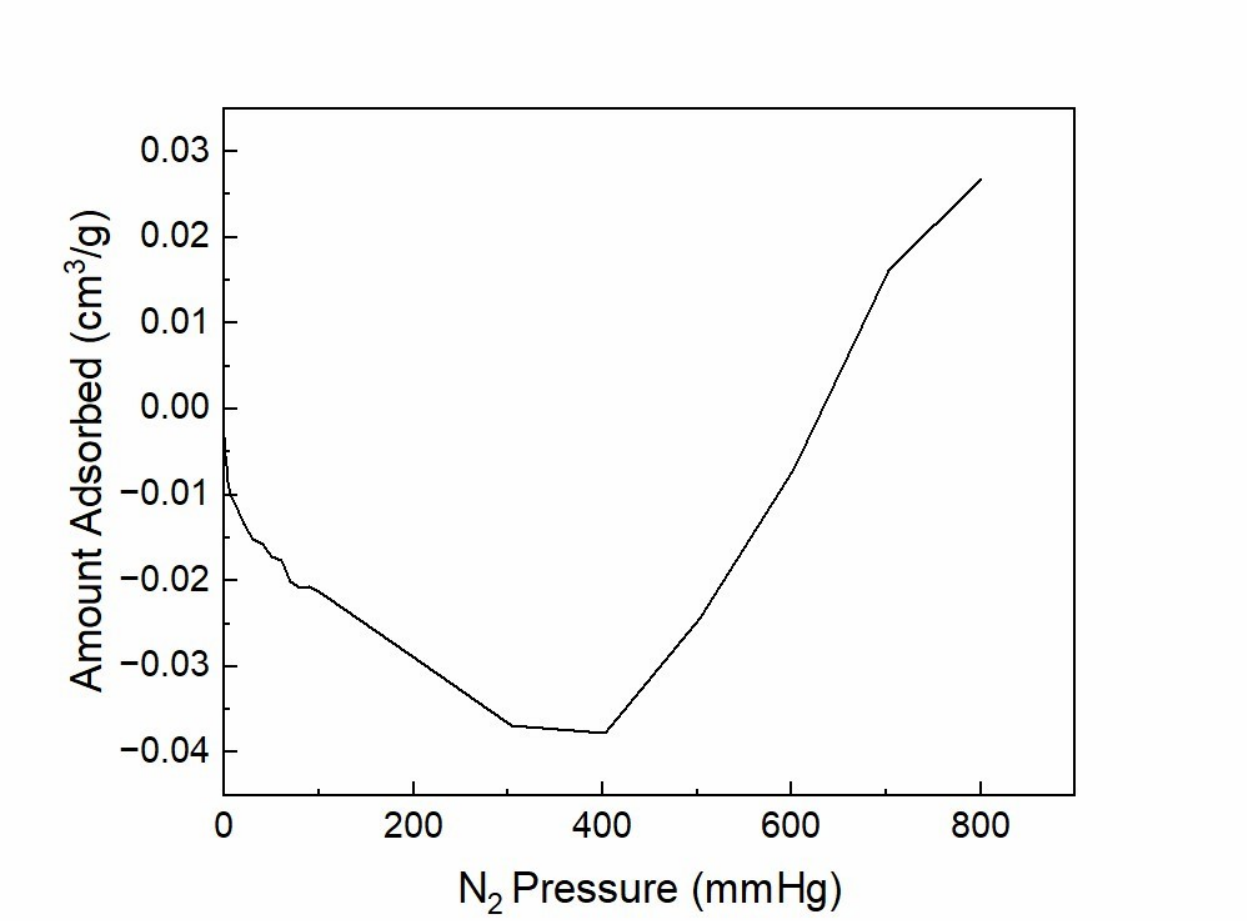

Figure S48. 12%Ni/4%Yb/12%K/Al_2O_3 N_2 chemisorption at 25°C.

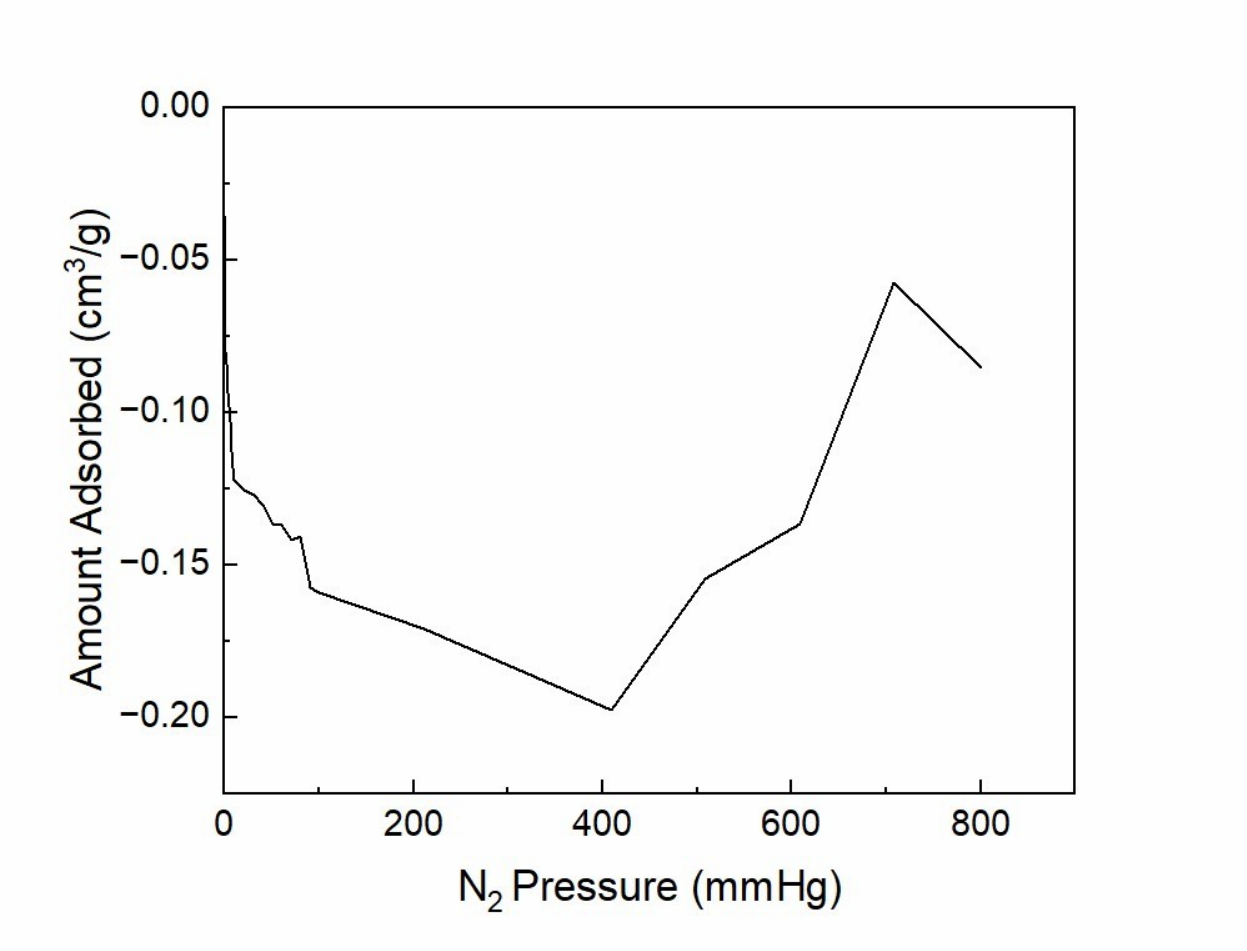

Figure S49. 12%Ni/4%Yb/12%K/Al_2O_3 N_2 chemisorption at 450°C.

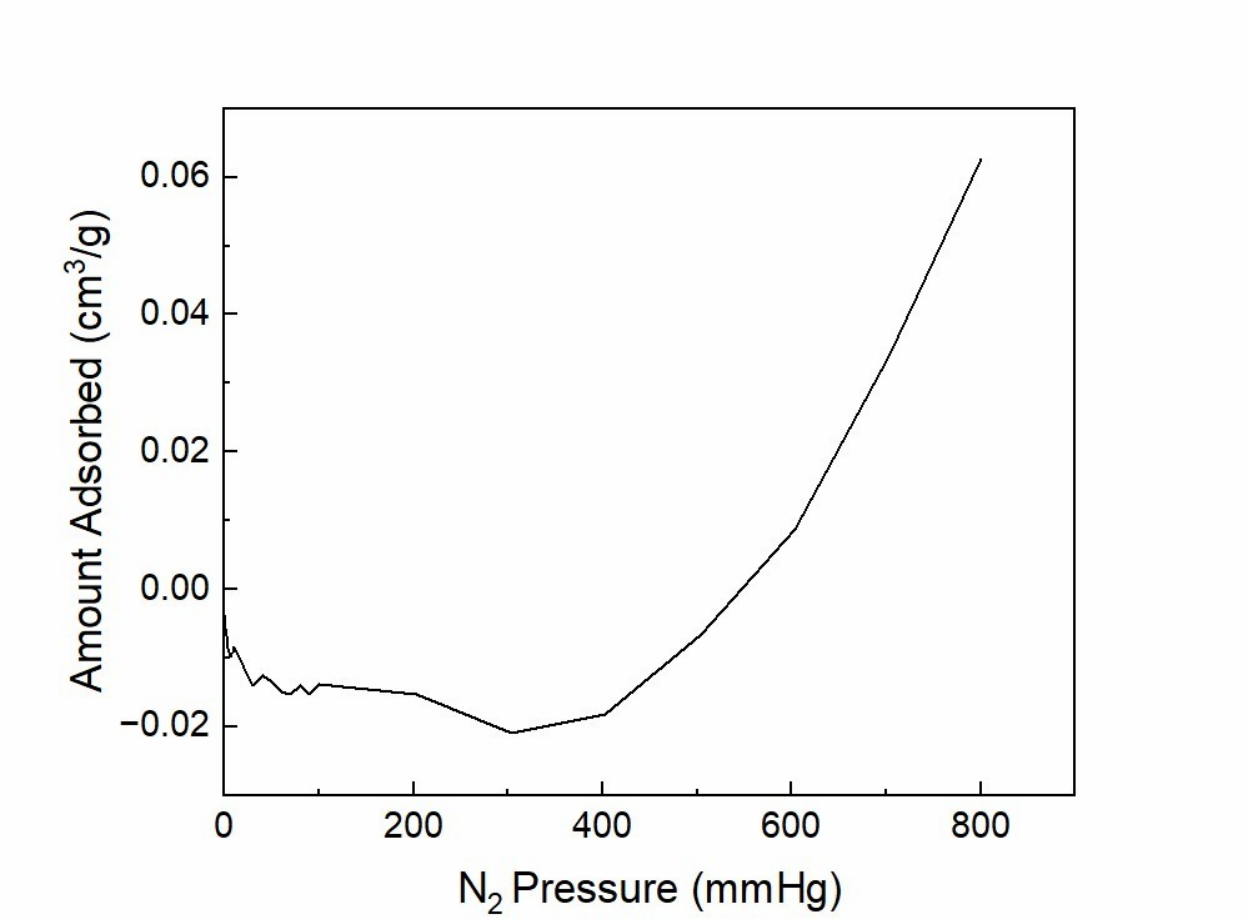

Figure S50. 12%Ni/4%Yb/12%Rb/Al_2O_3 N_2 chemisorption at 25°C.

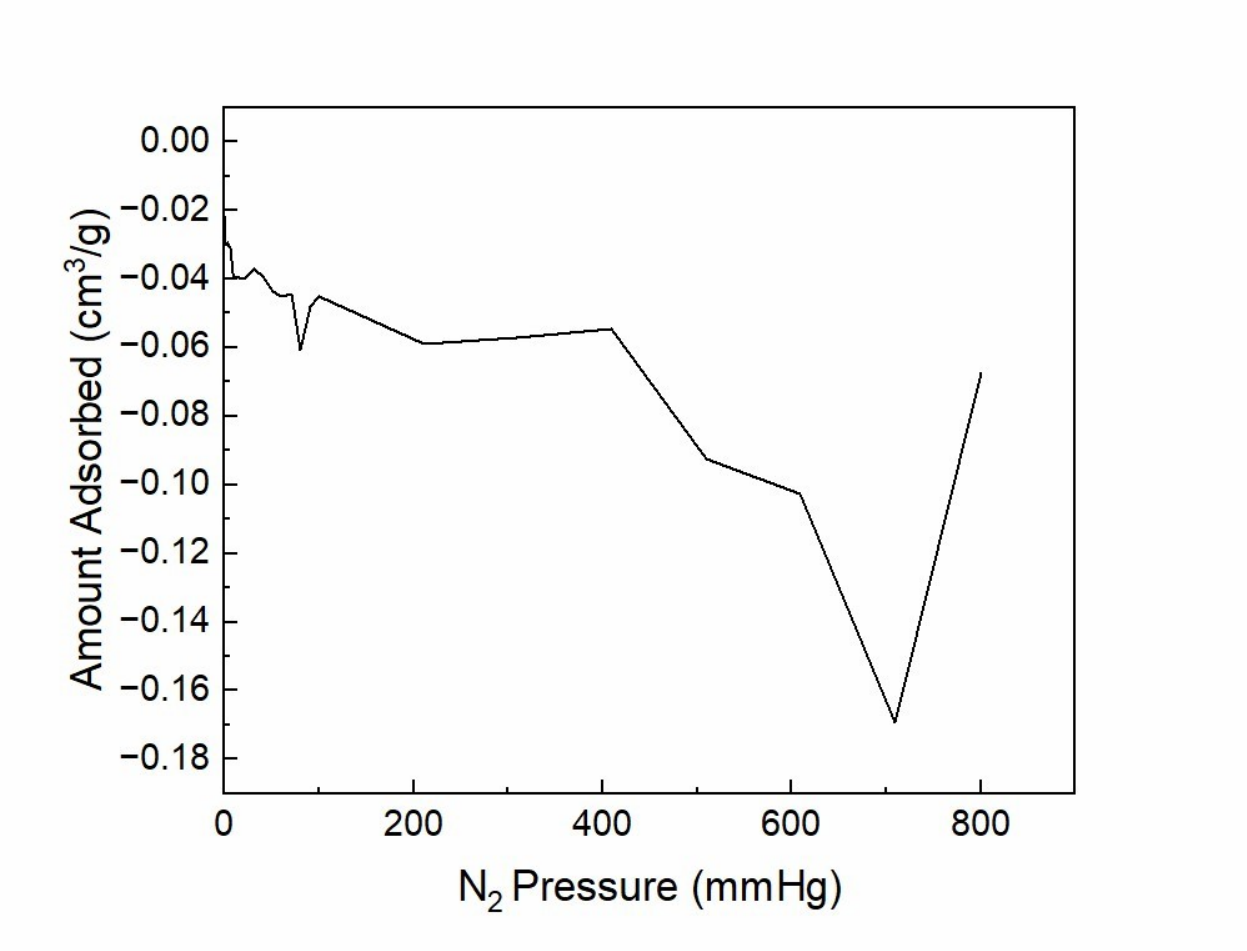

Figure S51. 12%Ni/4%Yb/12%Rb/Al_2O_3 N_2 chemisorption at 450°C.

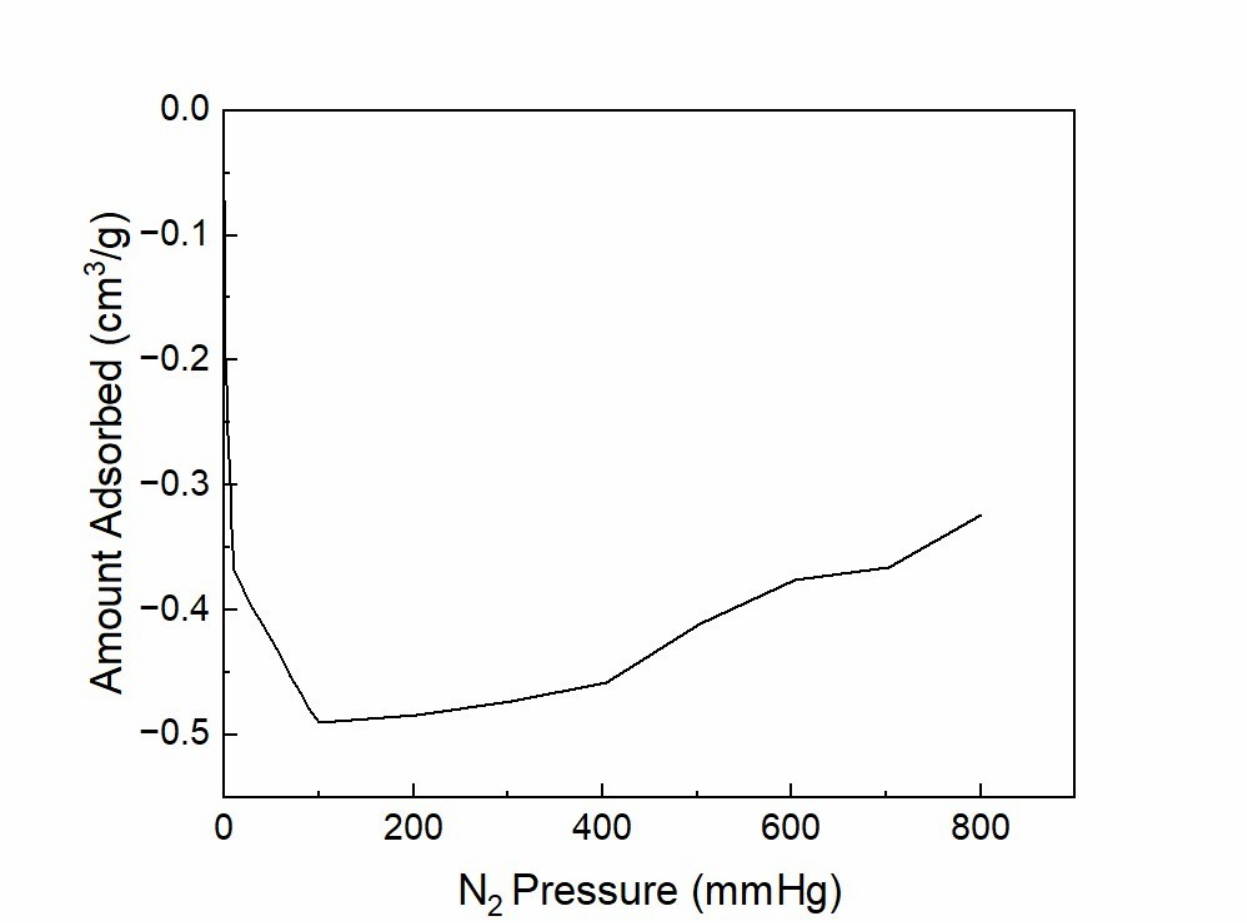

Figure S52. 12%Ni/4%Yb/12%Cs/Al_2O_3 N_2 chemisorption at 25°C.

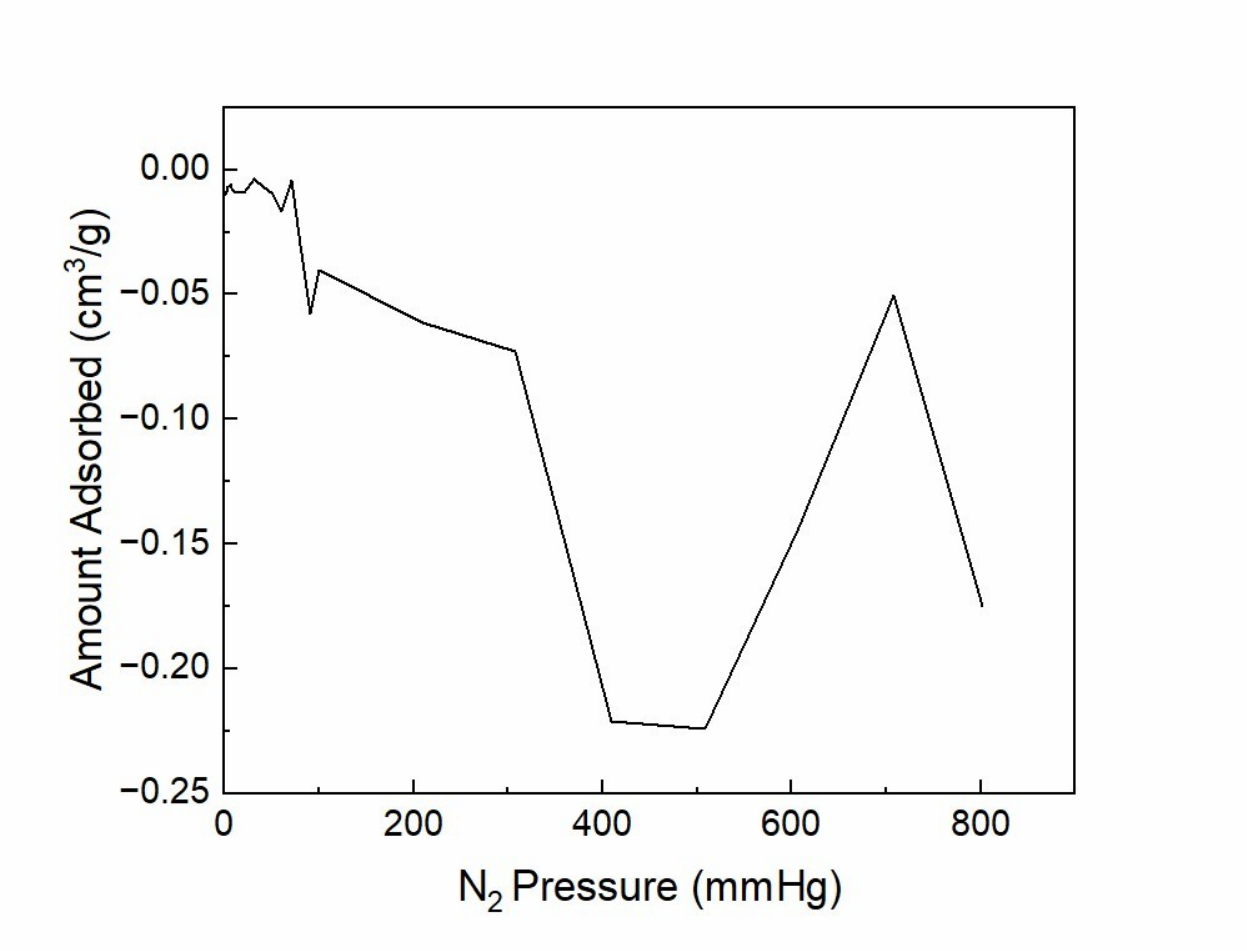

Figure S53. 12%Ni/4%Yb/12%Cs/Al_2O_3 N_2 chemisorption at 450°C.

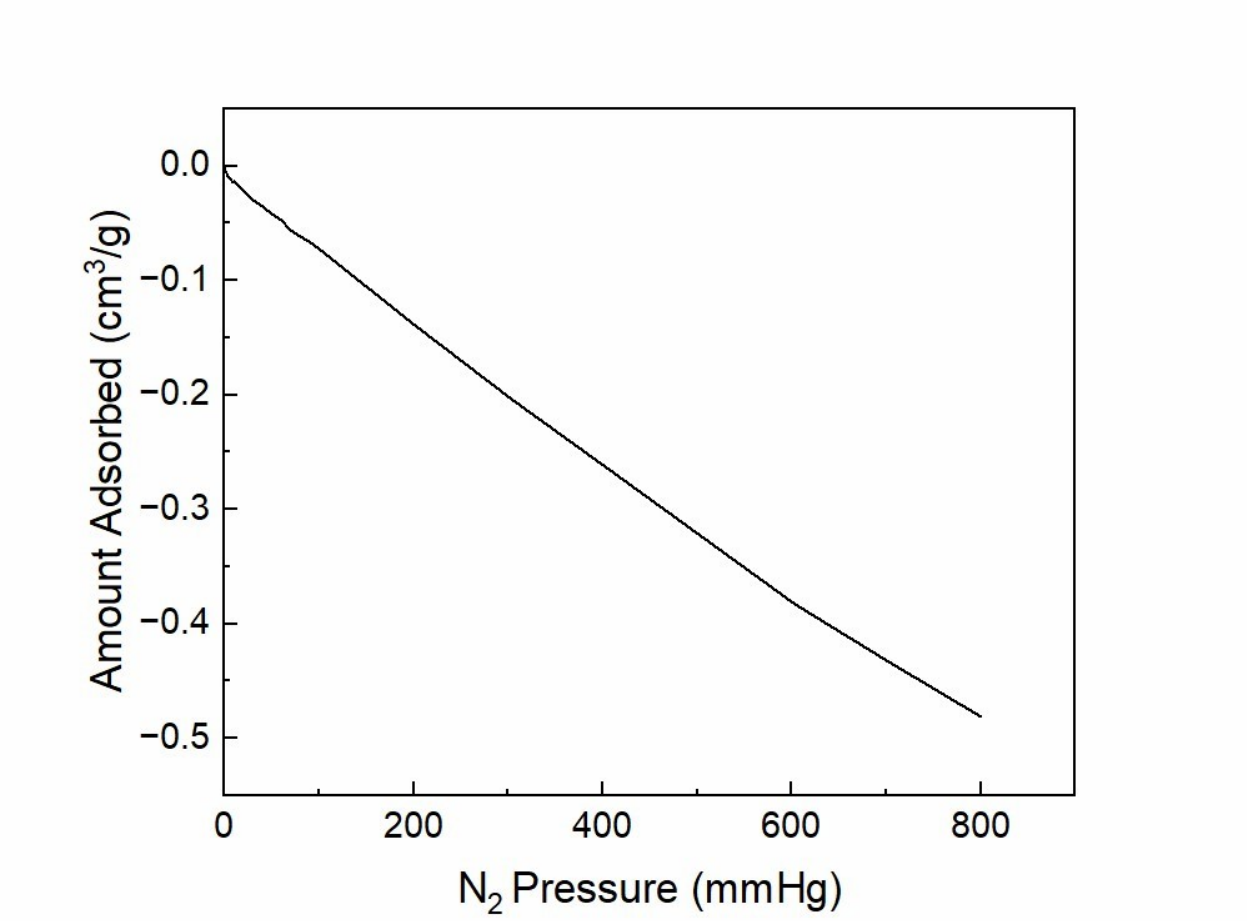

Figure S54. 12%Ni/4%Yb/12%Ca/Al_2O_3 N_2 chemisorption at 25°C.

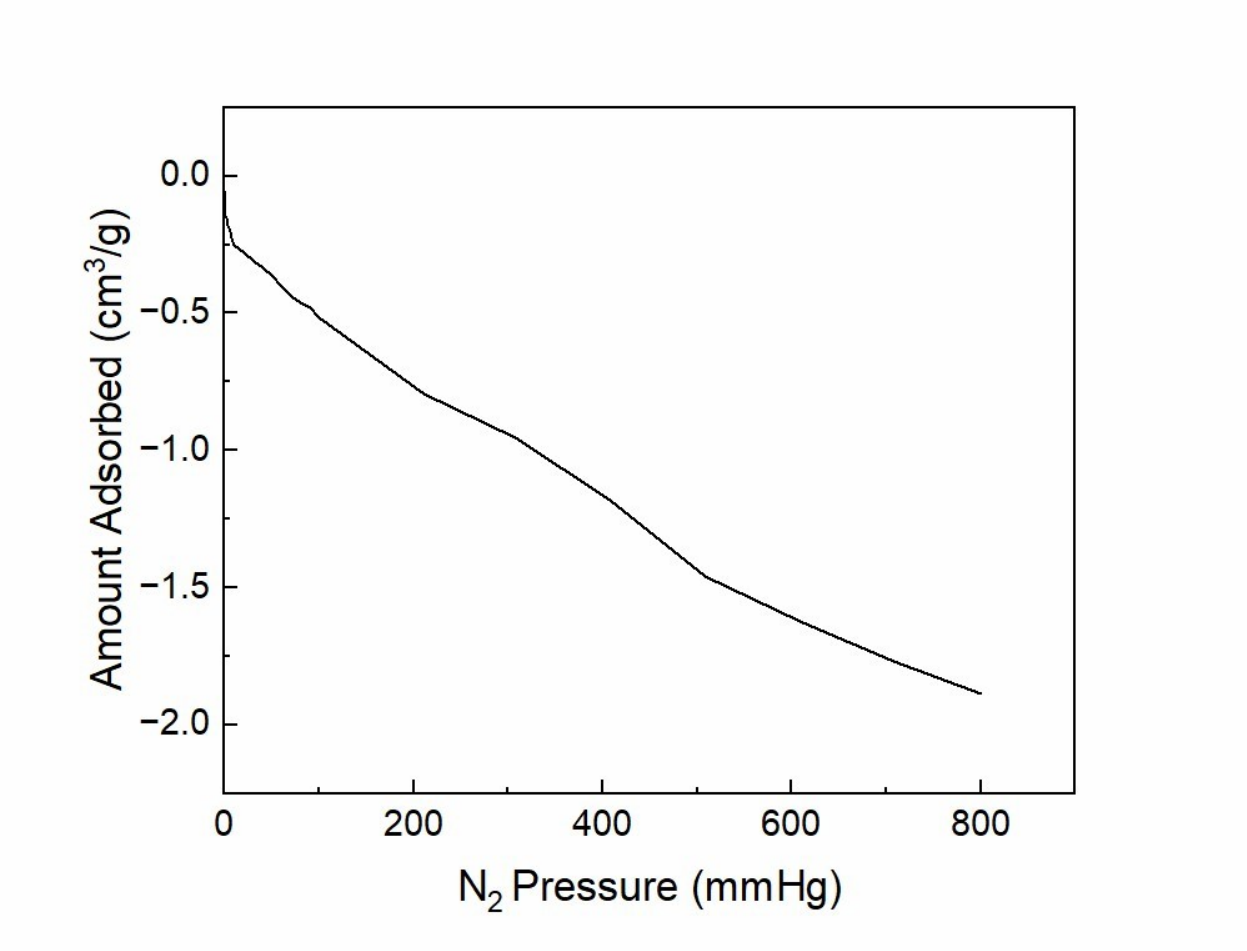

Figure S55. 12%Ni/4%Yb/12%Ca/Al_2O_3 N_2 chemisorption at 450°C.

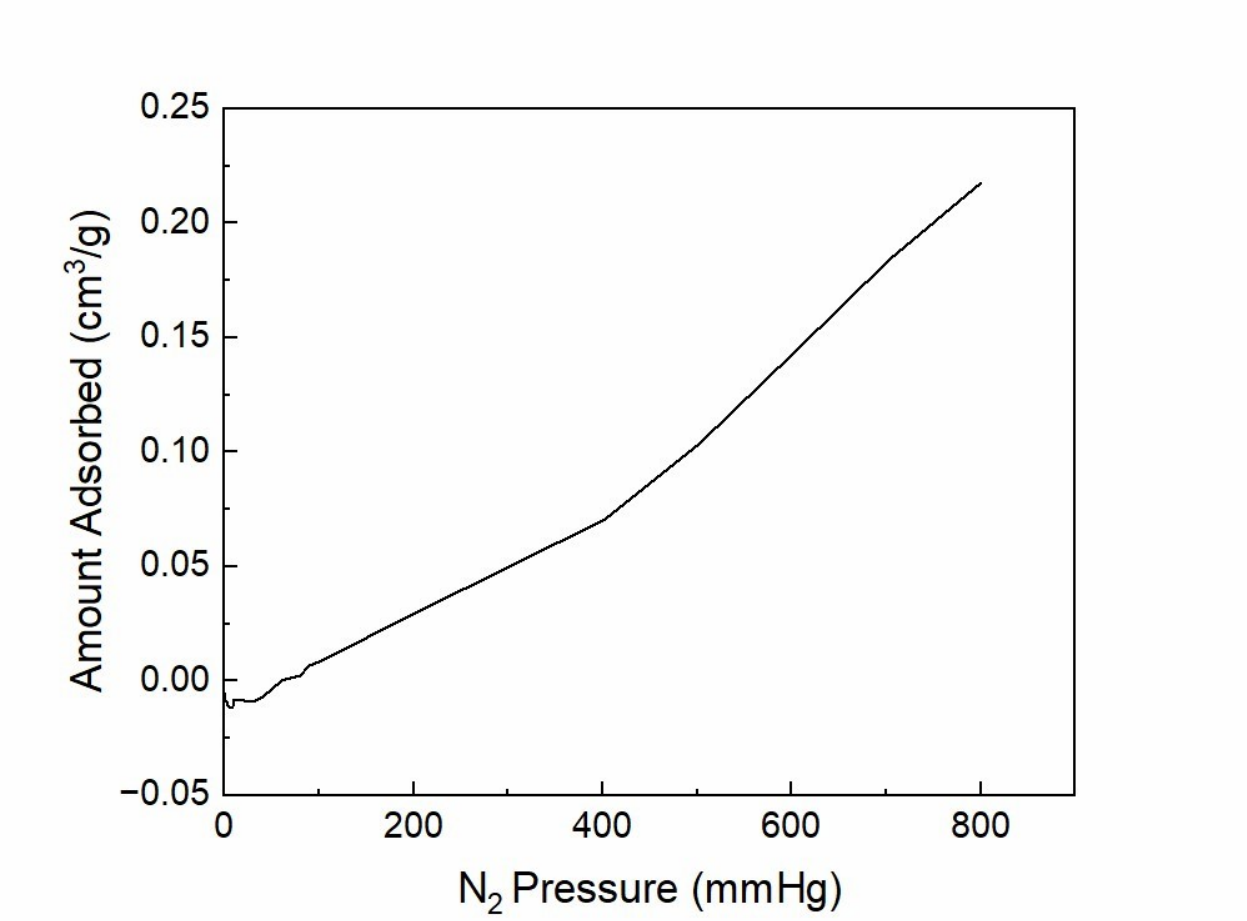

Figure S56. 12%Ni/4%Yb/12%Sr/Al_2O_3 N_2 chemisorption at 25°C.

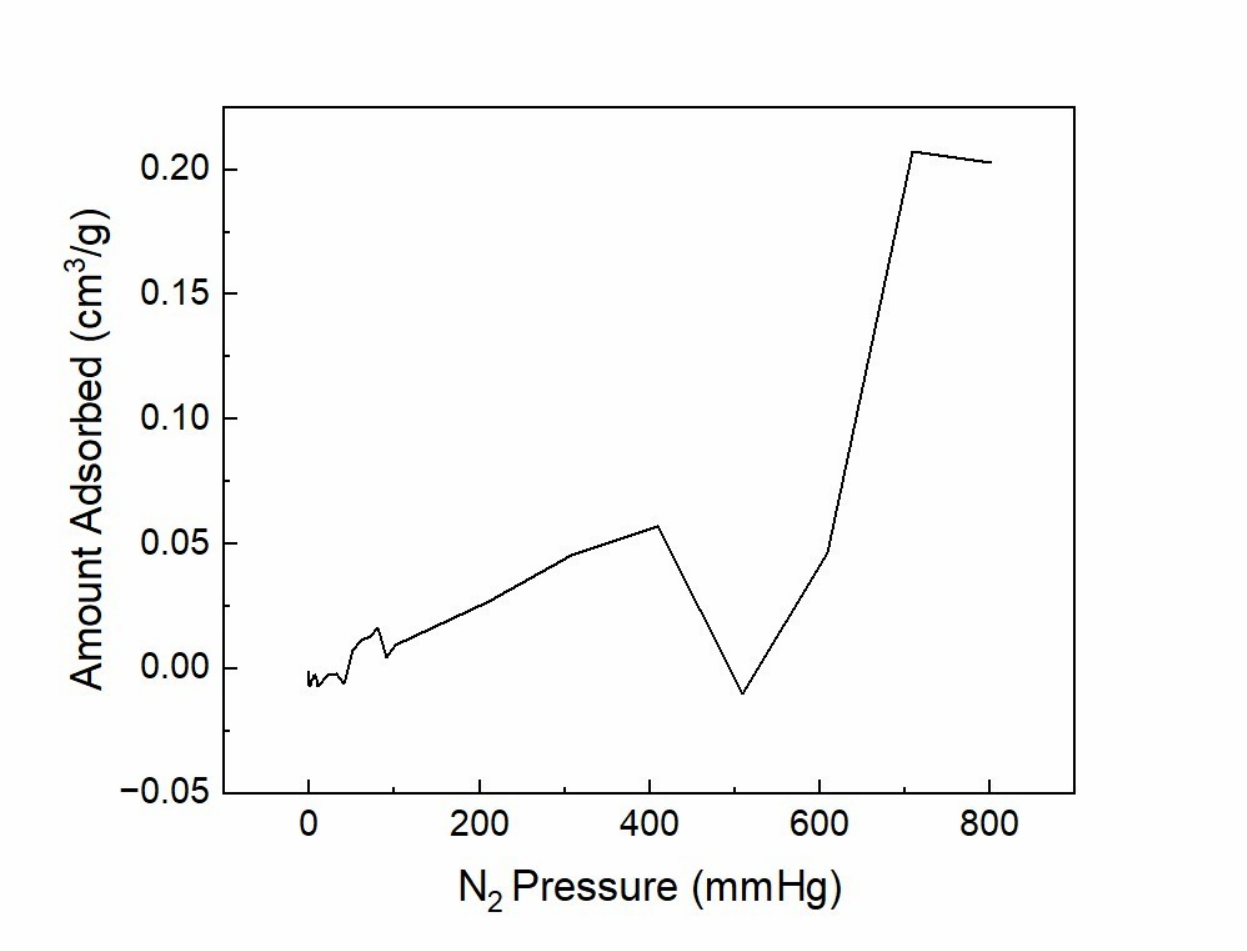

Figure S57. 12%Ni/4%Yb/12%Sr/Al_2O_3 N_2 chemisorption at 450°C.

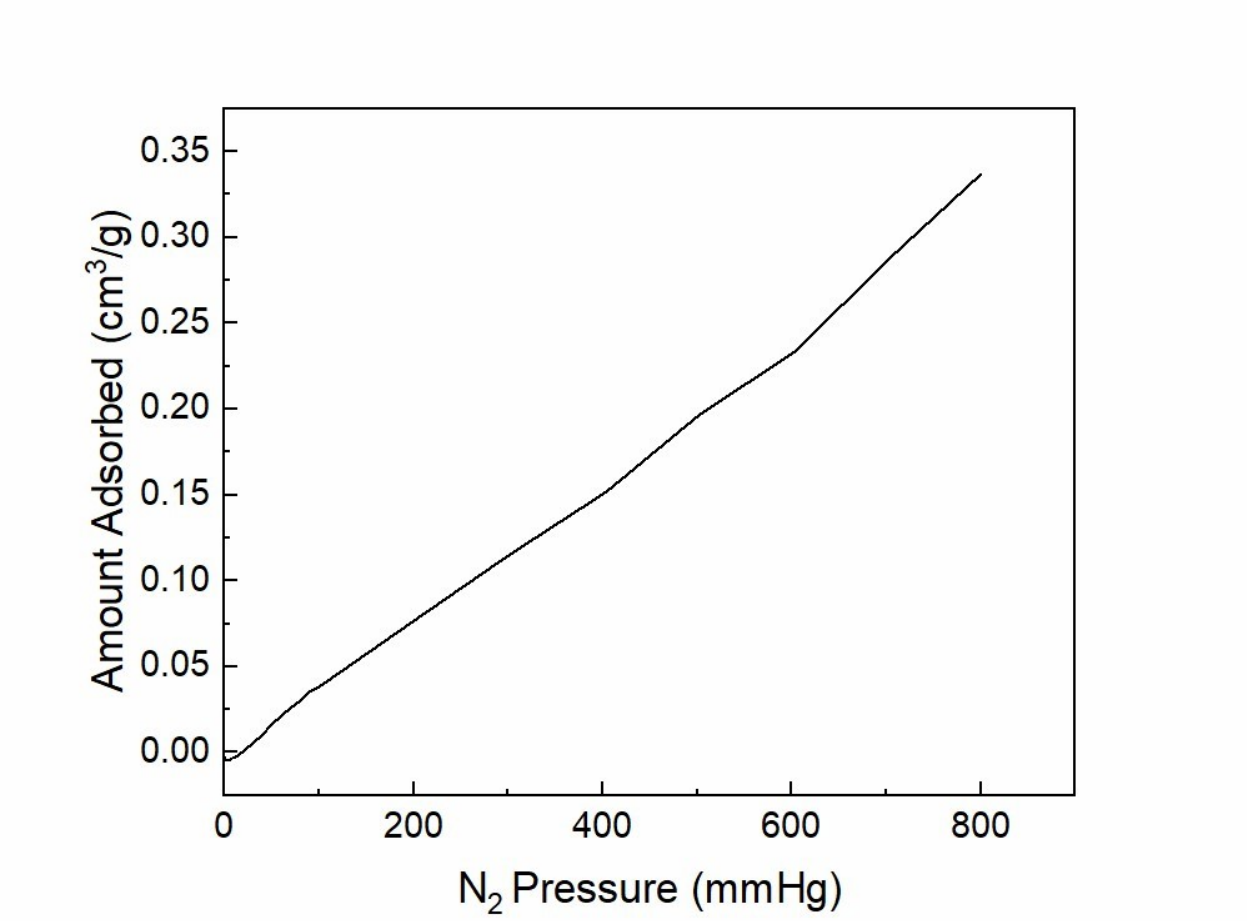

Figure S58. 12%Ni/4%Yb/12%Ba/Al_2O_3 N_2 chemisorption at 25°C.

Figure S59. 12%Ni/4%Yb/12%Ba/Al_2O_3 N_2 chemisorption at 450°C.

CO Chemisorption Data

Table S16. Median pore size and volume in pores calculated from CO chemisorption.

Sample	CO Adsorbed (mL/g)
12%Ni/4%Yb/12%Na/Al_2O_3	0.72
12%Ni/4%Yb/12%K/Al_2O_3	11.98
12%Ni/4%Yb/12%Rb/Al_2O_3	1.42
12%Ni/4%Yb/12%Cs/Al_2O_3	1.47
12%Ni/4%Yb/12%Ca/Al_2O_3	3.45
12%Ni/4%Yb/12%Sr/Al_2O_3	4.07
12%Ni/4%Yb/12%Ba/Al_2O_3	7.16
12%Ni/Al_2O_3	7.47
Al_2O_3	1.32

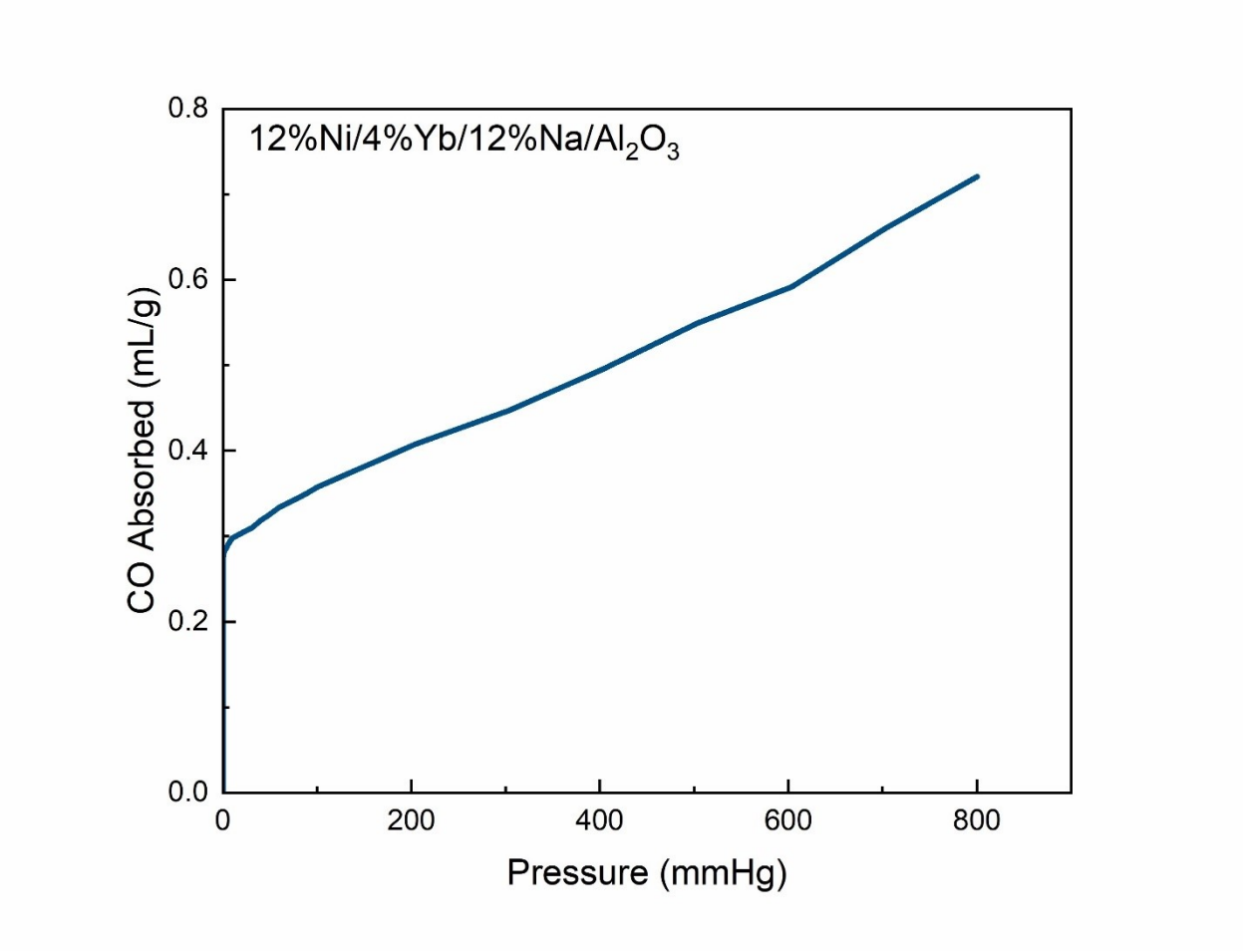

Figure S60. CO chemisorption data of the 12%Ni/4%Yb/12%Na/Al_2O_3 catalyst.

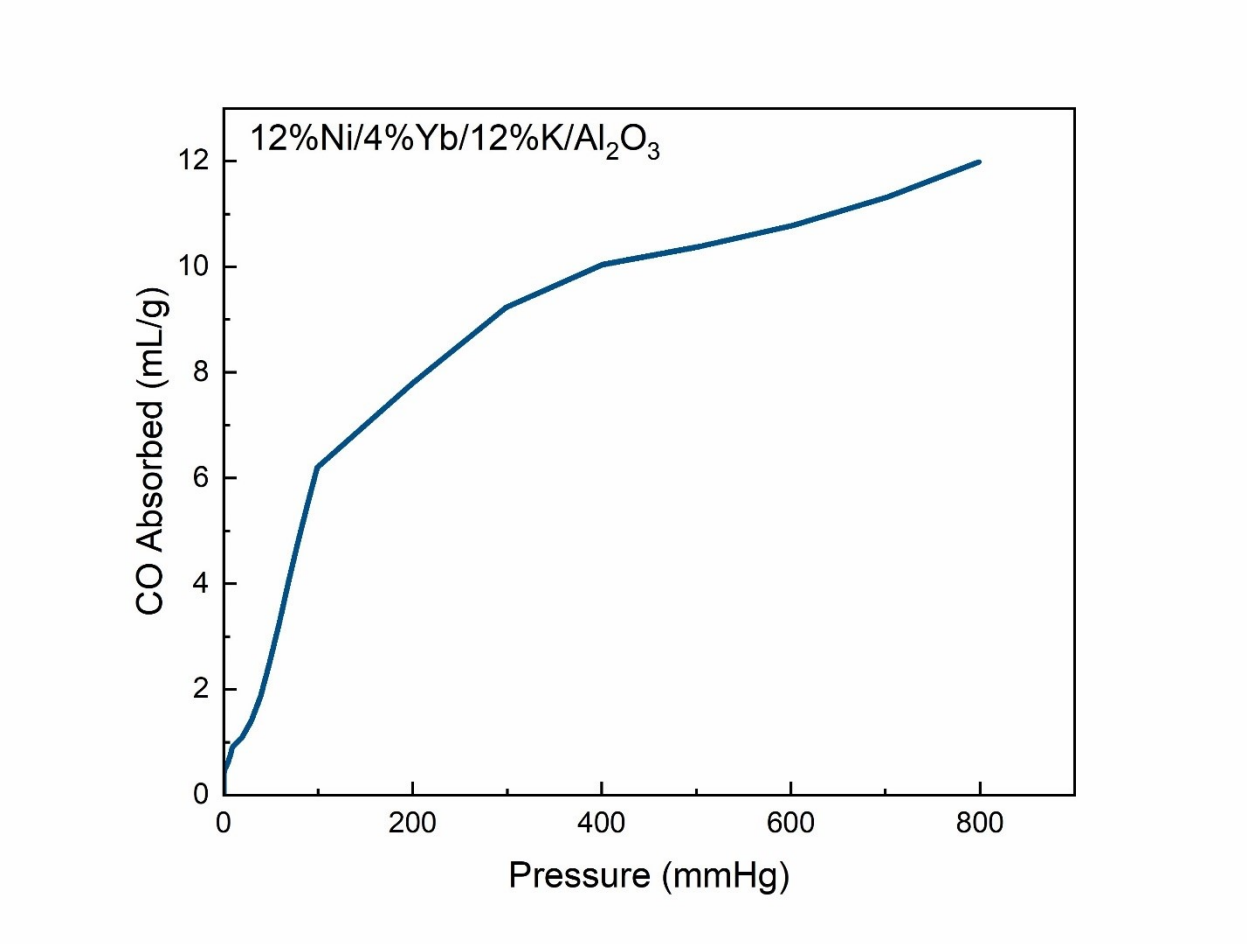

Figure S61. CO chemisorption data of the 12%Ni/4%Yb/12%K/Al_2O_3 catalyst.

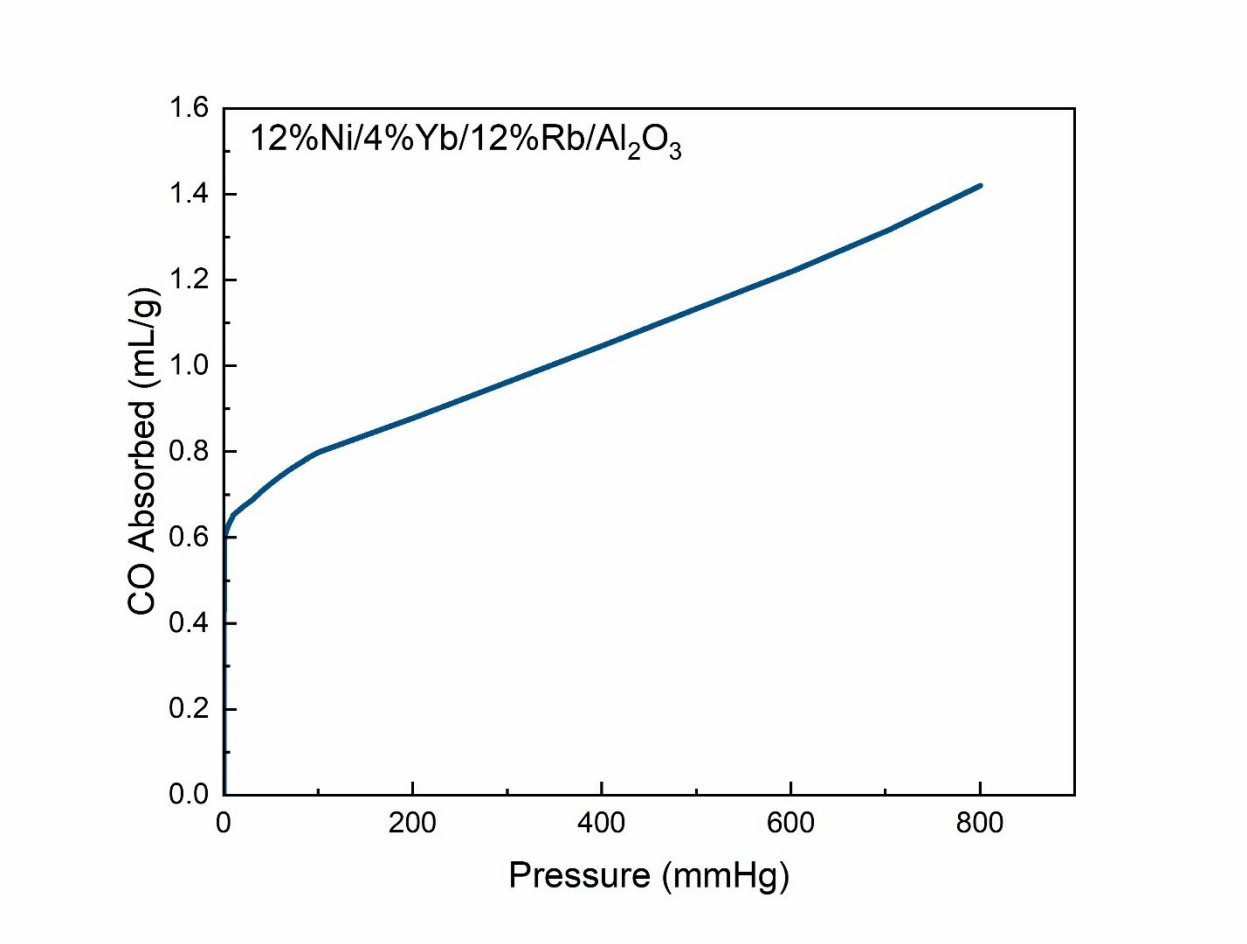

Figure S62. CO chemisorption data of the 12%Ni/4%Yb/12%Rb/Al_2O_3 catalyst.

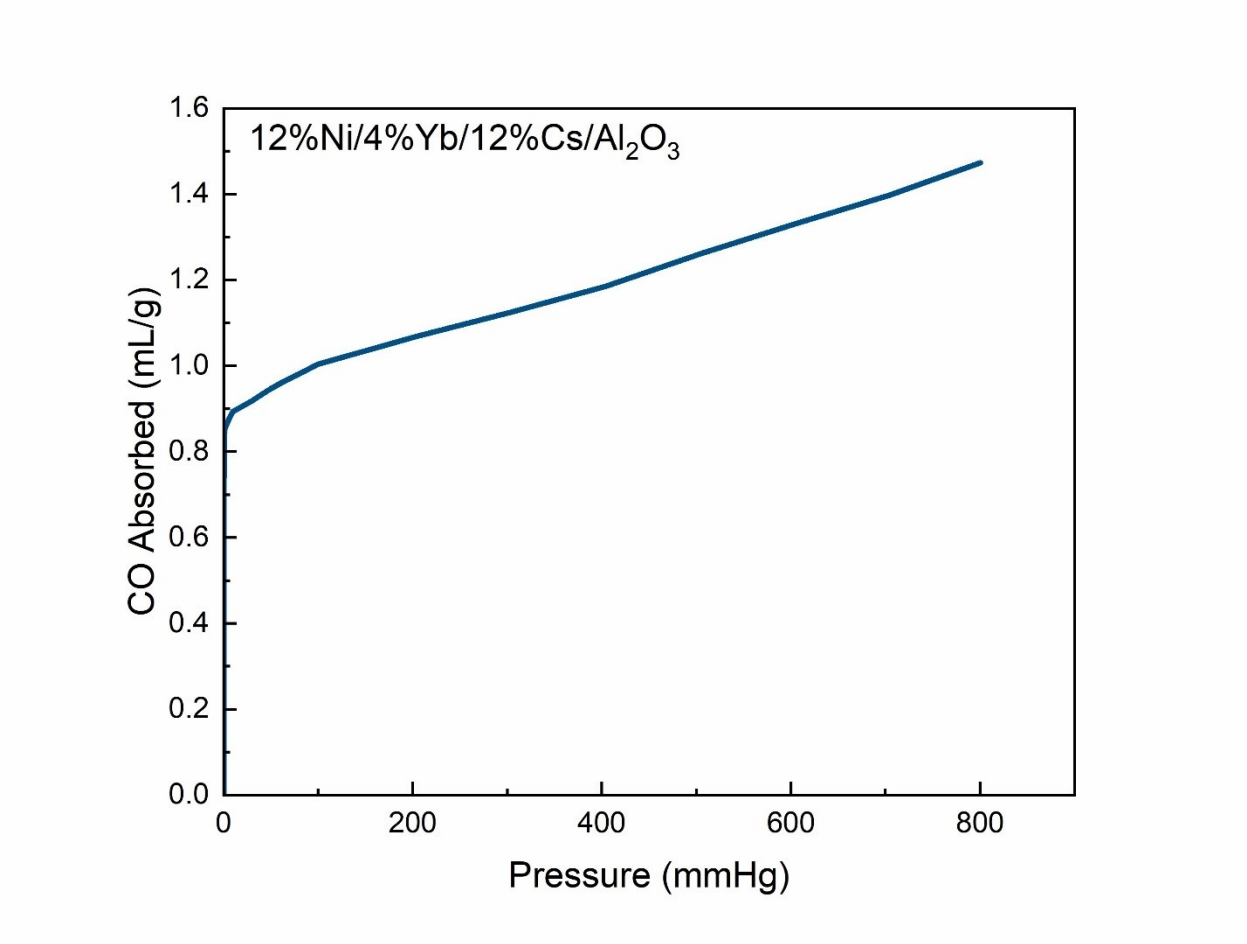

Figure S63. CO chemisorption data of the 12%Ni/4%Yb/12%Cs/Al_2O_3 catalyst.

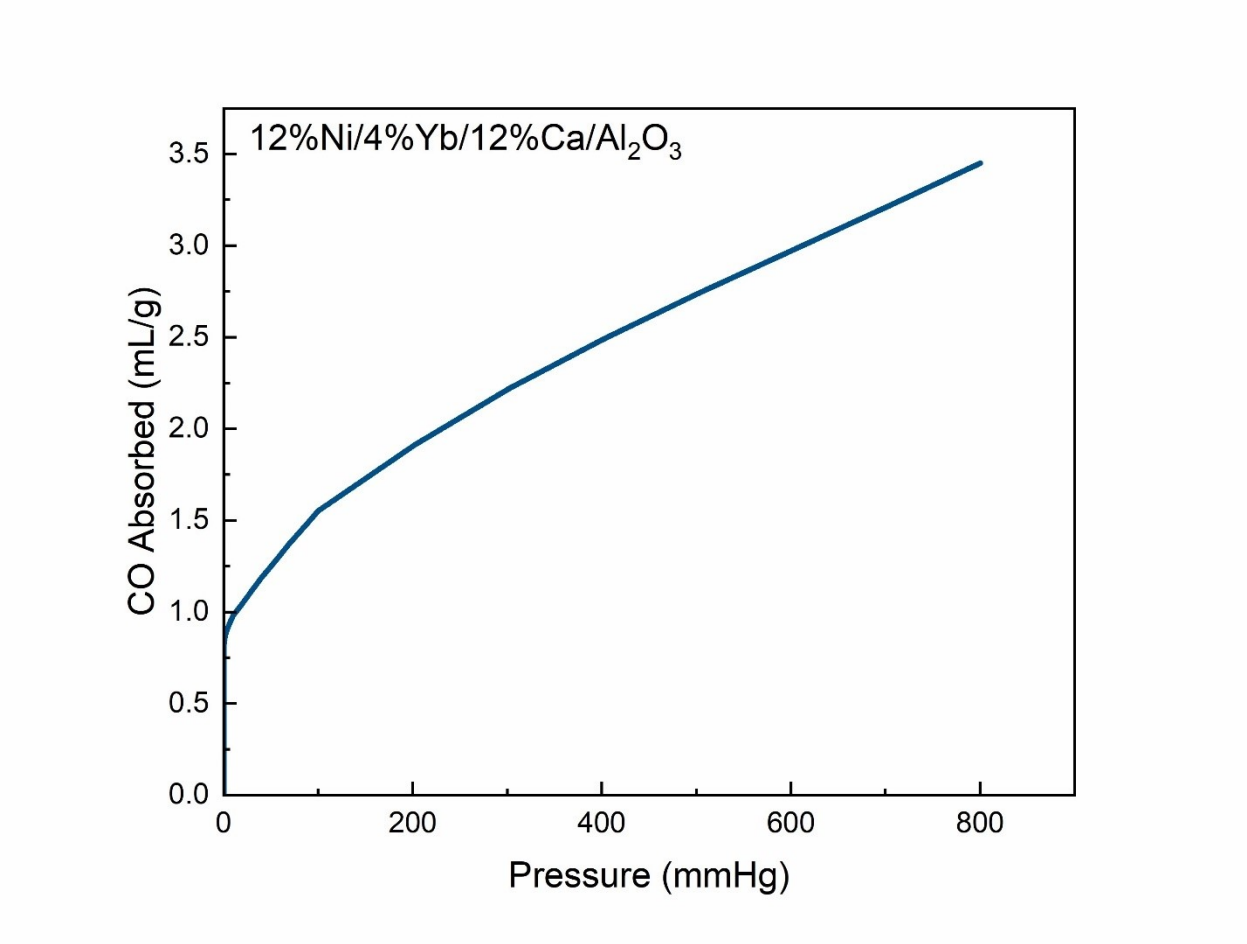

Figure S64. CO chemisorption data of the 12%Ni/4%Yb/12%Ca/Al_2O_3 catalyst.

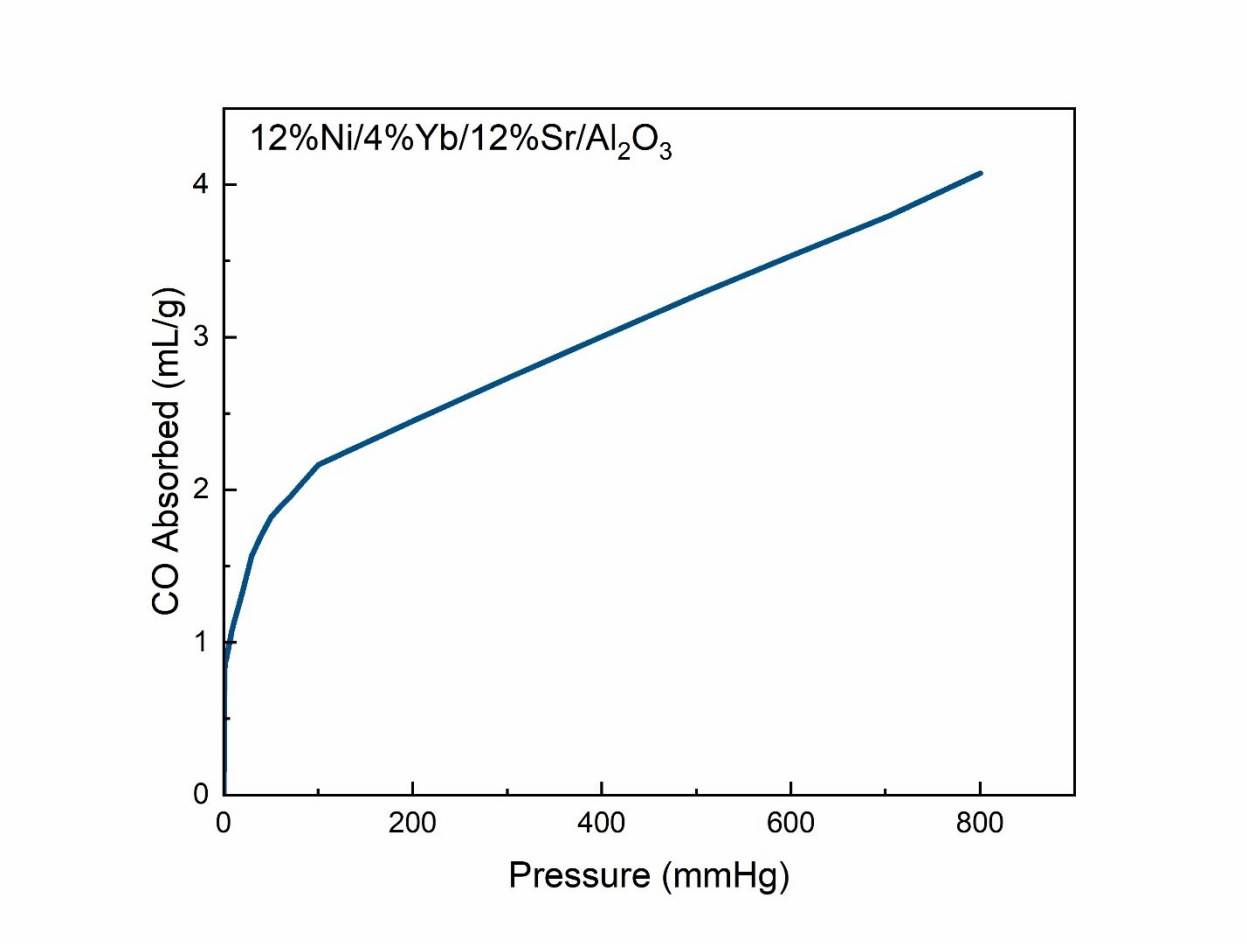

Figure S65. CO chemisorption data of the 12%Ni/4%Yb/12%Sr/Al_2O_3 catalyst.

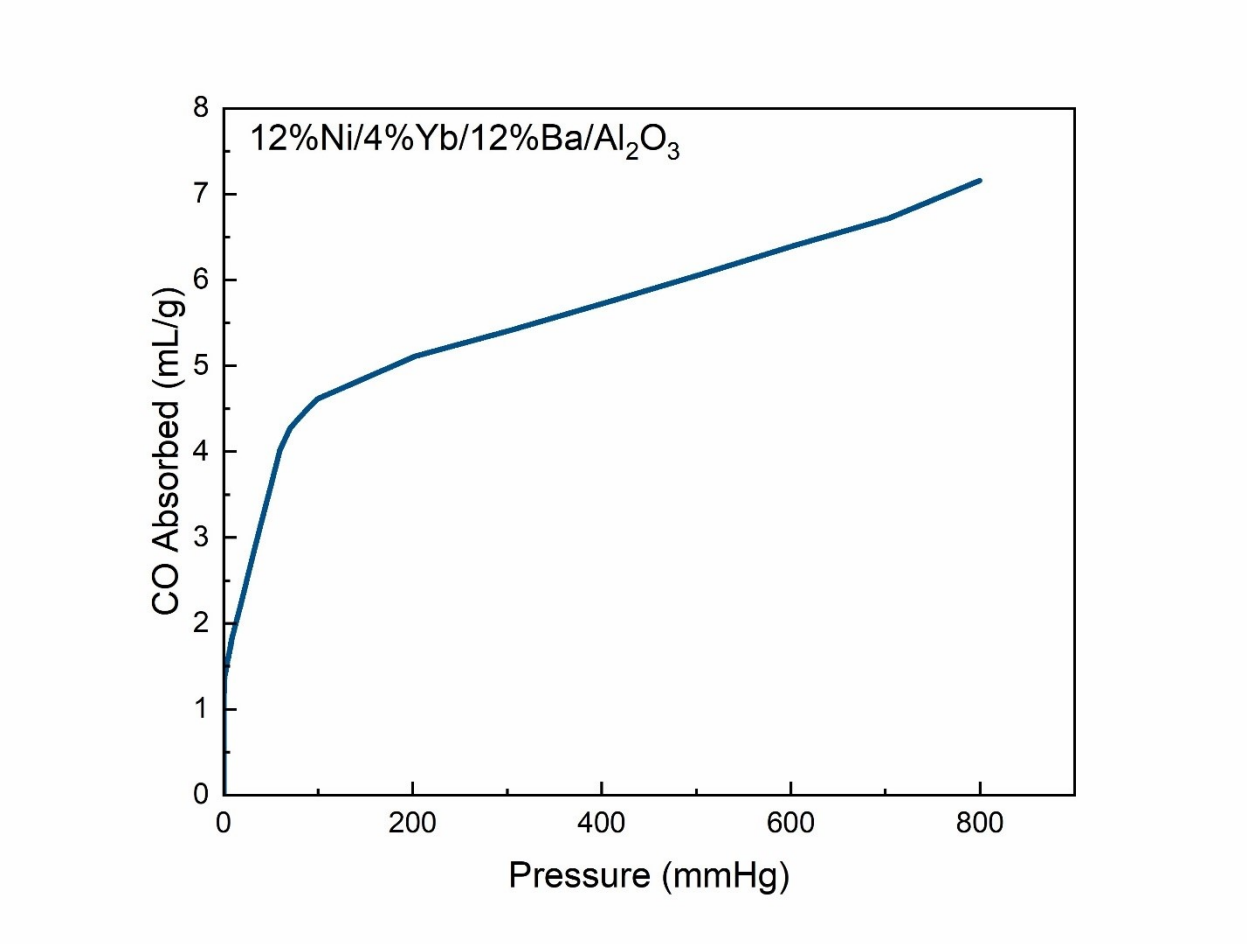

Figure S66. CO chemisorption data of the 12%Ni/4%Yb/12%Ba/Al_2O_3 catalyst.

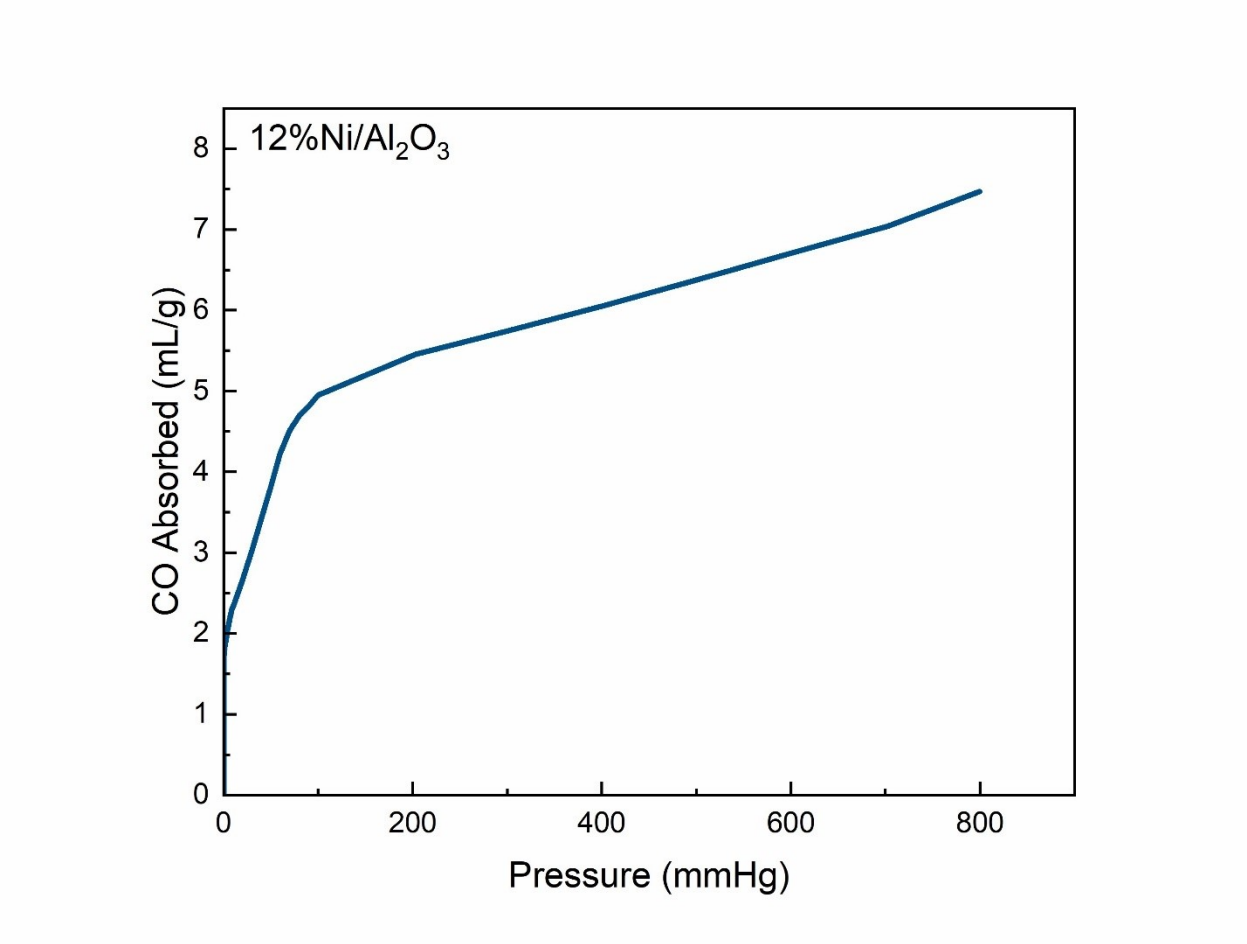

Figure S67. DR CO chemisorption data of the 12%Ni/Al_2O_3 catalyst.

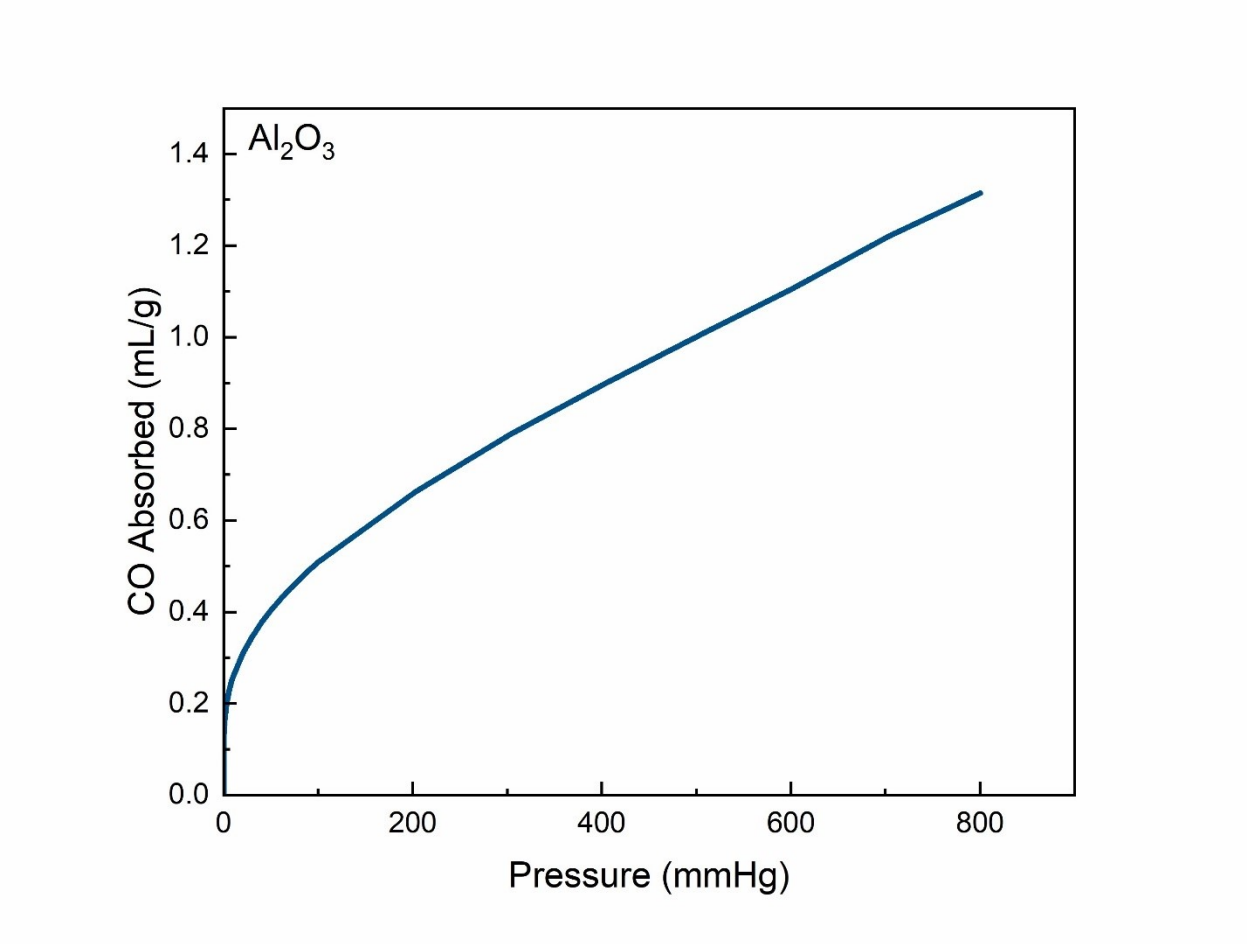

Figure S68. CO chemisorption data of the Al_2O_3 support.

X-Ray Photoelectron Spectroscopy (XPS) Data

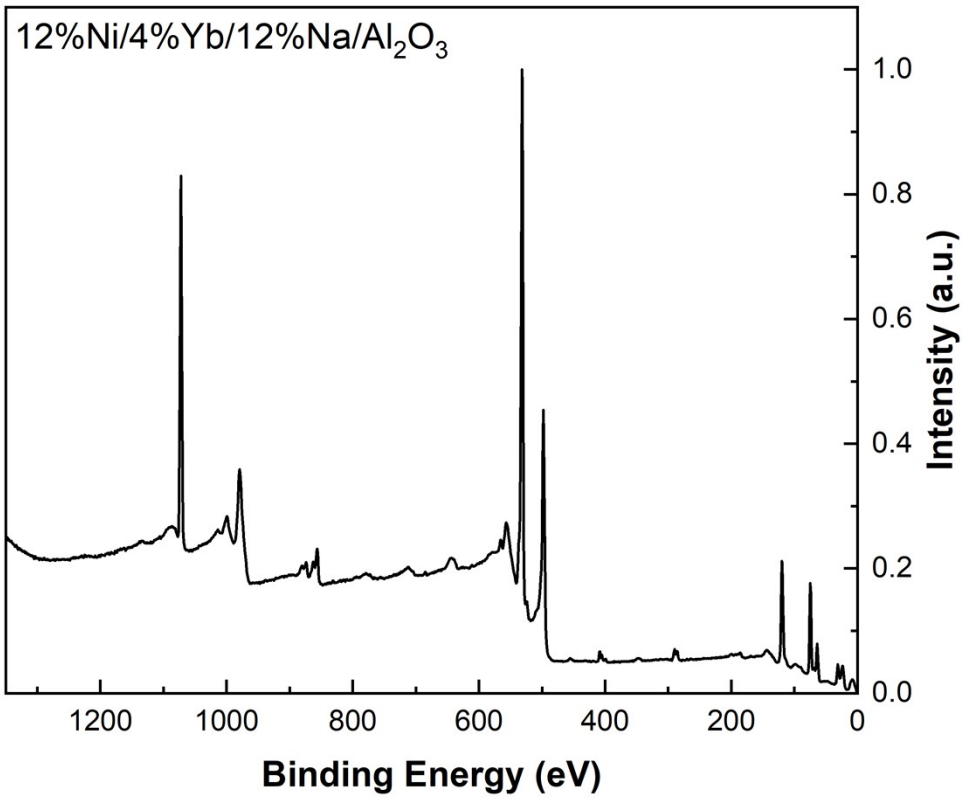

Figure S69. XPS spectrum of the 12%Ni/4%Yb/12%Na/Al_2O_3 catalyst.

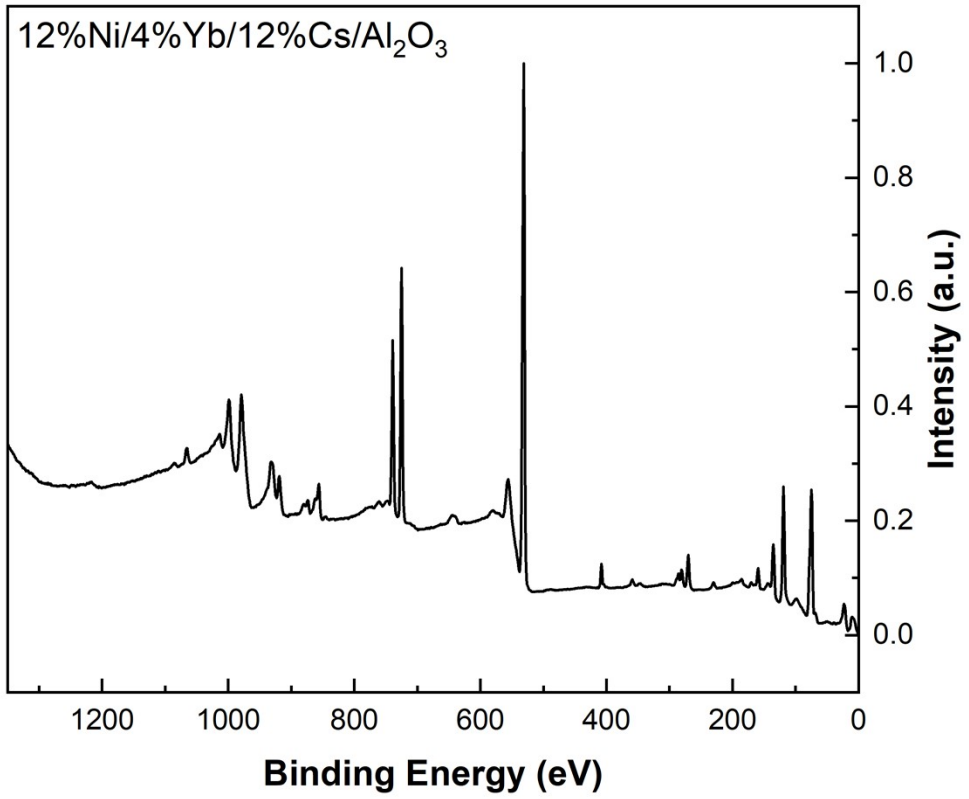

Figure S70. XPS spectrum of the 12%Ni/4%Yb/12%Cs/Al_2O_3 catalyst.

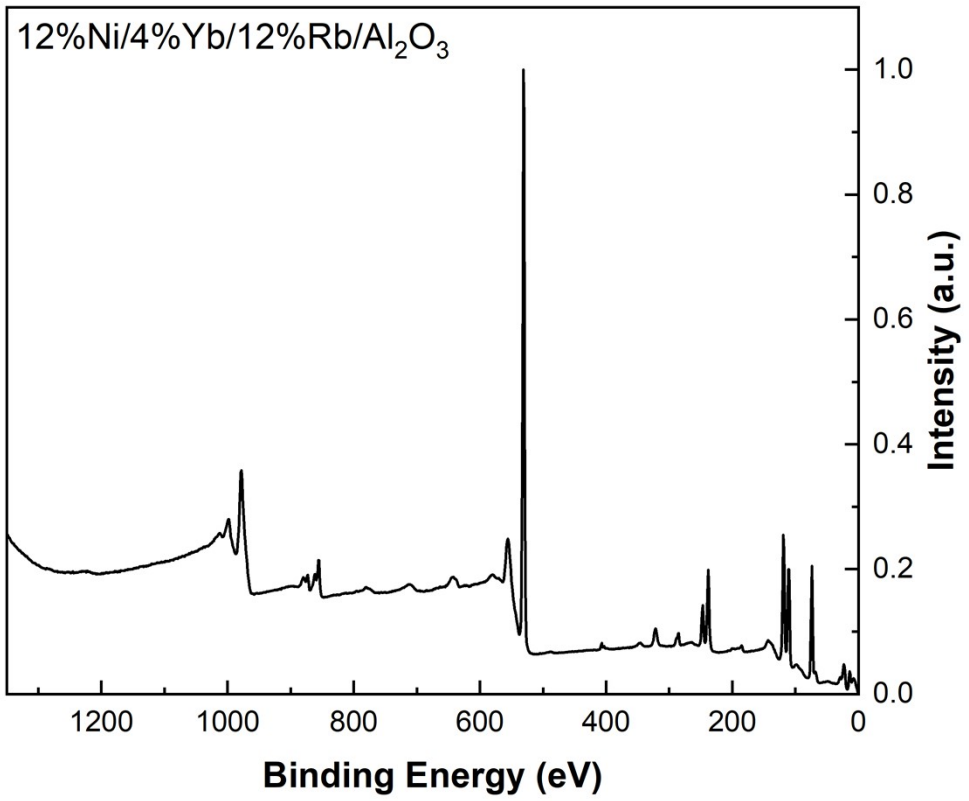

Figure S71. XPS spectrum of the 12%Ni/4%Yb/12%Rb/Al_2O_3 catalyst.

Figure S72. XPS spectrum of the 12%Ni/4%Yb/12%Cs/Al_2O_3 catalyst.

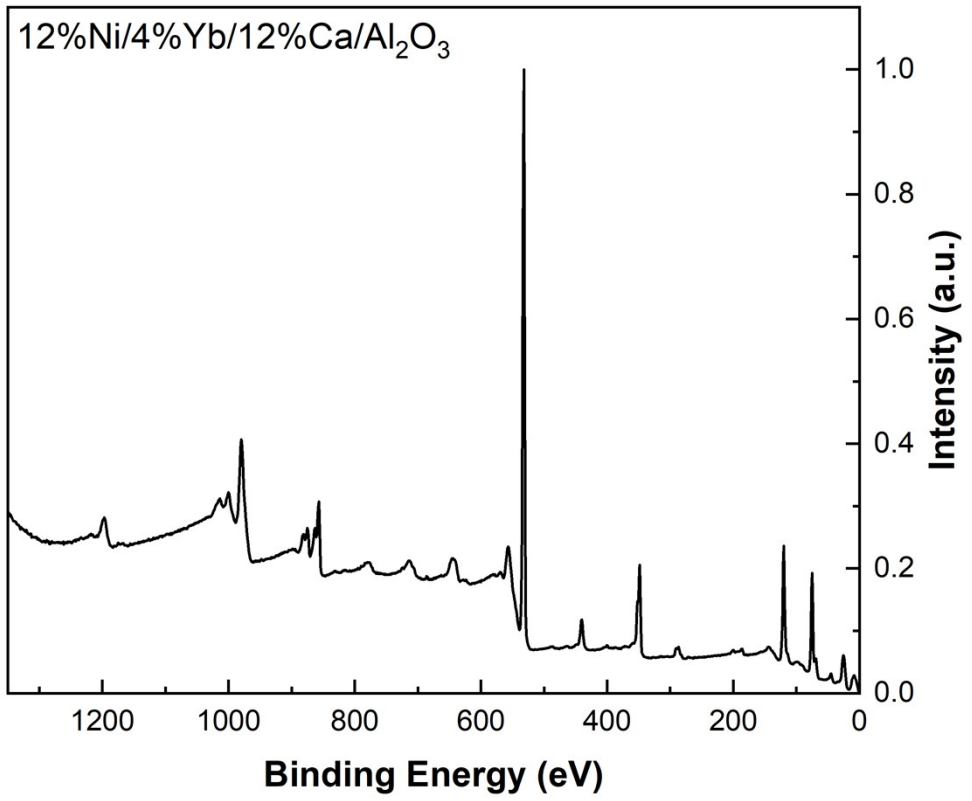

Figure S73. XPS spectrum of the 12%Ni/4%Yb/12%Ca/Al_2O_3 catalyst.

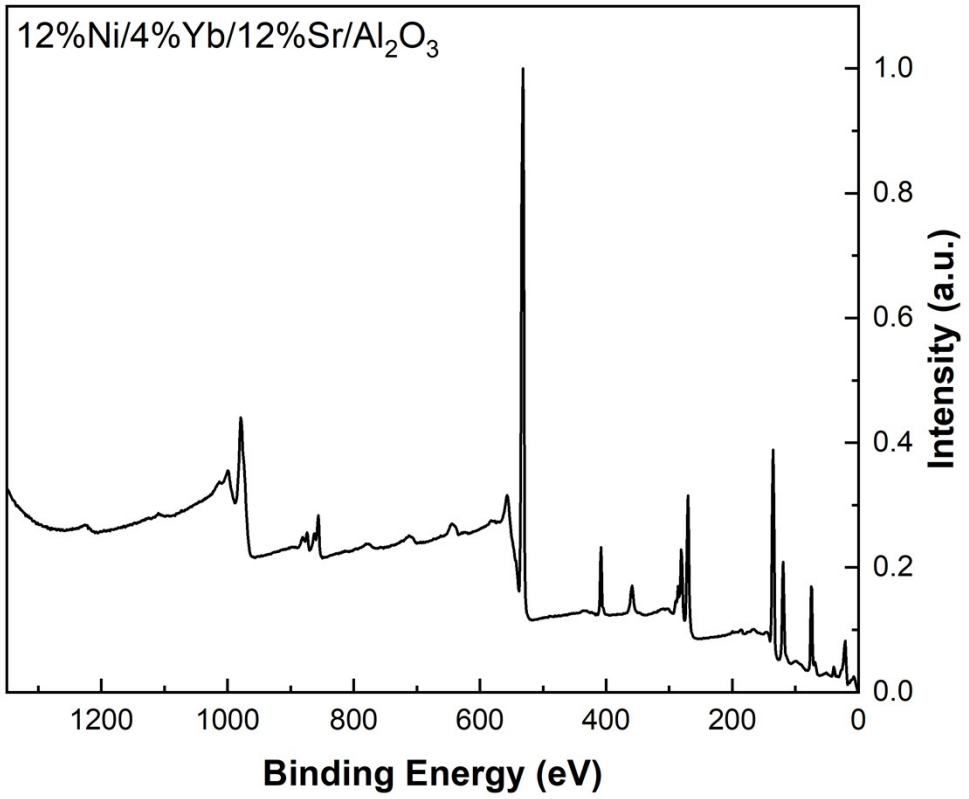

Figure S74. XPS spectrum of the 12%Ni/4%Yb/12%Sr/Al_2O_3 catalyst.

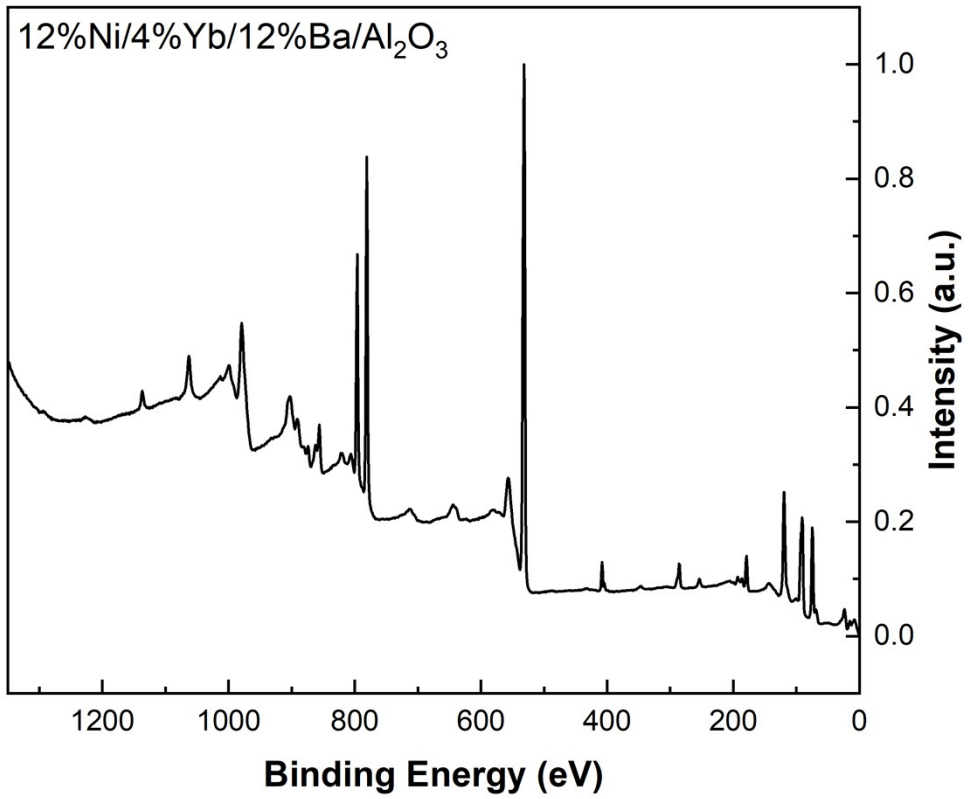

Figure S75. XPS spectrum of the 12%Ni/4%Yb/12%Ba/Al_2O_3 catalyst.

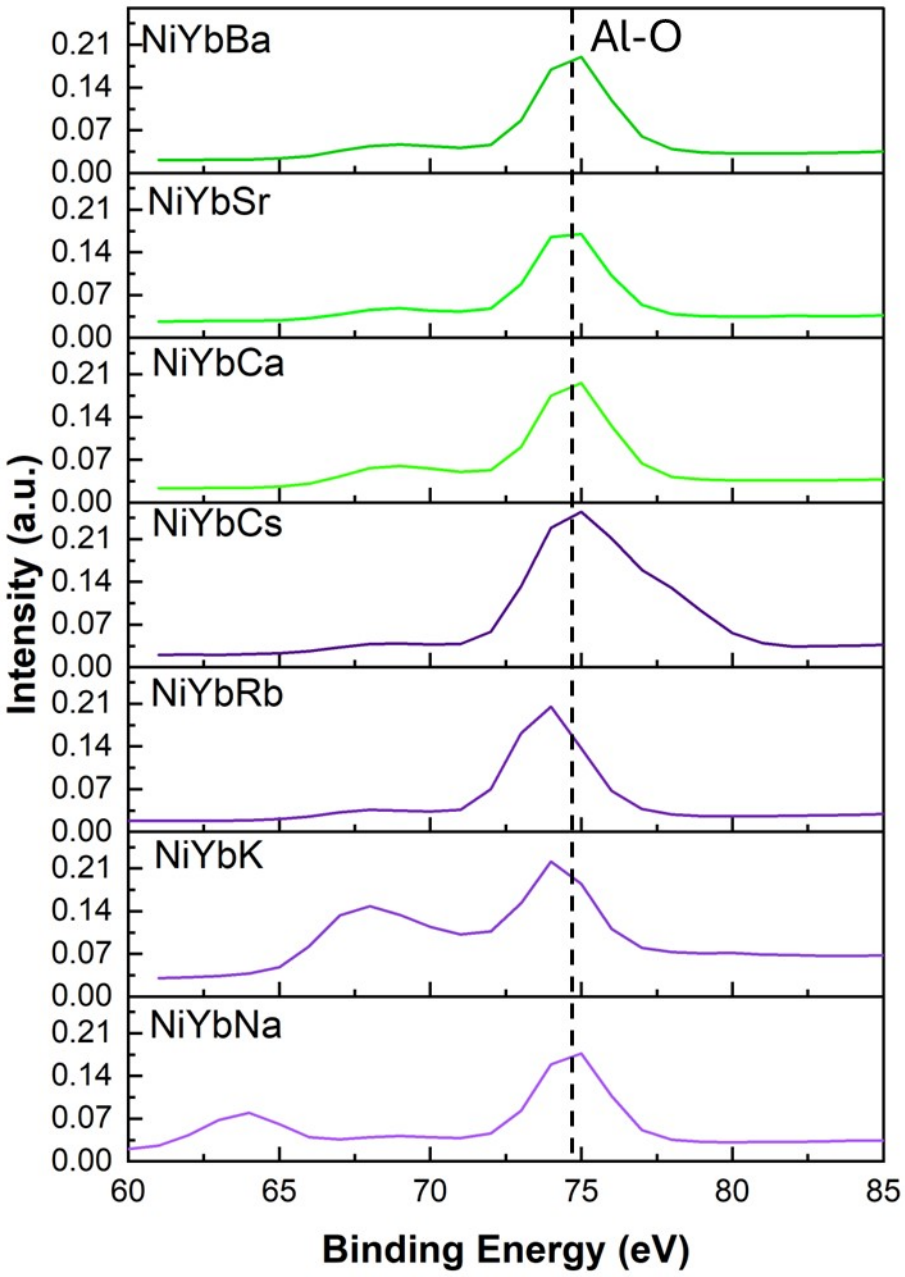

Figure S76. Comparison of the alumina peaks in the XPS spectrum across the seven NiYbM catalysts.

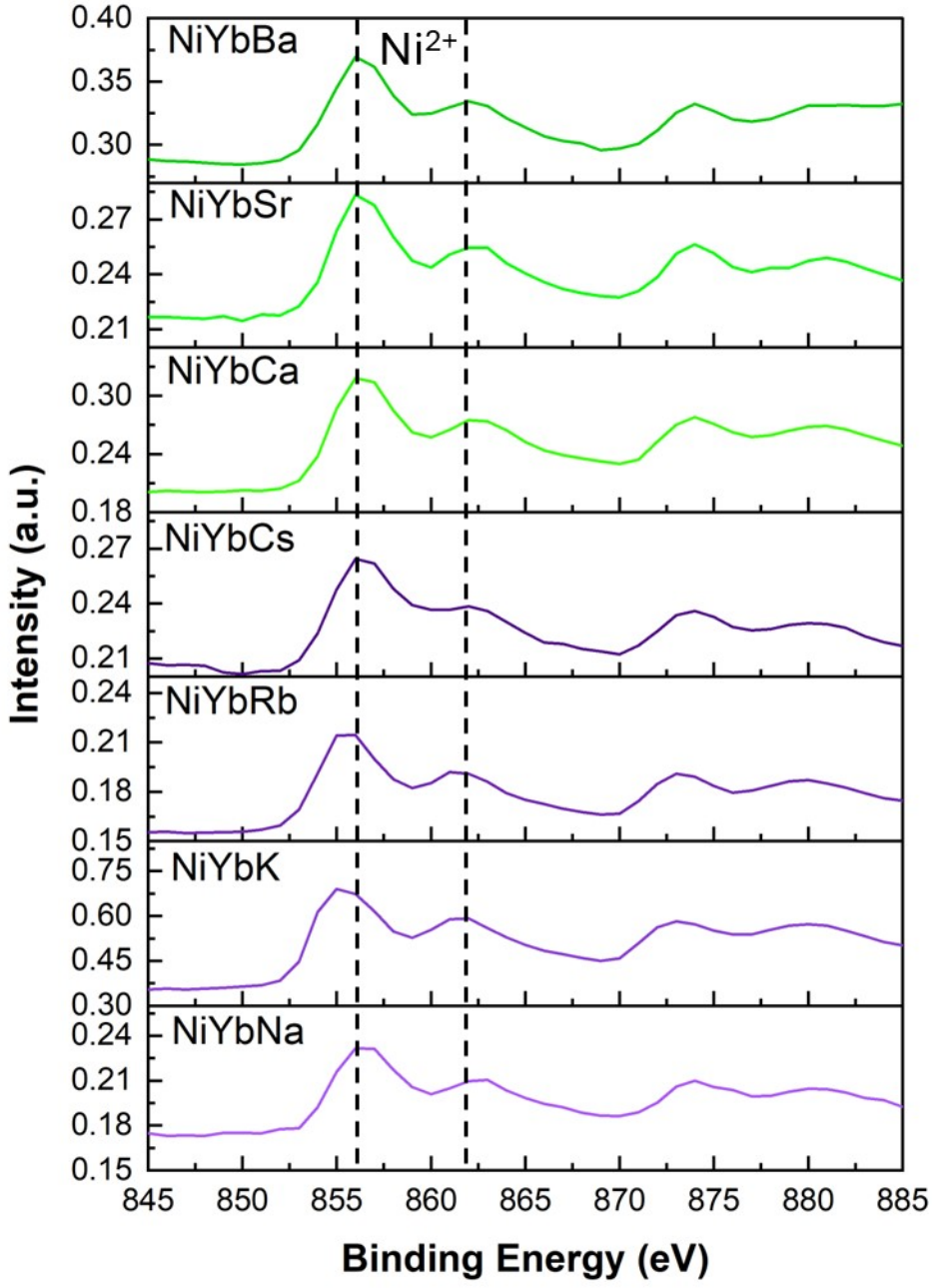

Figure S77. Comparison of the nickel peaks in the XPS spectrum across the seven NiYbM catalysts.

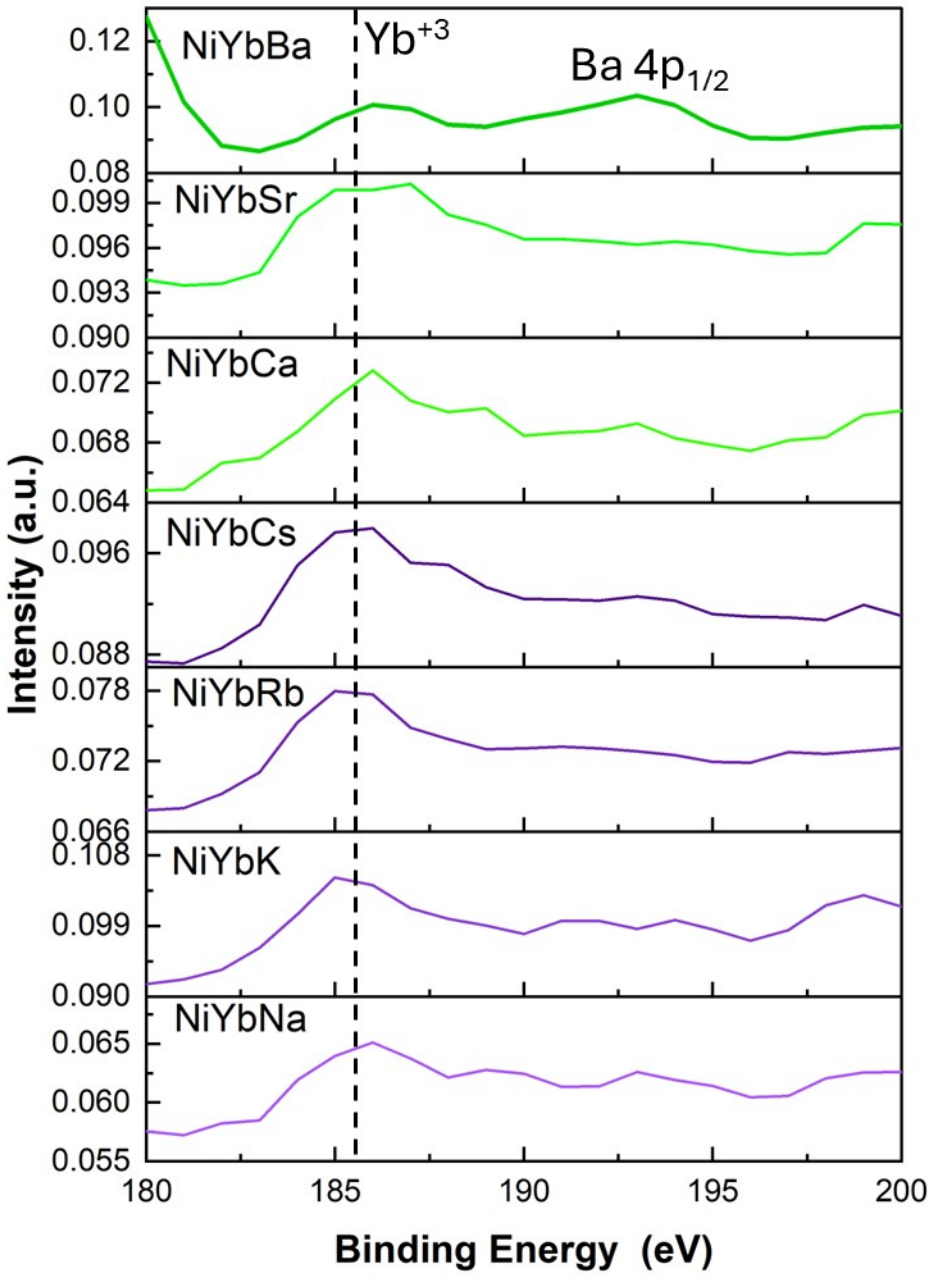

Figure S78. Comparison of the ytterbium peaks in the XPS spectrum across the seven NiYbM catalysts.

CO DRIFTS Data

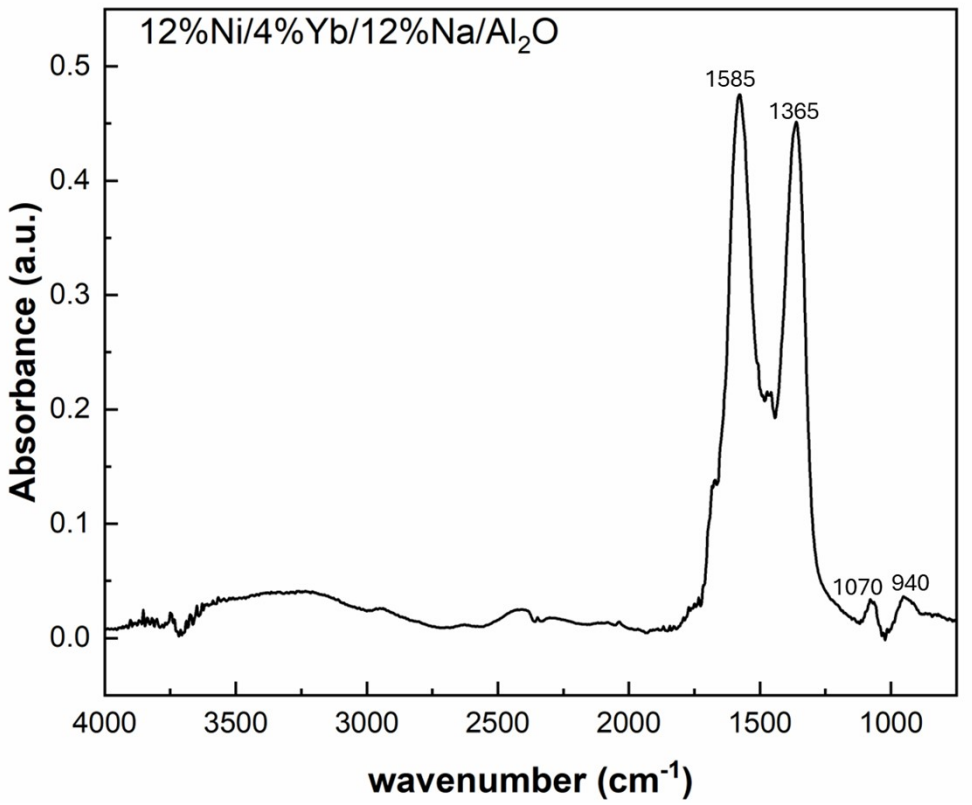

Figure S79. DRIFTS spectrum of the 12%Ni/4%Yb/12%Na/Al_2O_3 catalyst with CO adsorbed on the catalyst.

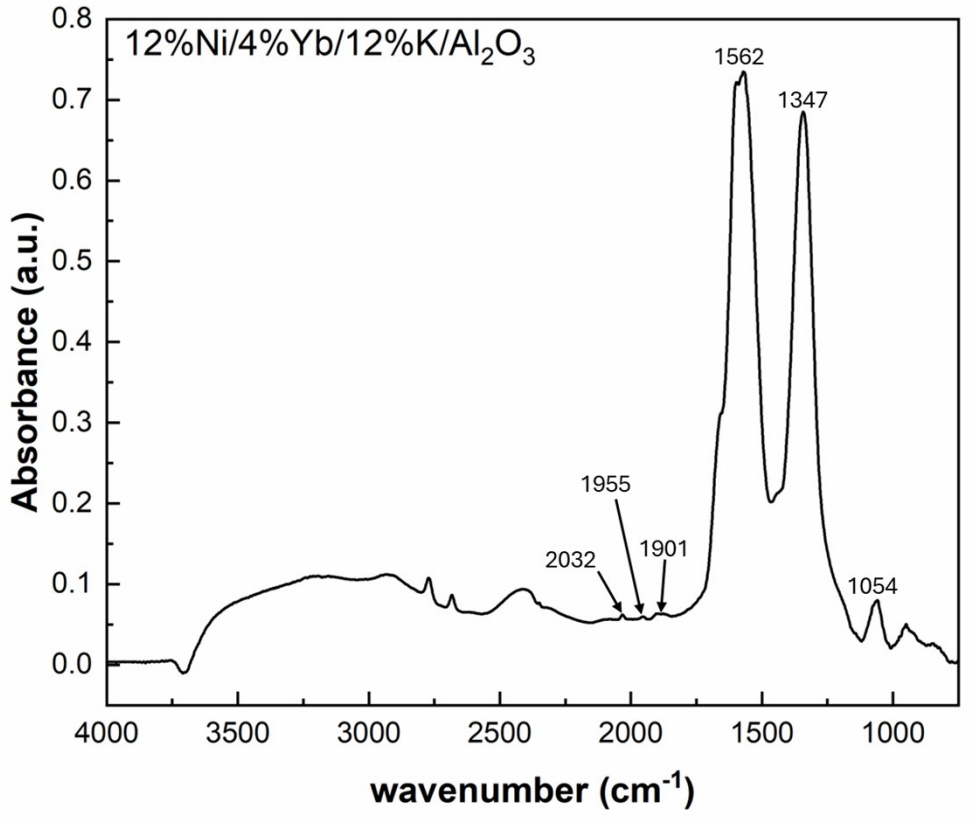

Figure S80. DRIFTS spectrum of the 12%Ni/4%Yb/12%K/Al_2O_3 catalyst with CO adsorbed on the catalyst.

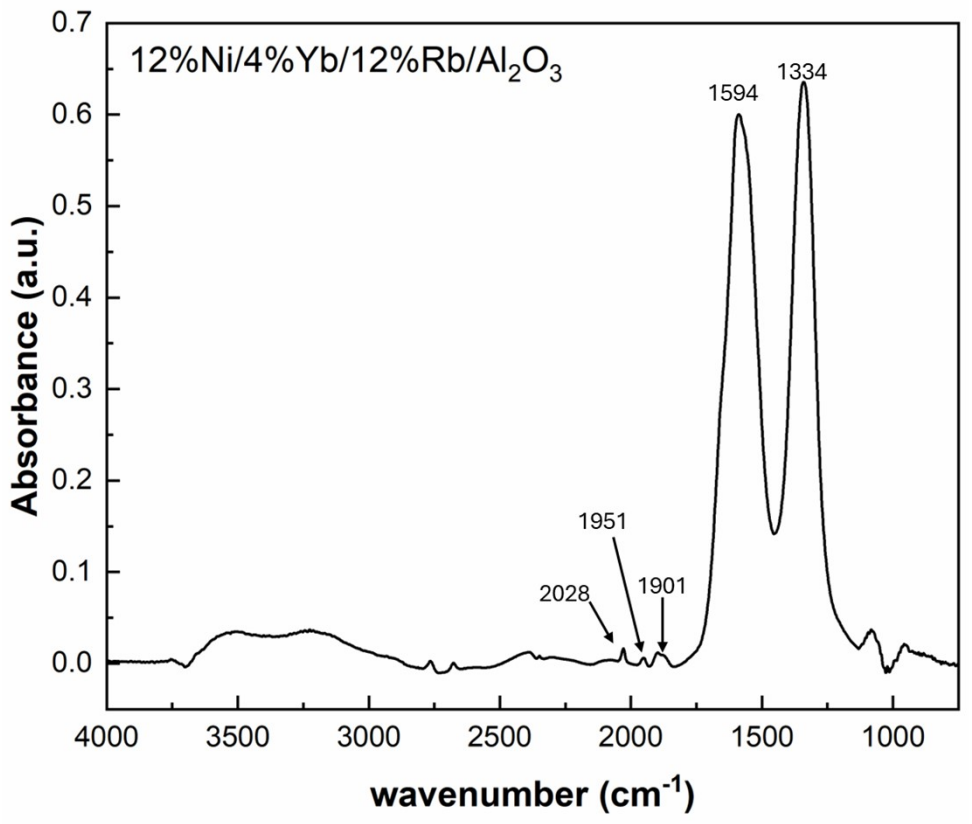

Figure S81. DRIFTS spectrum of the 12%Ni/4%Yb/12%Rb/Al_2O_3 catalyst with CO adsorbed on the catalyst.

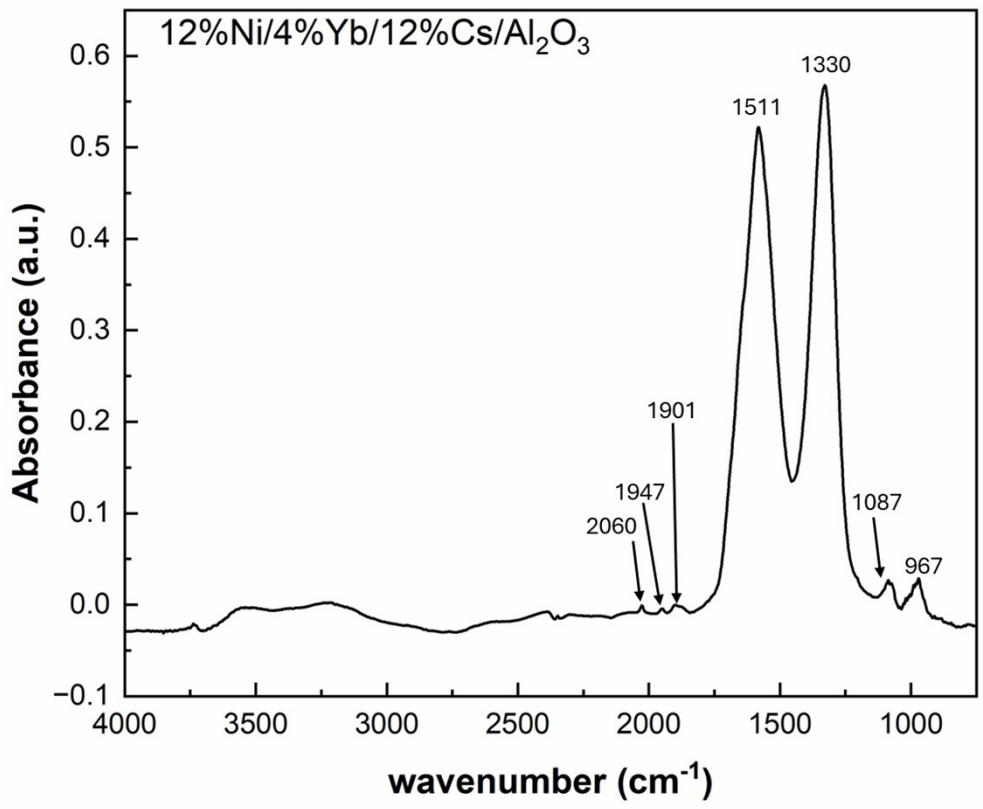

Figure S82. DRIFTS spectrum of the 12%Ni/4%Yb/12%Cs/Al_2O_3 catalyst with CO adsorbed on the catalyst.

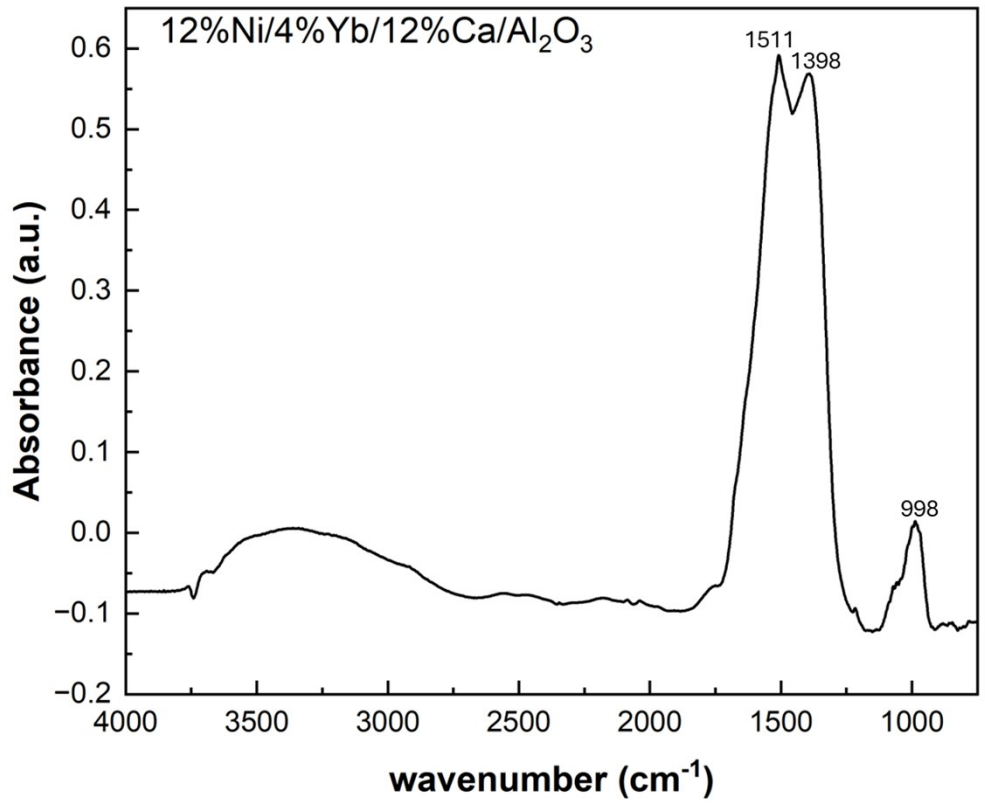

Figure S83. DRIFTS spectrum of the 12%Ni/4%Yb/12%Ca/Al_2O_3 catalyst with CO adsorbed on the catalyst.

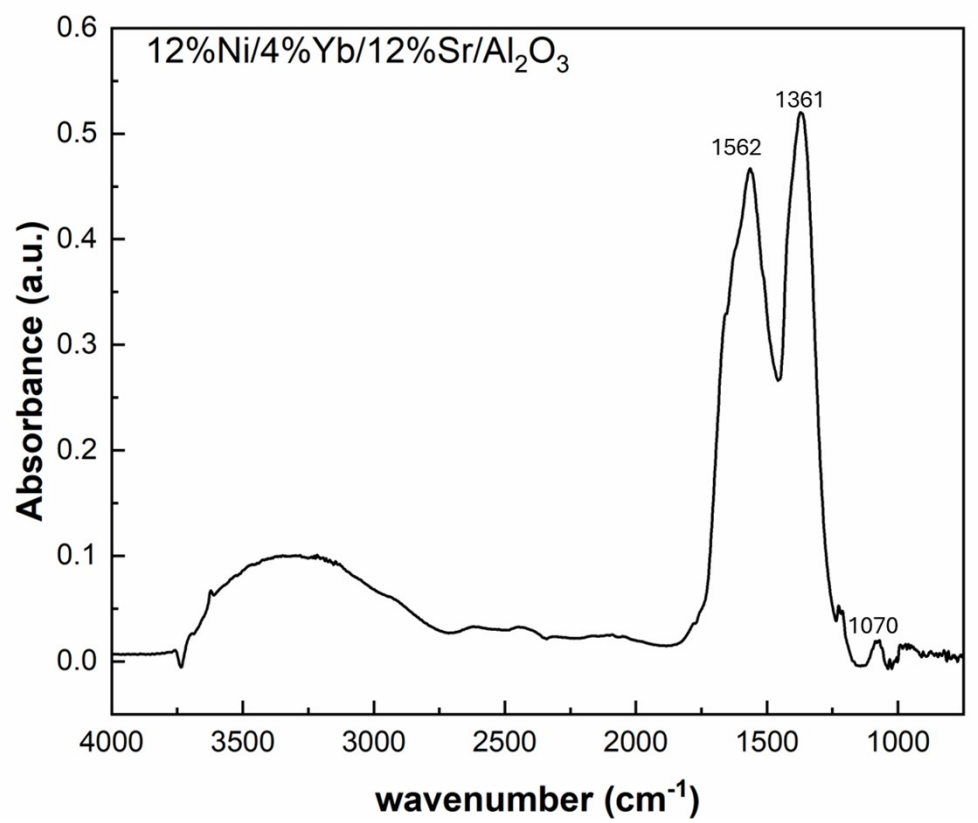

Figure S84. DRIFTS spectrum of the 12%Ni/4%Yb/12%Sr/Al_2O_3 catalyst with CO adsorbed on the catalyst.

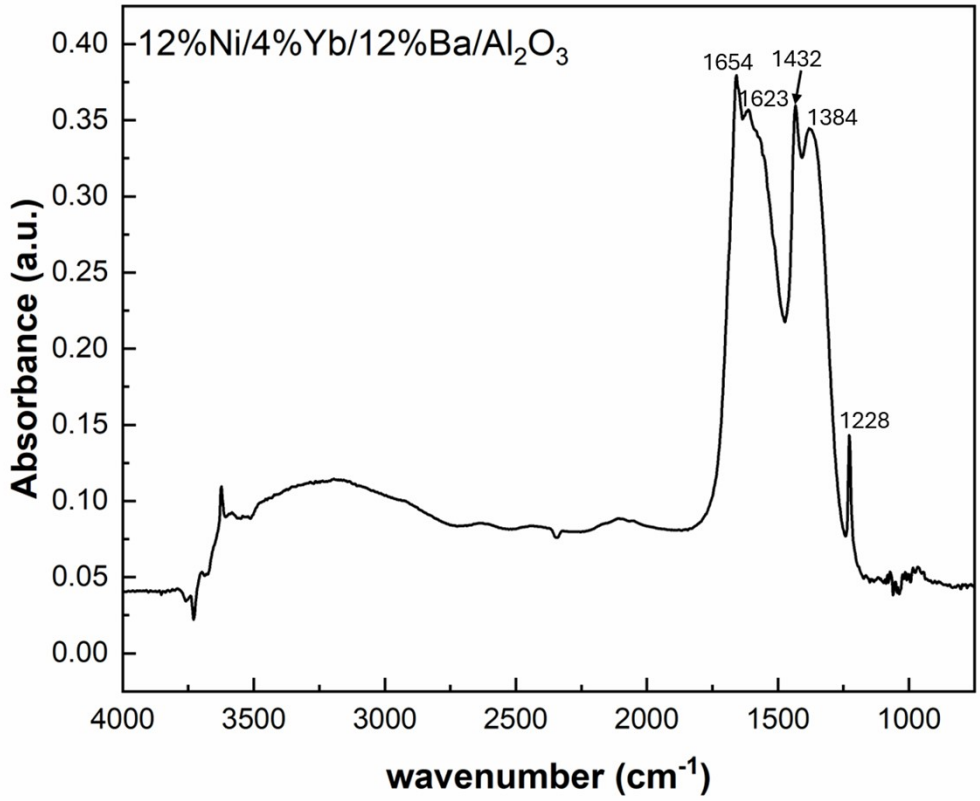

Figure S85. DRIFTS spectrum of the 12%Ni/4%Yb/12%Ba/Al_2O_3 catalyst with CO adsorbed on the catalyst.

Scanning Electron Microscopy

A note regarding EDX is that the nickel Kα and ytterbium Lα peaks overlap and the maps may conflate the two, which is why weight percentages were not utilized from the EDX.

SEM of the Catalyst Cross Section and Outer Shell before and after reaction

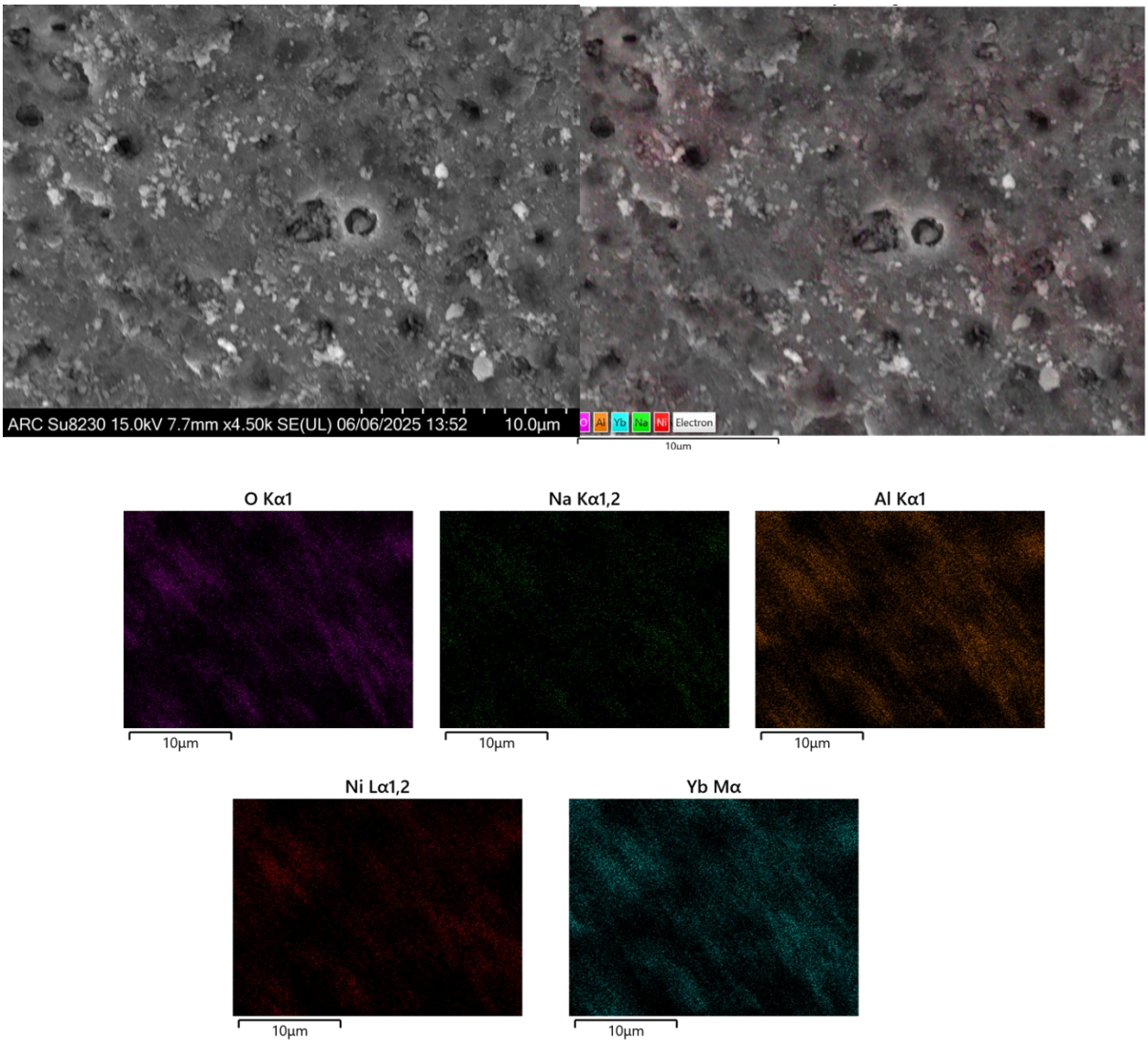

Figure S86. SEM of the NiYbNa before reaction of the outer shell.

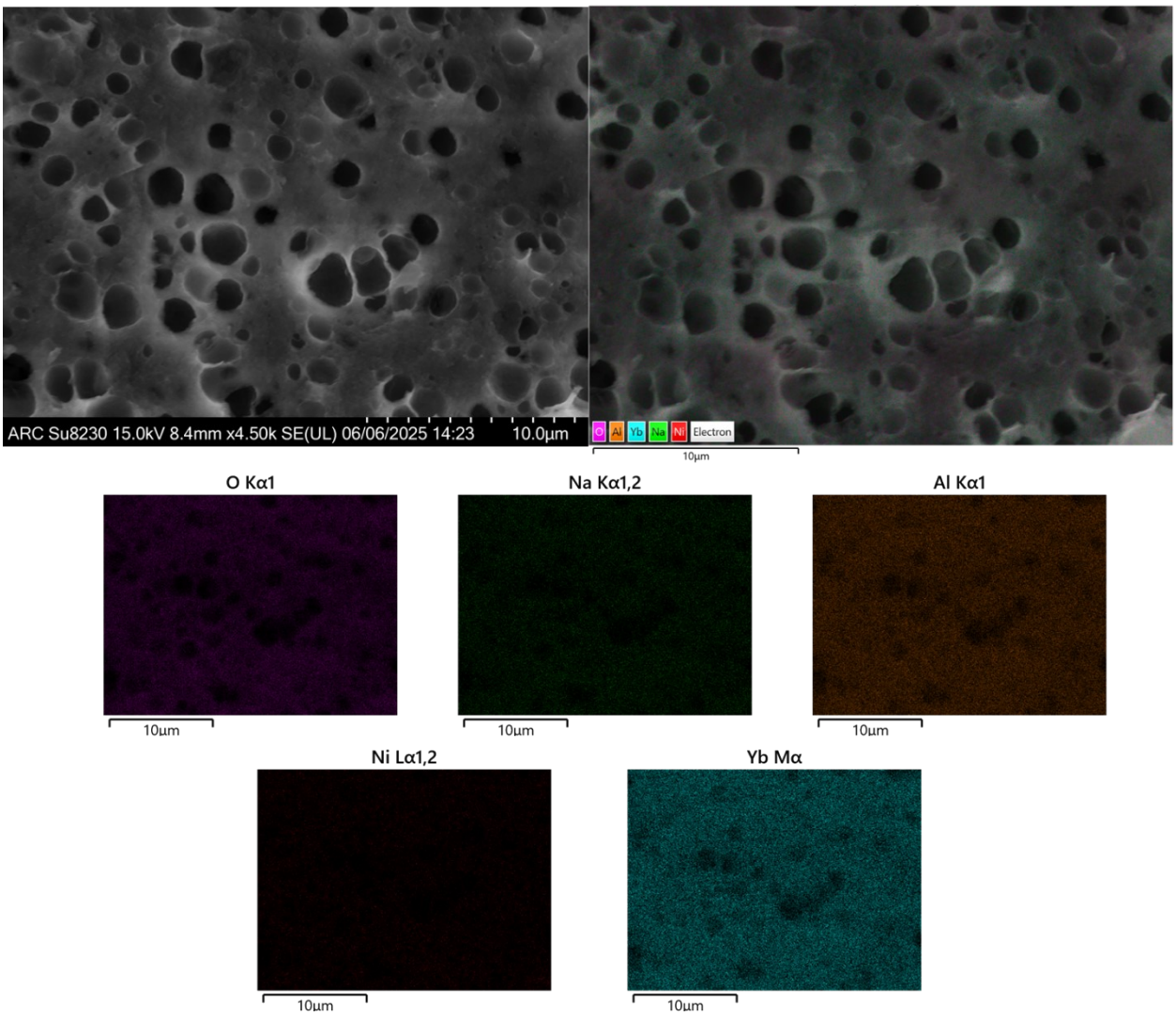

Figure S 87. SEM of the NiYbNa before reaction of the cross section.

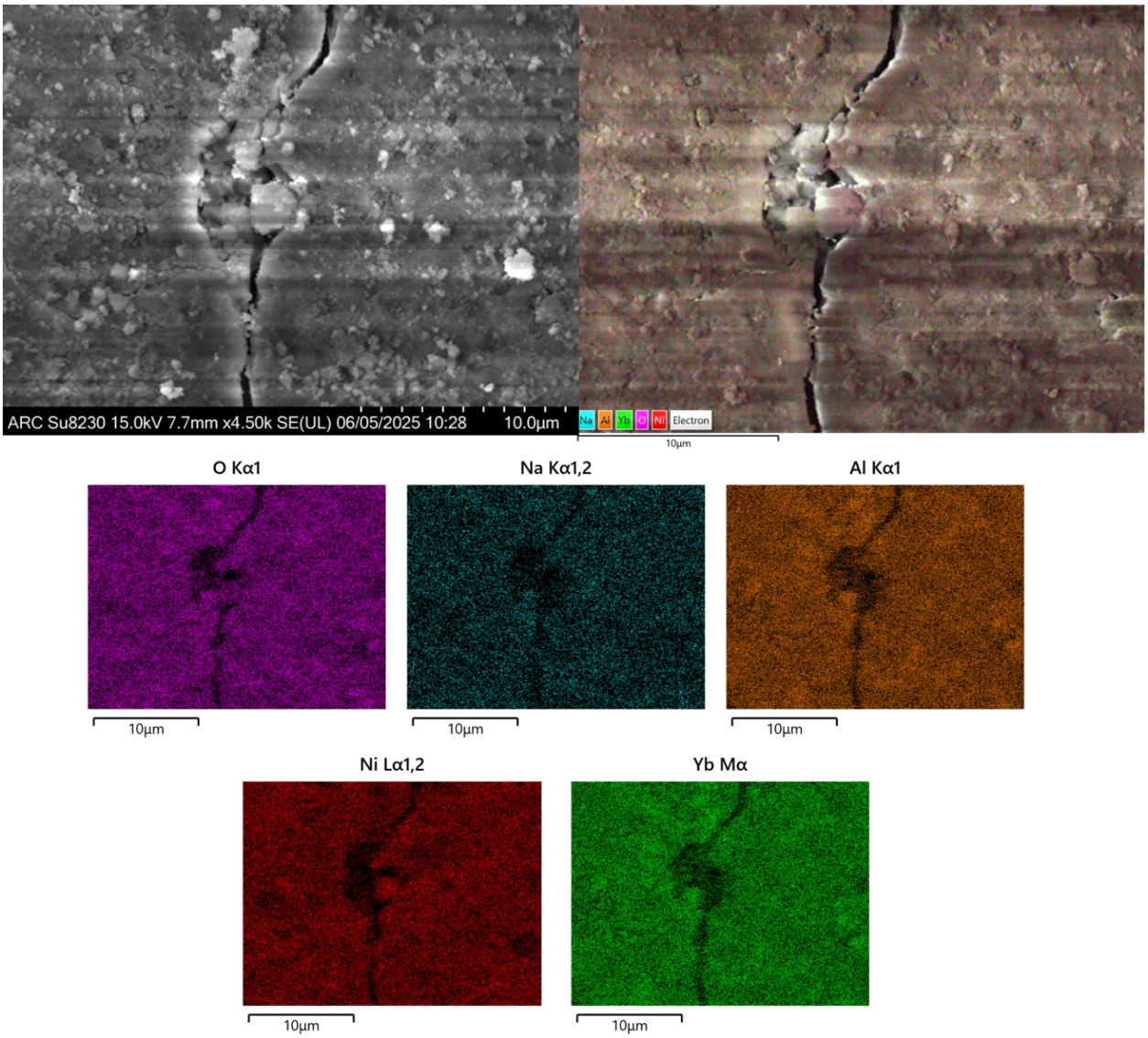

Figure S88. SEM of the NiYbNa after reaction of the outer shell.

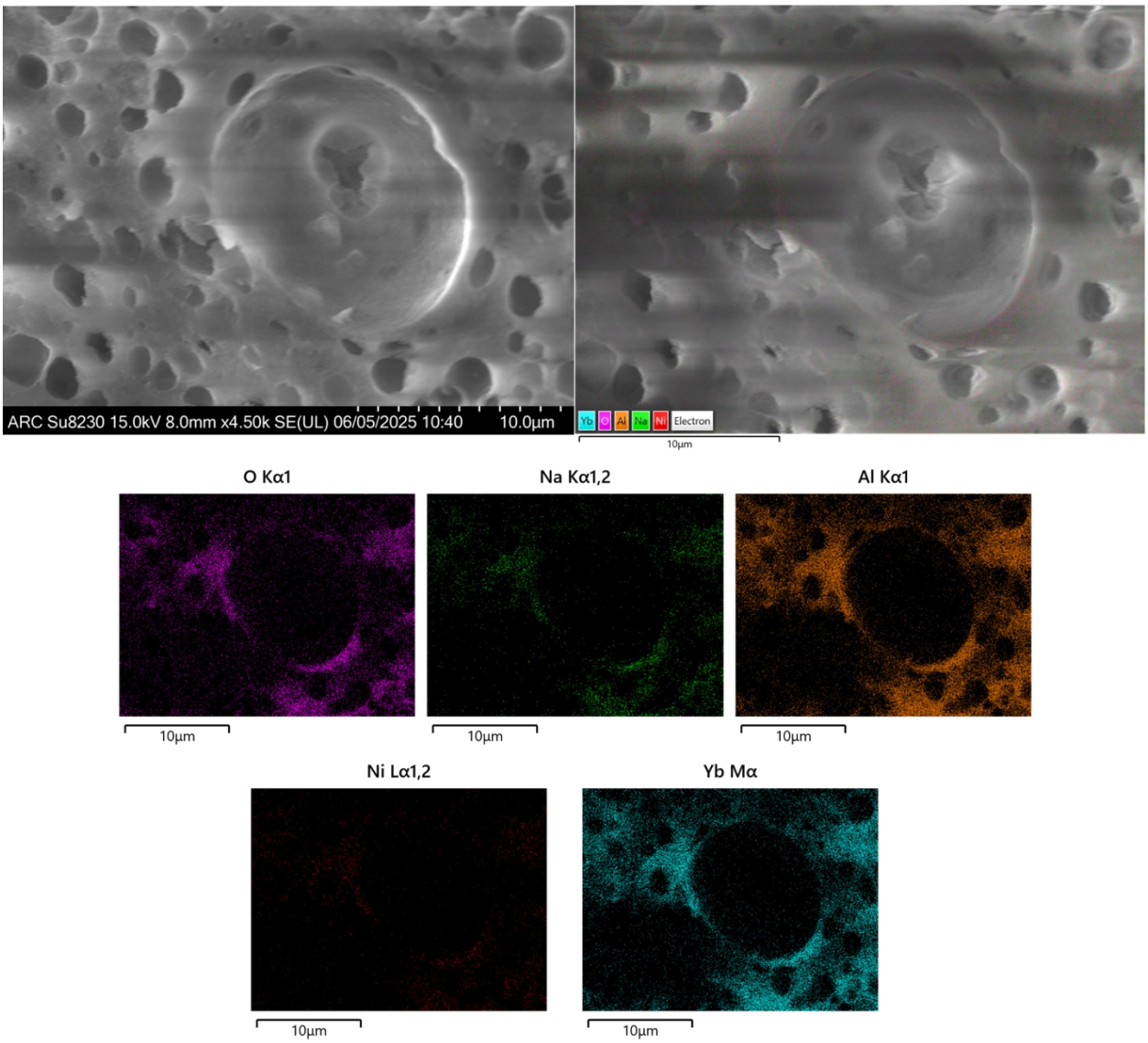

Figure S89. SEM of the NiYbNa after reaction of the cross section.

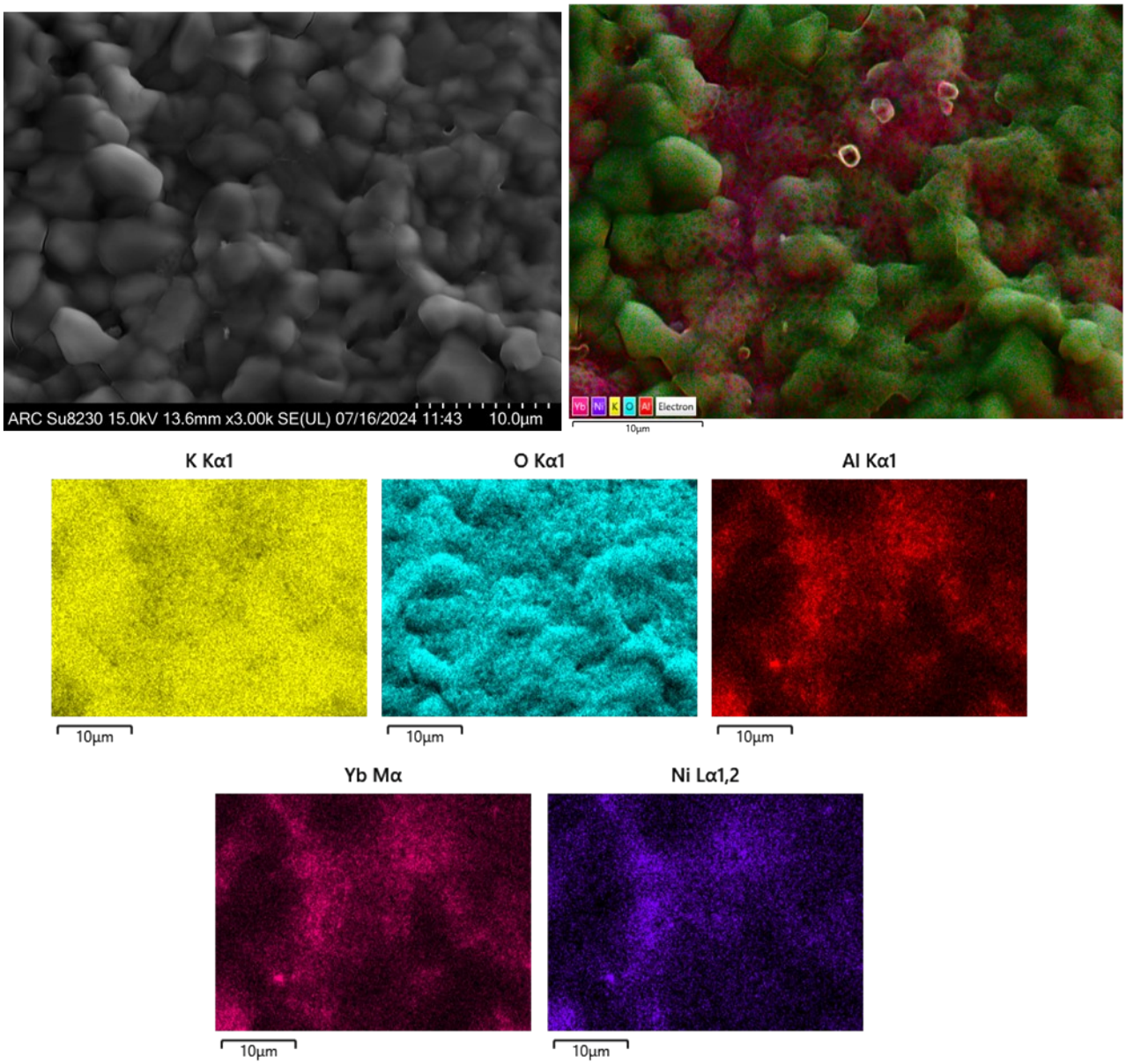

Figure S90. SEM of the NiYbK before reaction of the outer shell.

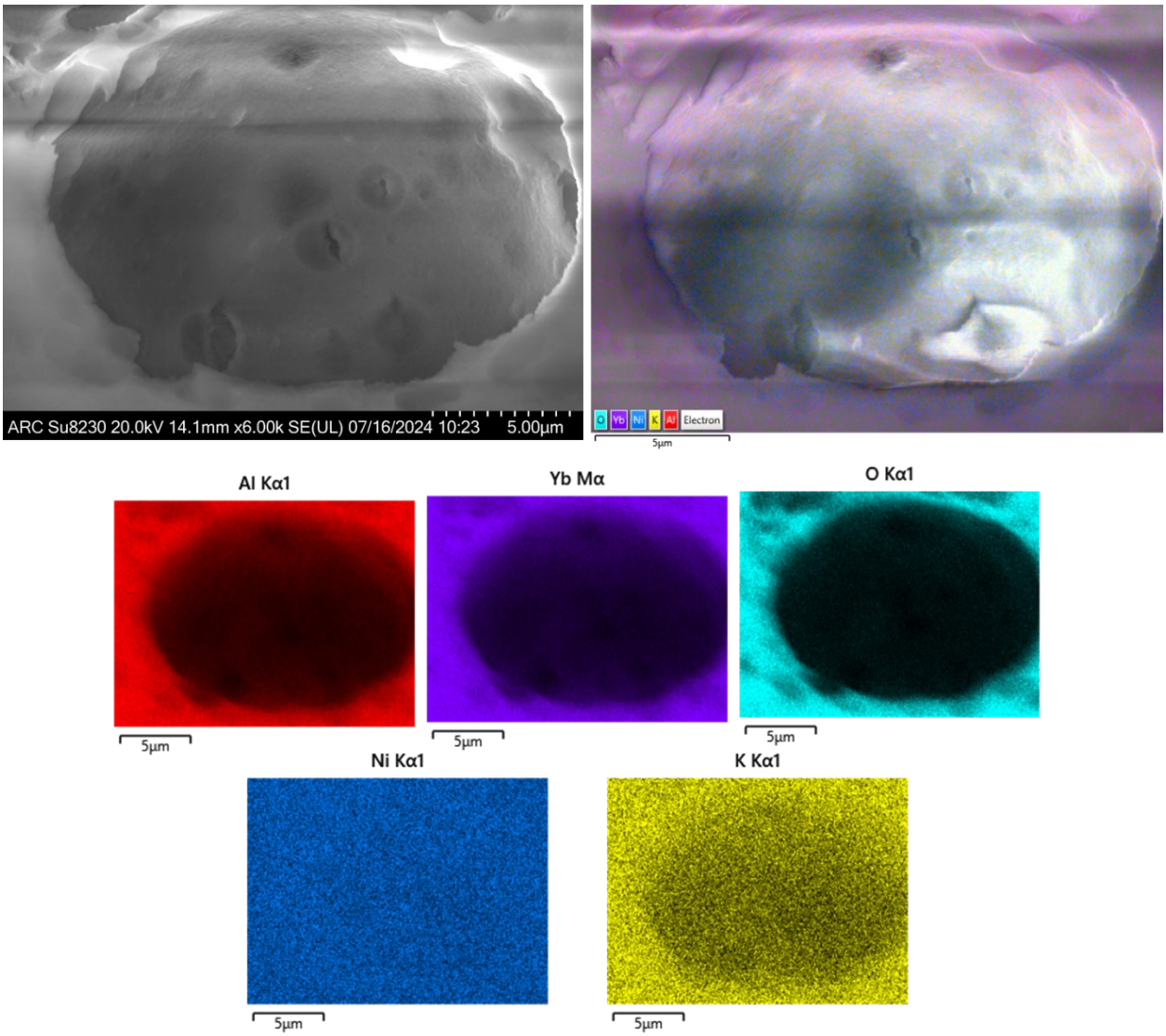

Figure S91. SEM of the NiYbK before reaction of the cross section.

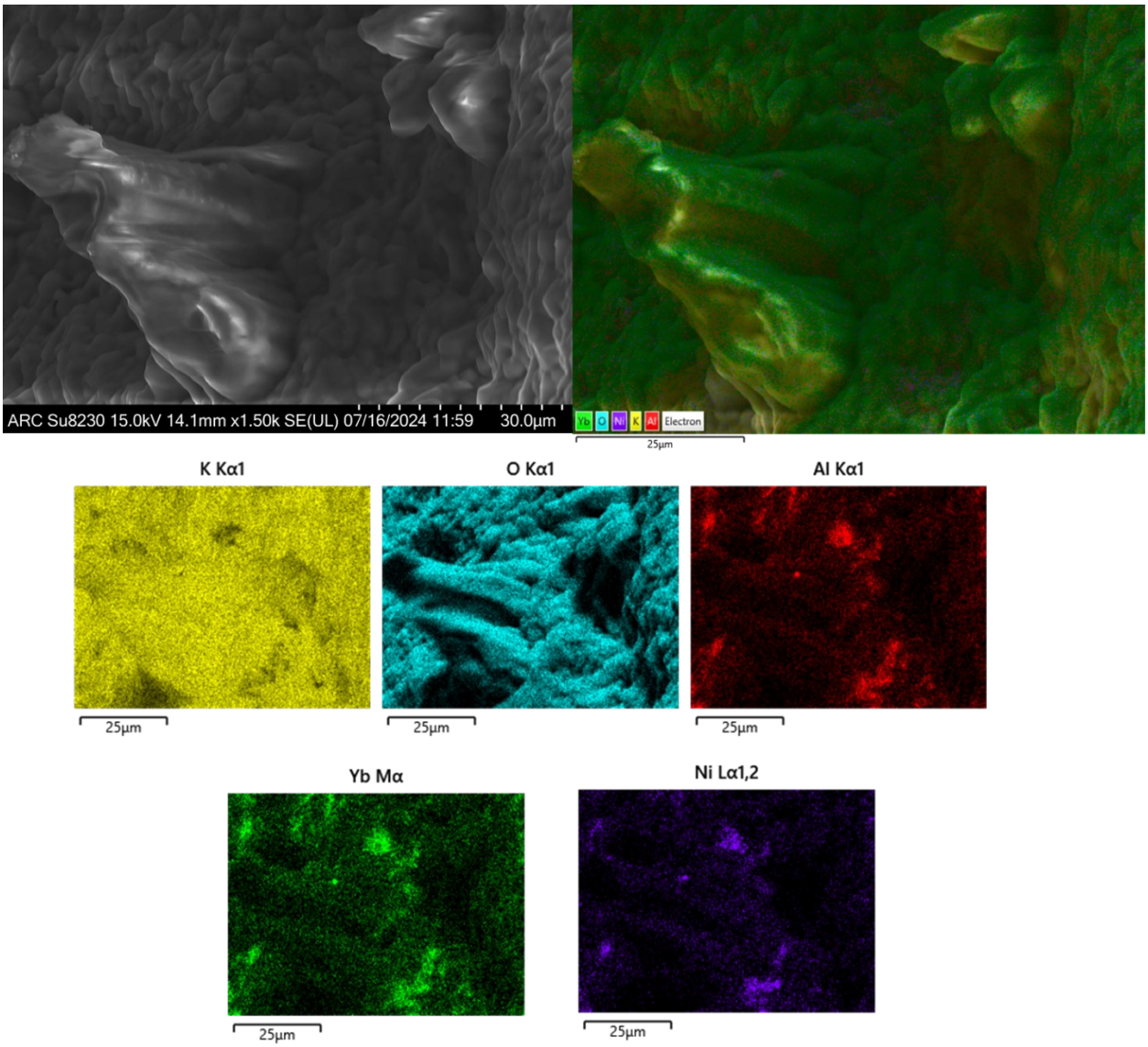

Figure S92. SEM of the NiYbK after reaction of the outer shell.

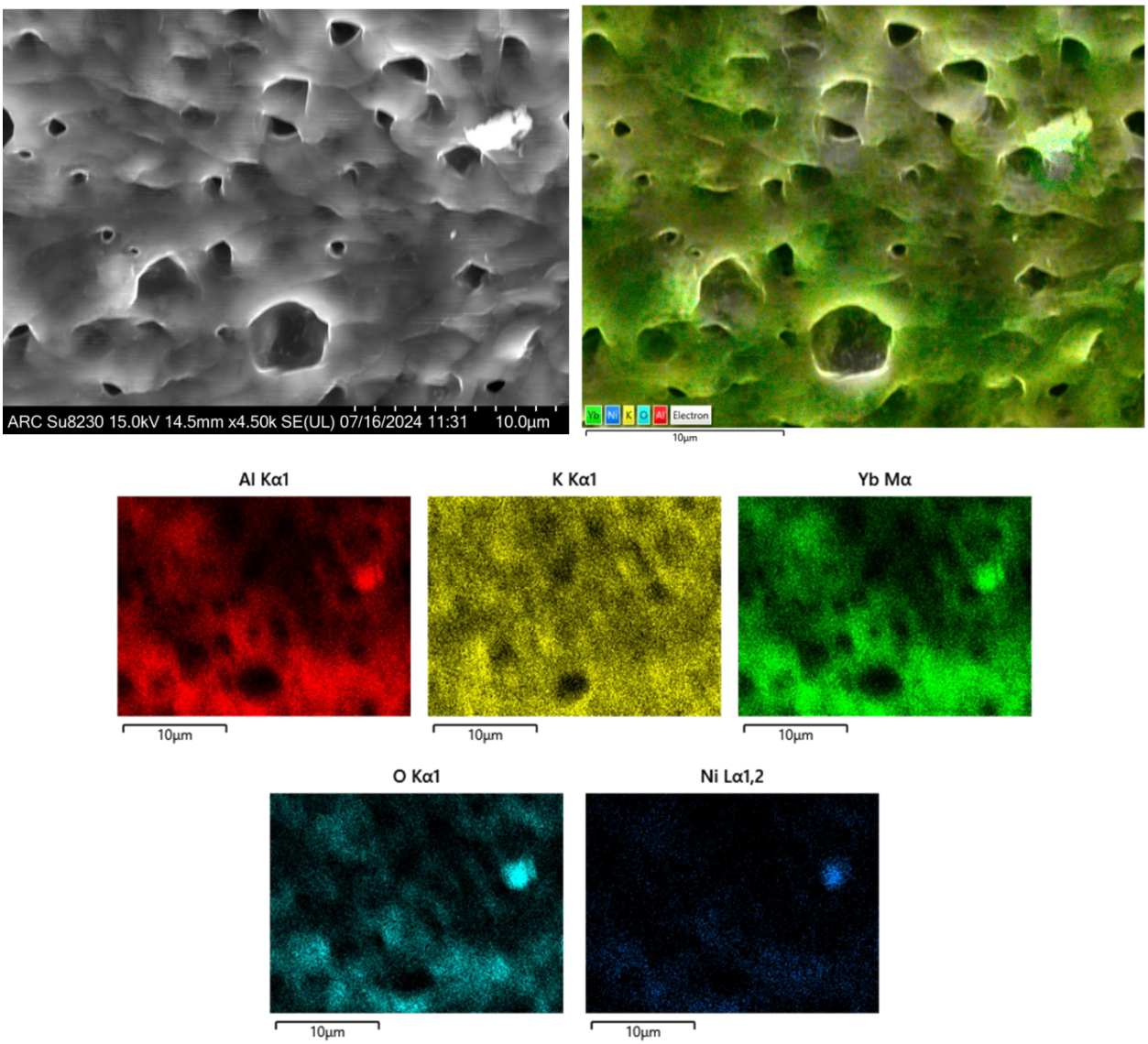

Figure S93. SEM of the NiYbK after reaction of the cross section.

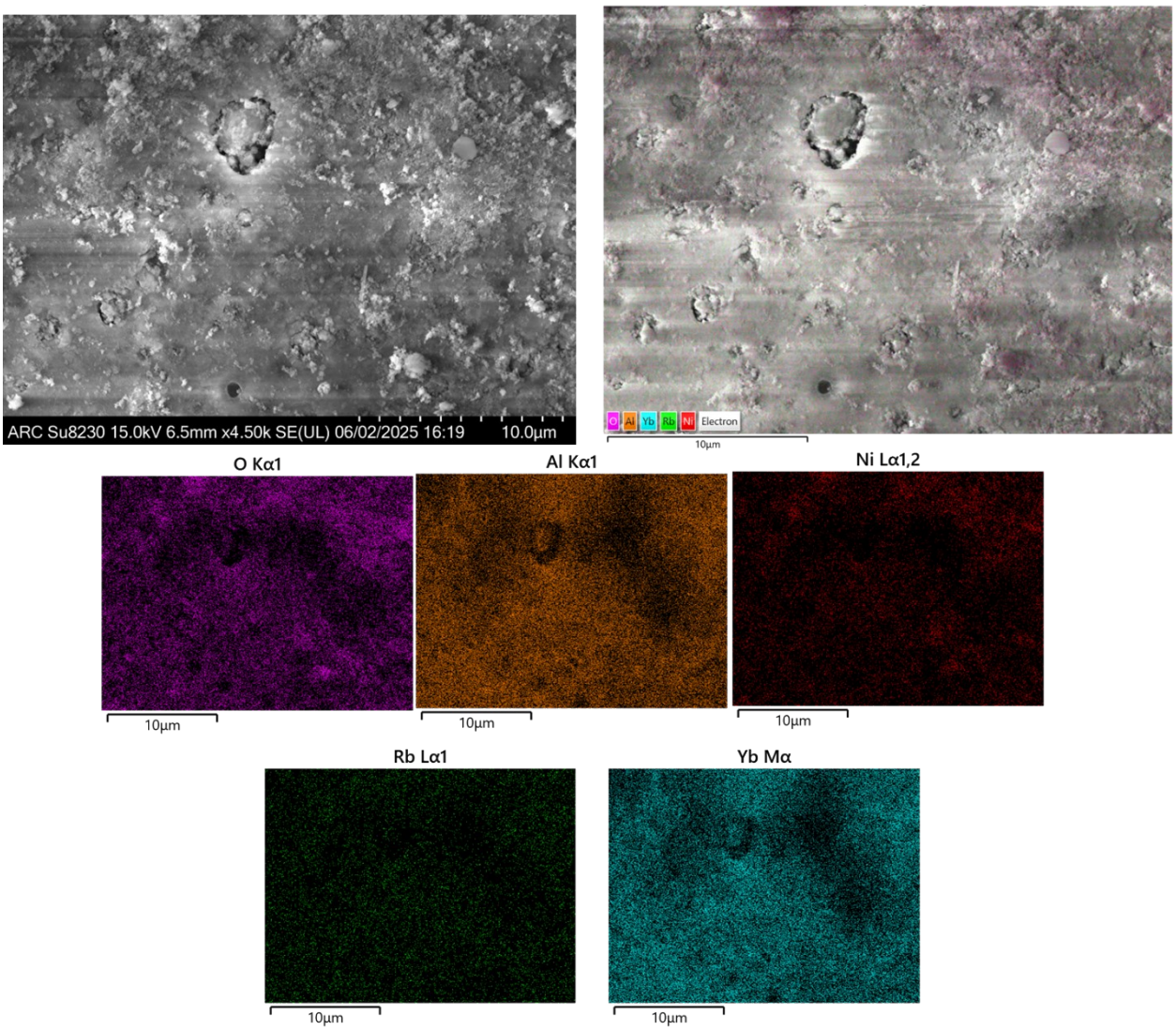

Figure S 94. SEM of the NiYbRb catalyst outer shell before reaction.

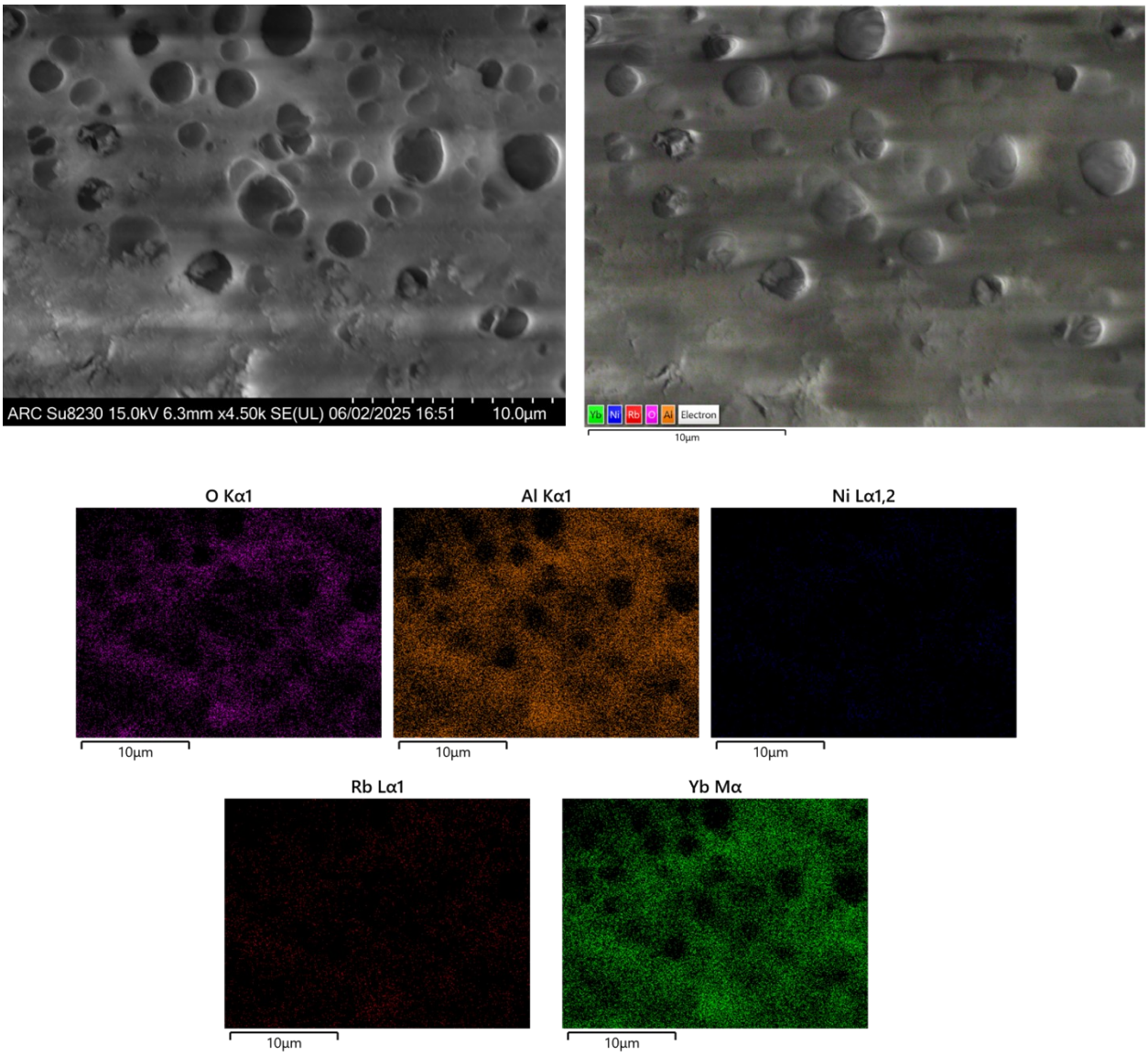

Figure S 95. SEM of the NiYbRb catalyst cross section before reaction.

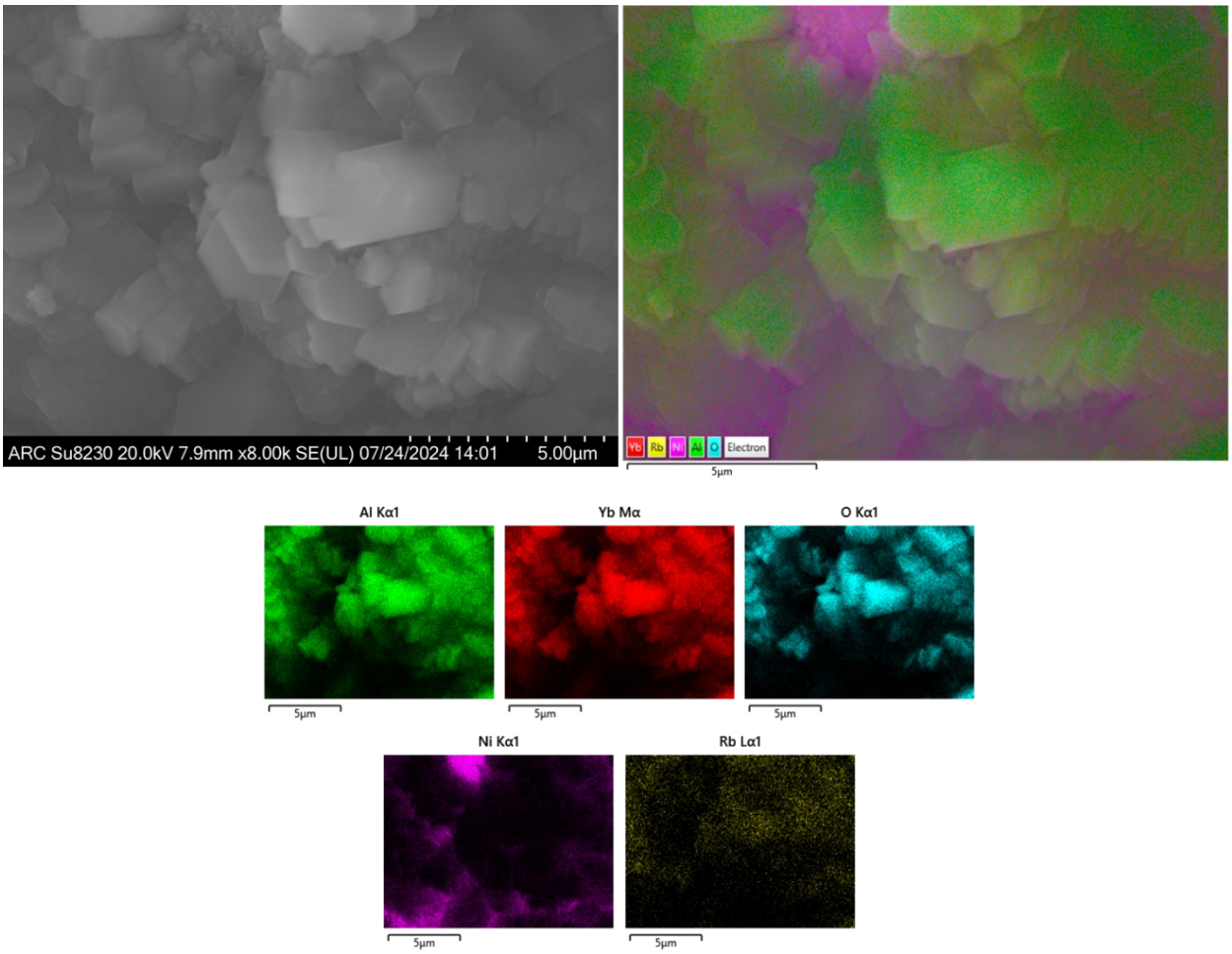

Figure S96. SEM of the NiYbRb catalyst after reaction of the outer shell.

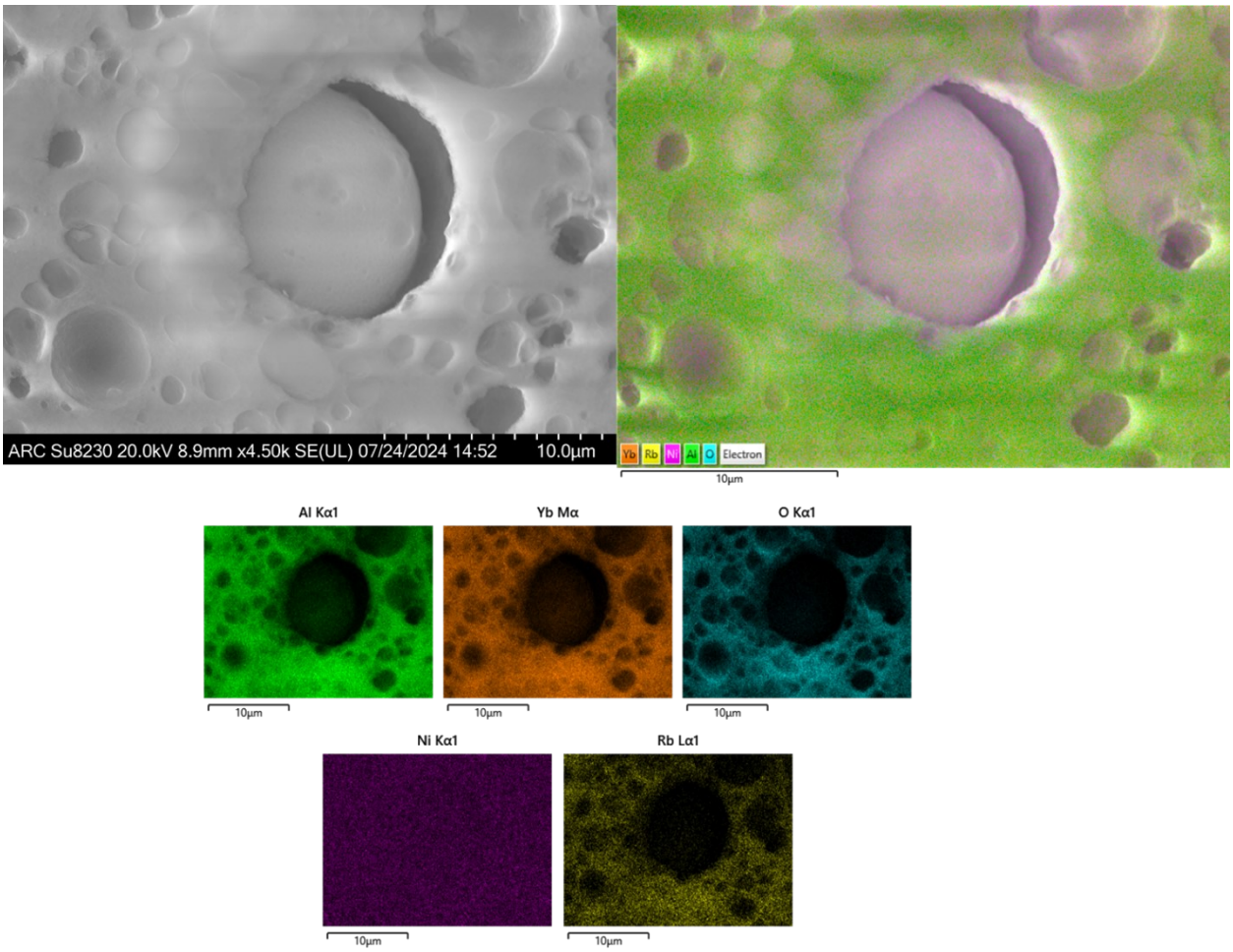

Figure S97. SEM of the NiYbRb catalysts after reaction with ammonia of the cross section.

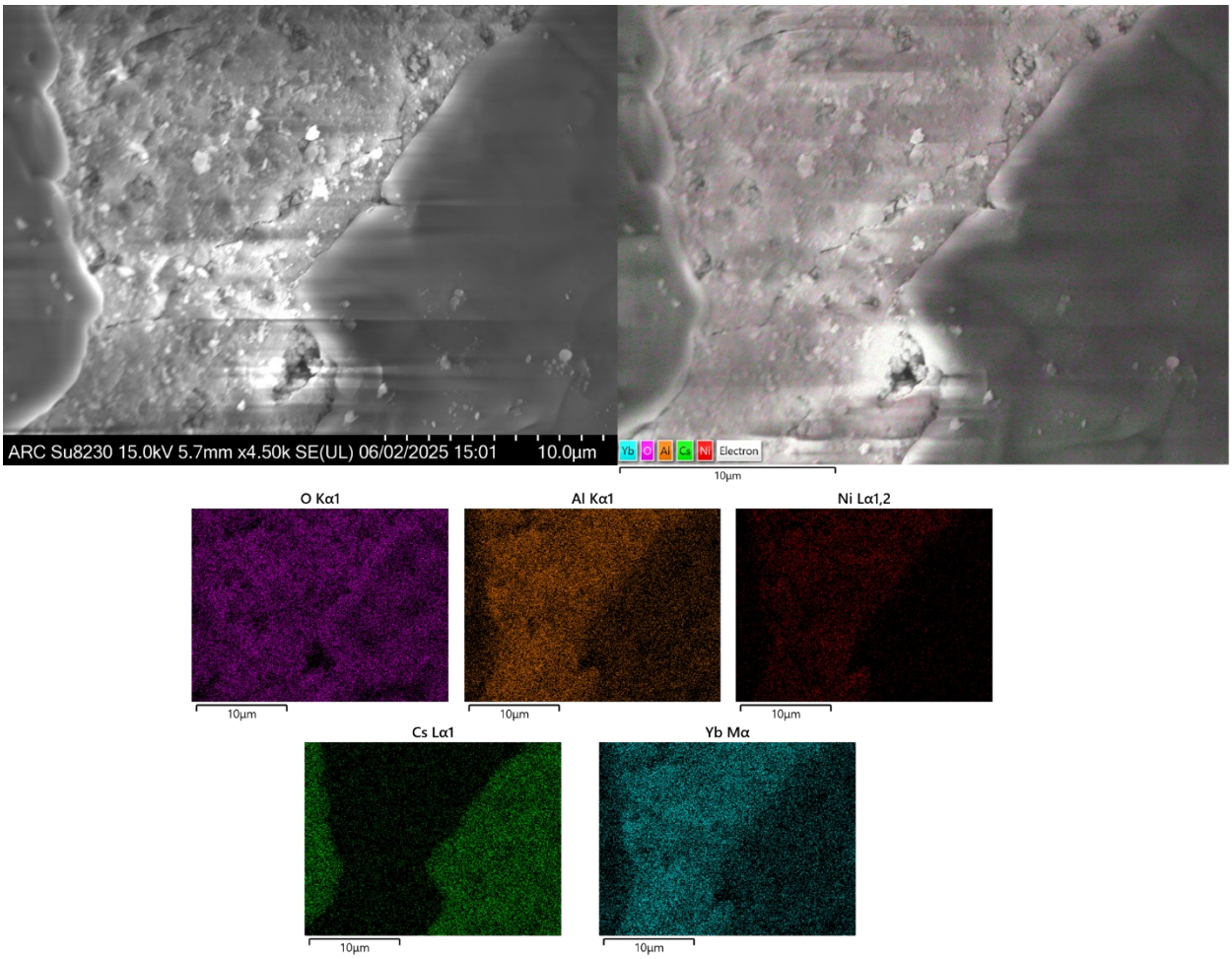

Figure S98. SEM of the NiYbCs catalyst outer shell before reaction.

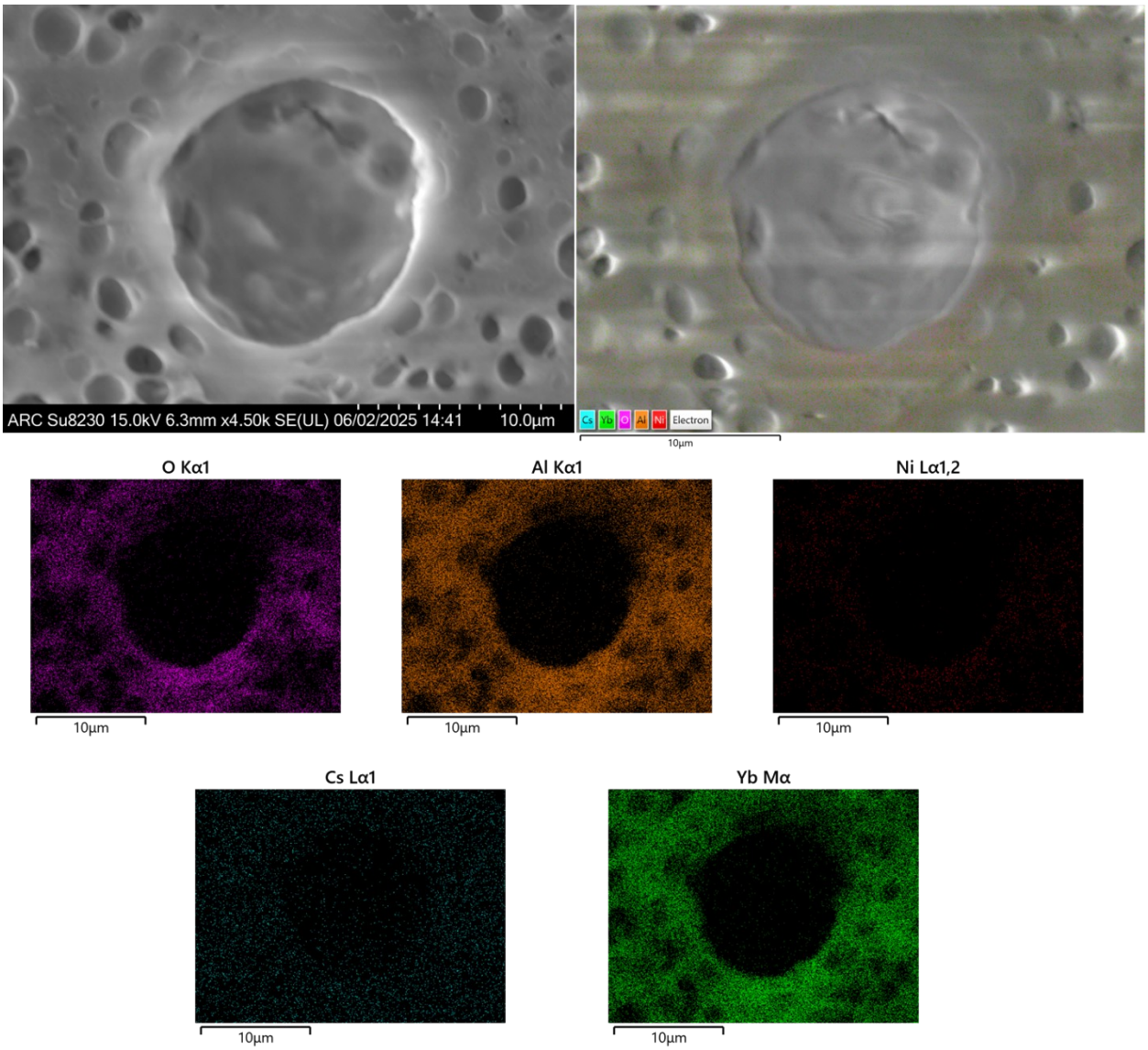

Figure S 99. SEM of the NiYbCs catalyst cross section before reaction.

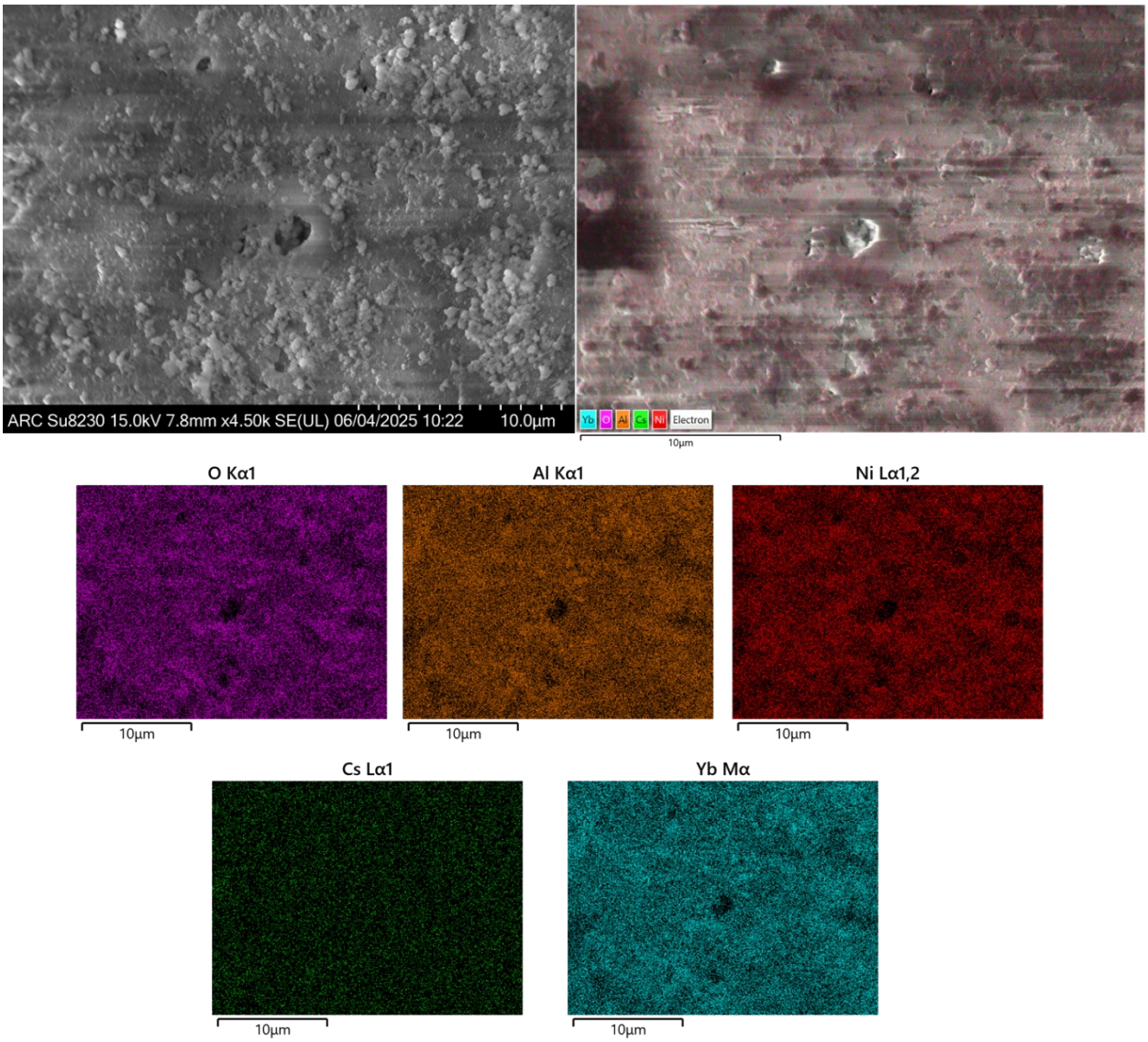

Figure S 100. SEM of NiYbCs catalyst outer shell after reaction.

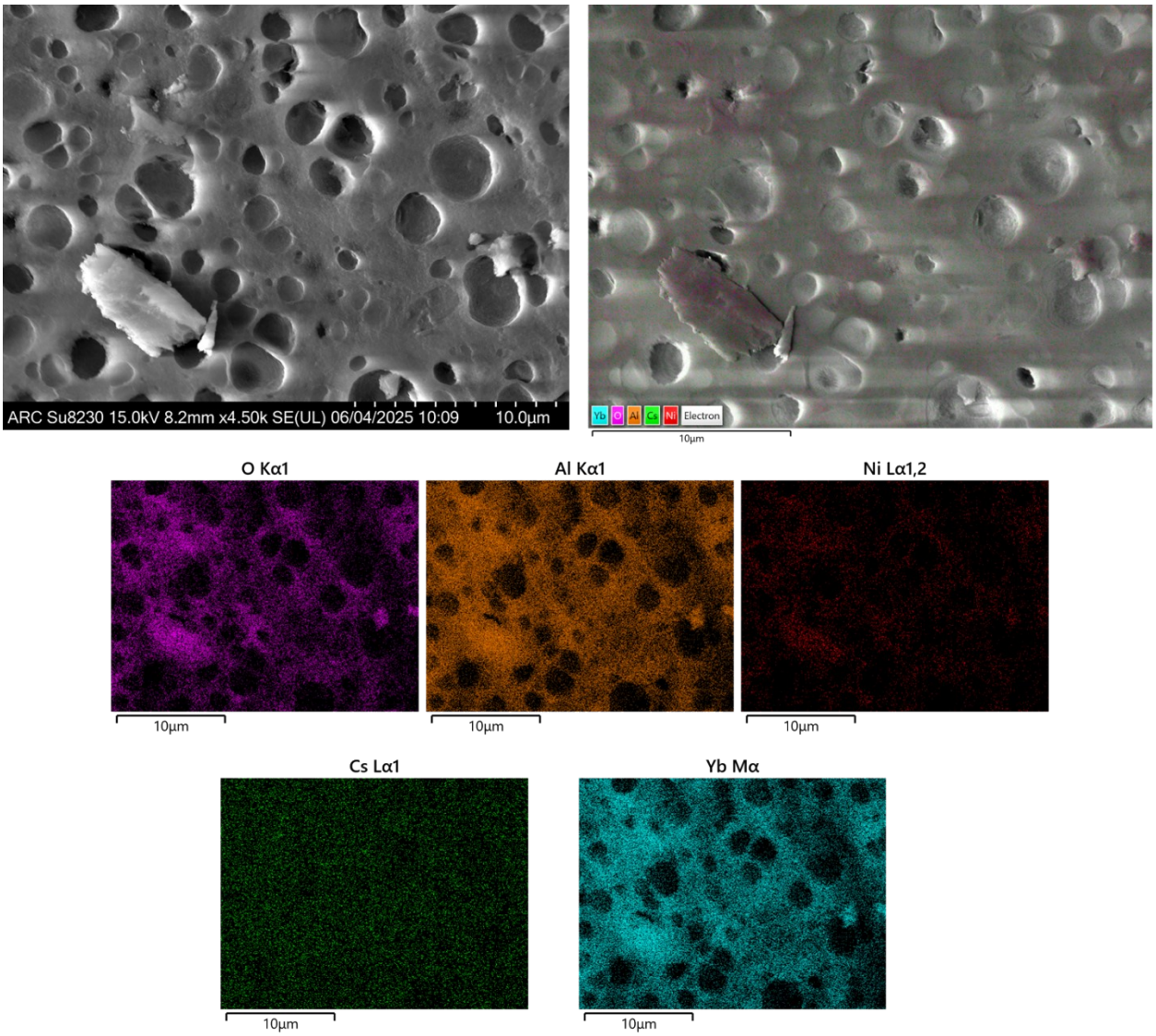

Figure S101. SEM of the NiYbCs catalyst cross section after reaction.

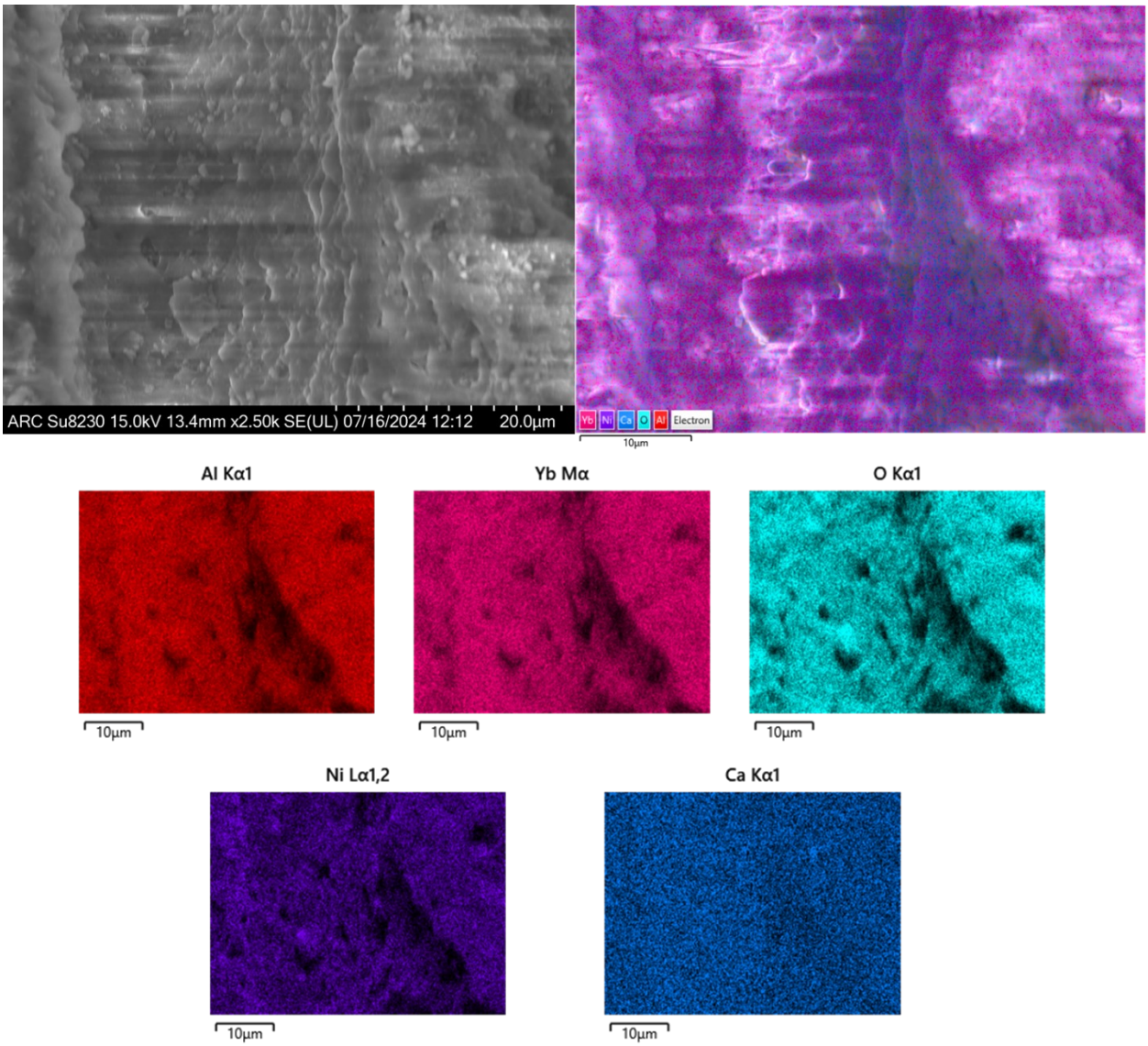

Figure S 102. SEM of the NiYbCa before reaction of the outer shell.

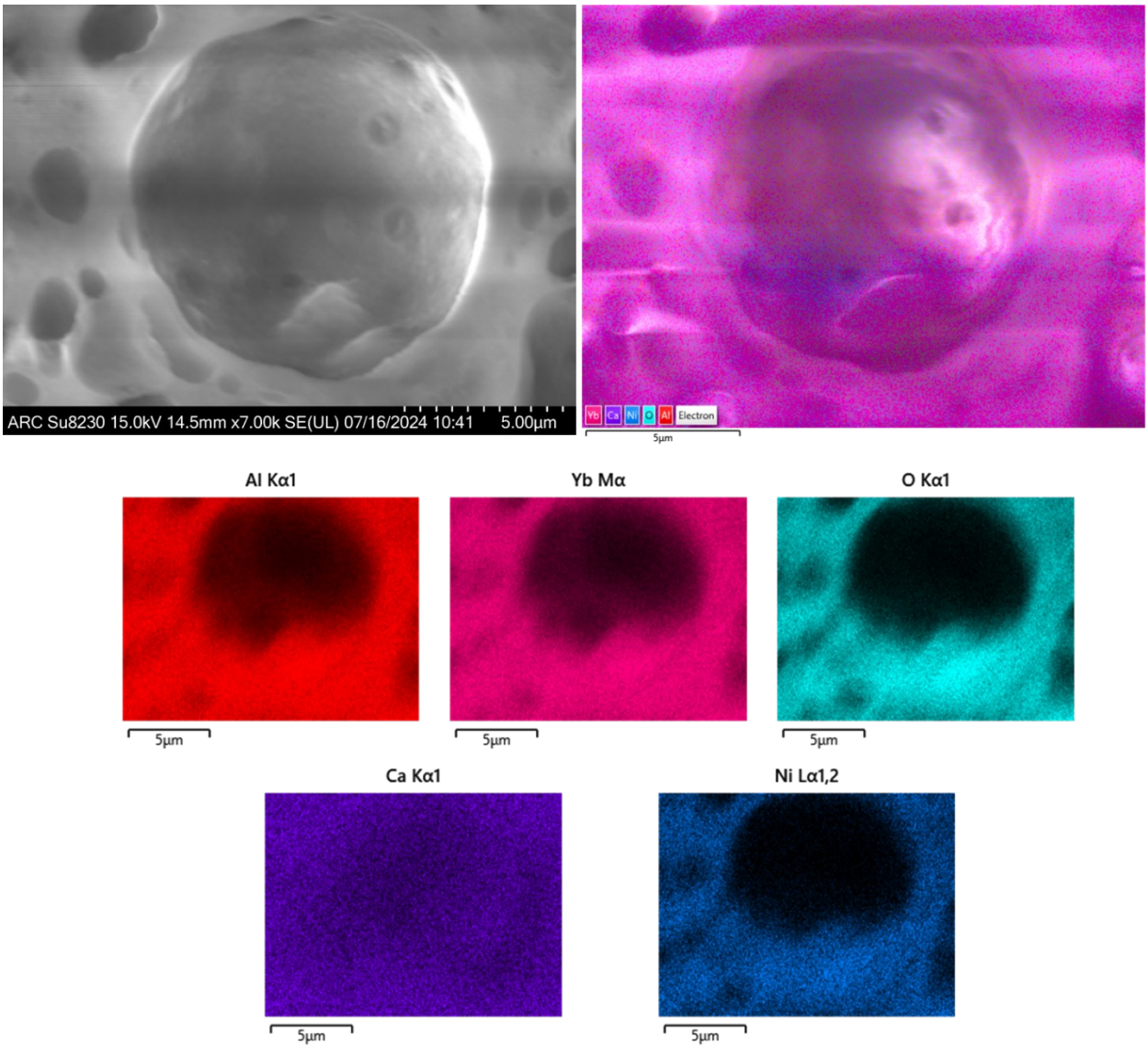

Figure S103. SEM of the NiYbCa catalyst cross section before reaction.

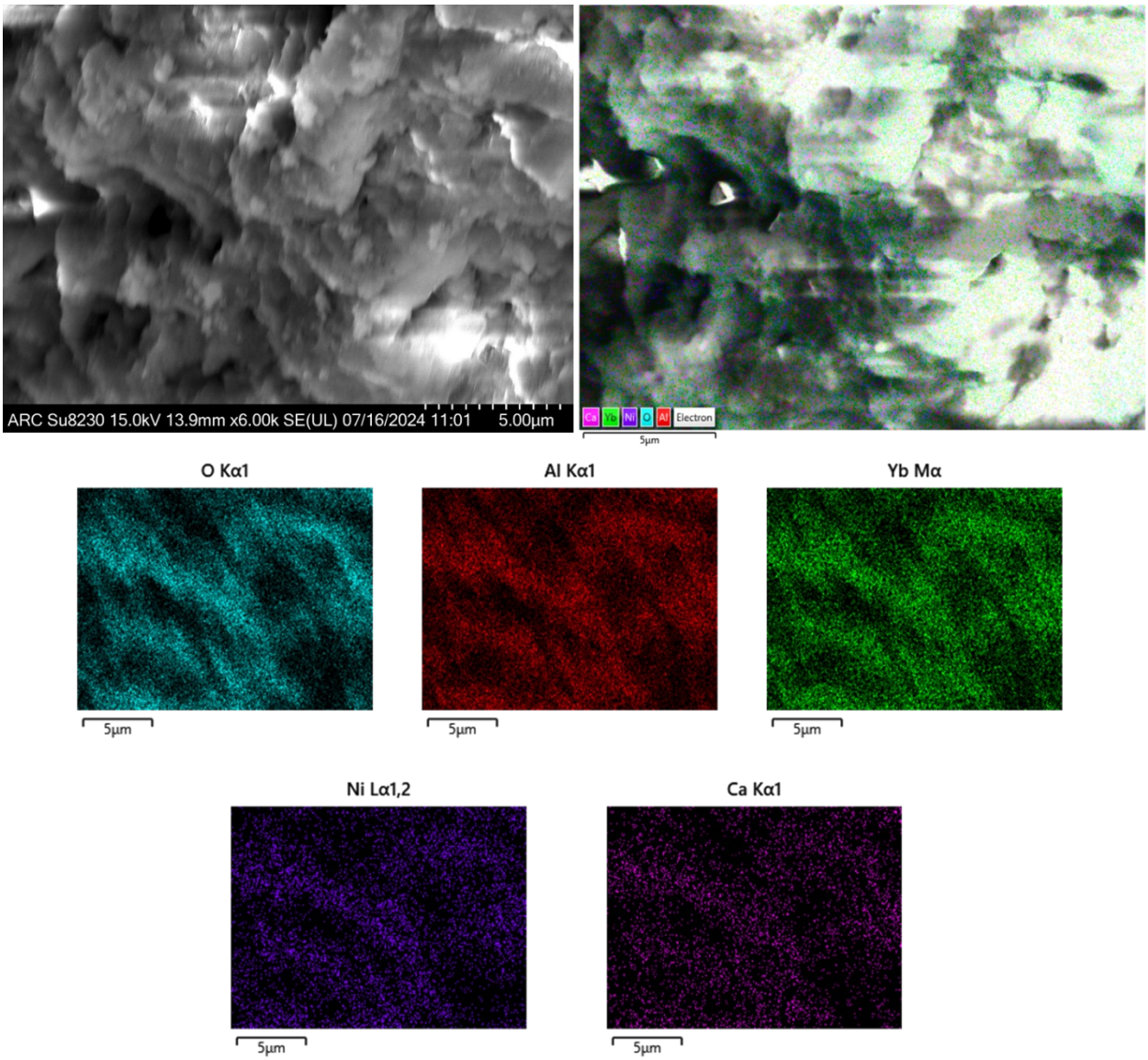

Figure S 104. SEM of the NiYbCa after reaction of the outer shell.

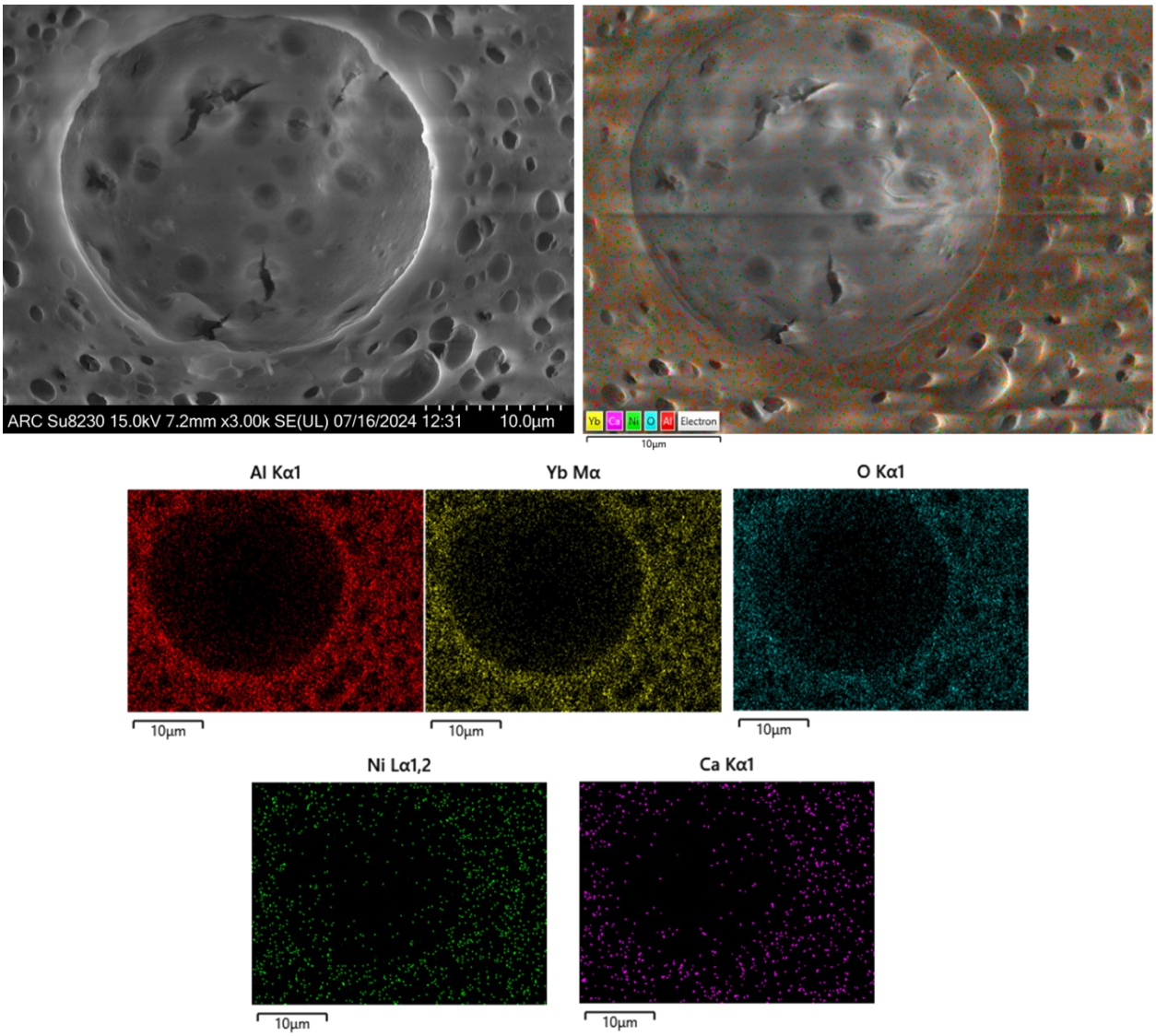

Figure S105. SEM of the NiYbCa catalyst of the cross section after reaction.

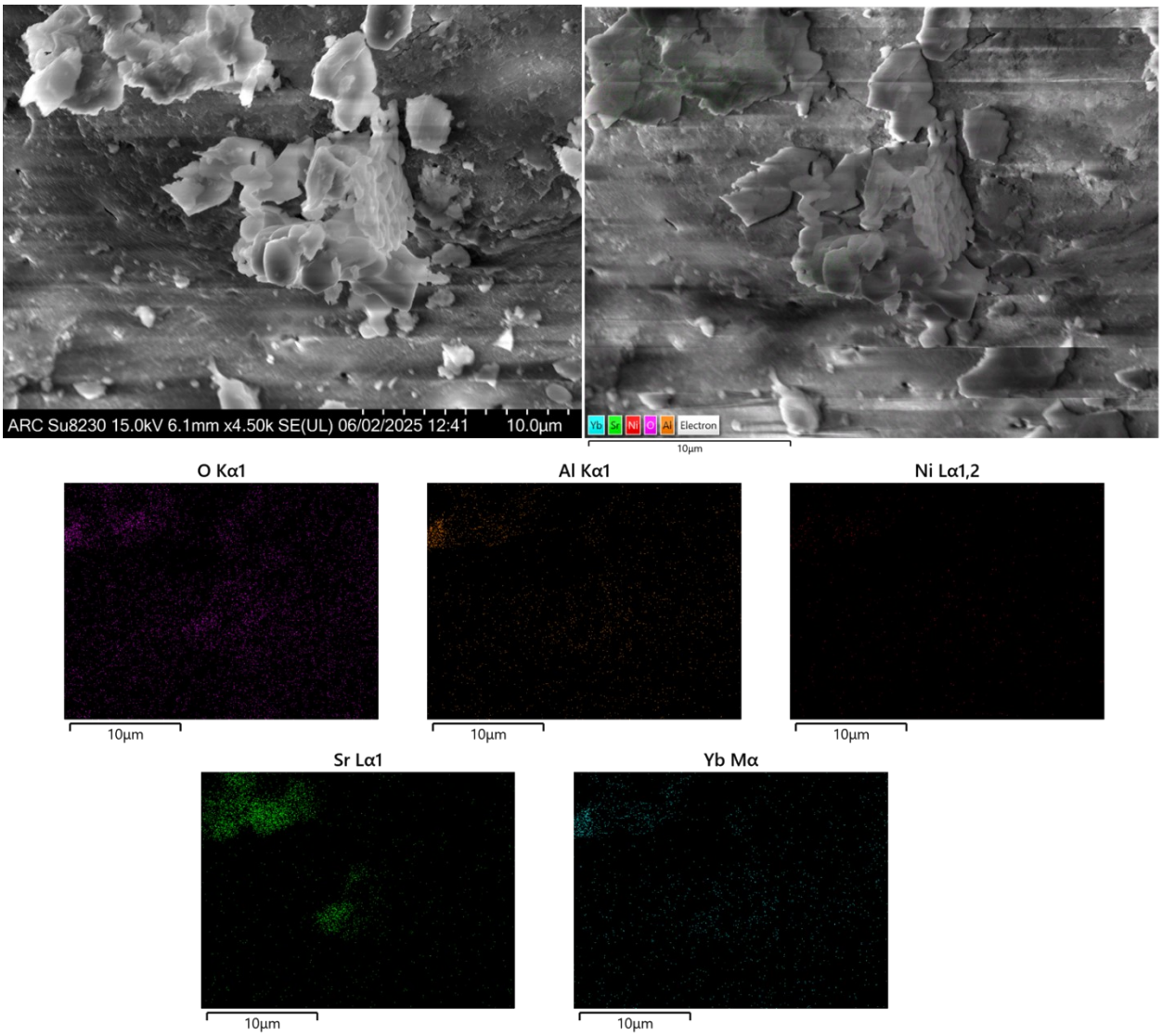

Figure S106. SEM of the NiYbSr catalyst outer shell before reaction.

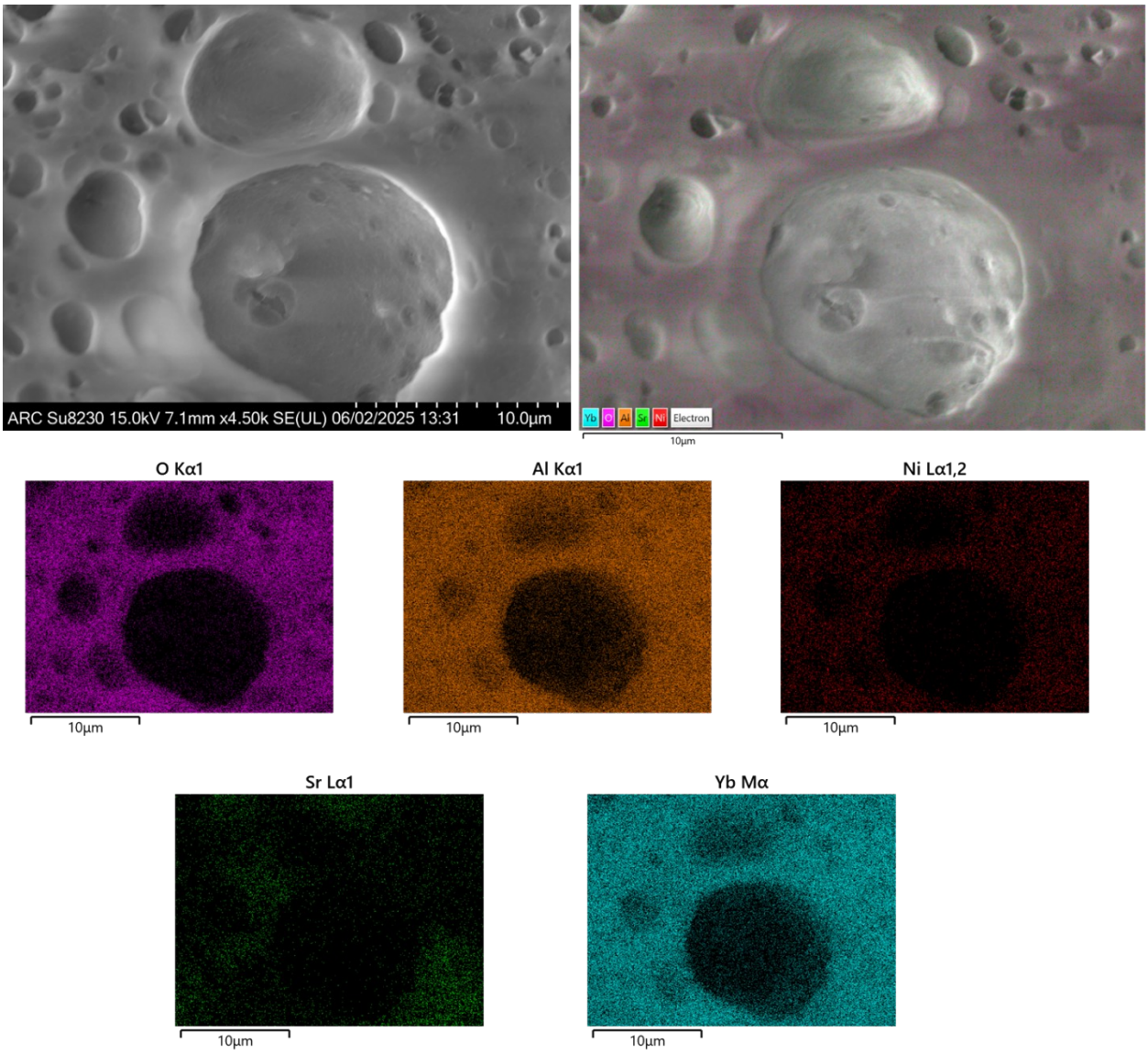

Figure S107. SEM of the NiYbSr catalyst cross section before reaction.

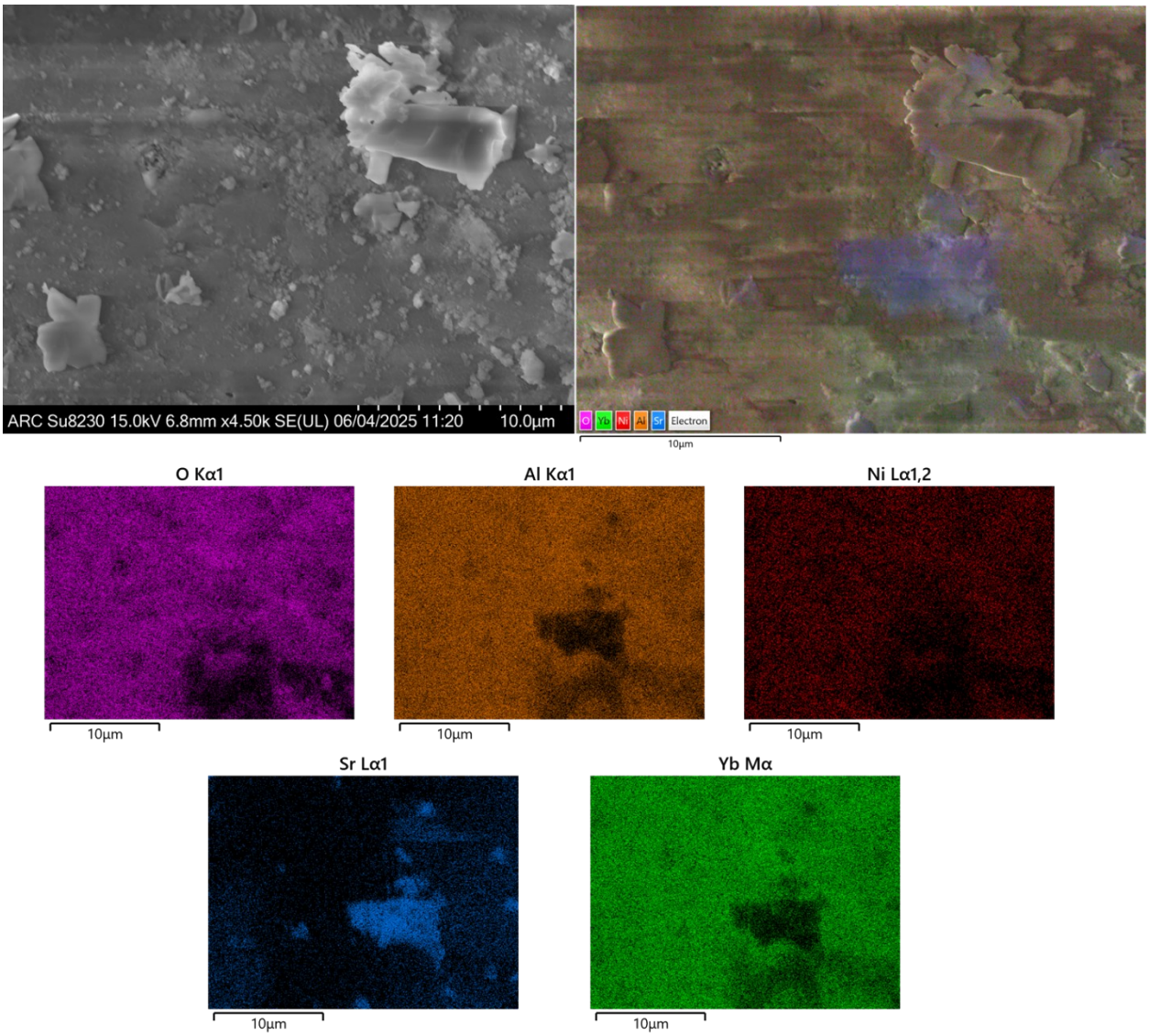

Figure S 108. SEM of the NiYbSr catalyst outer shell after reaction.

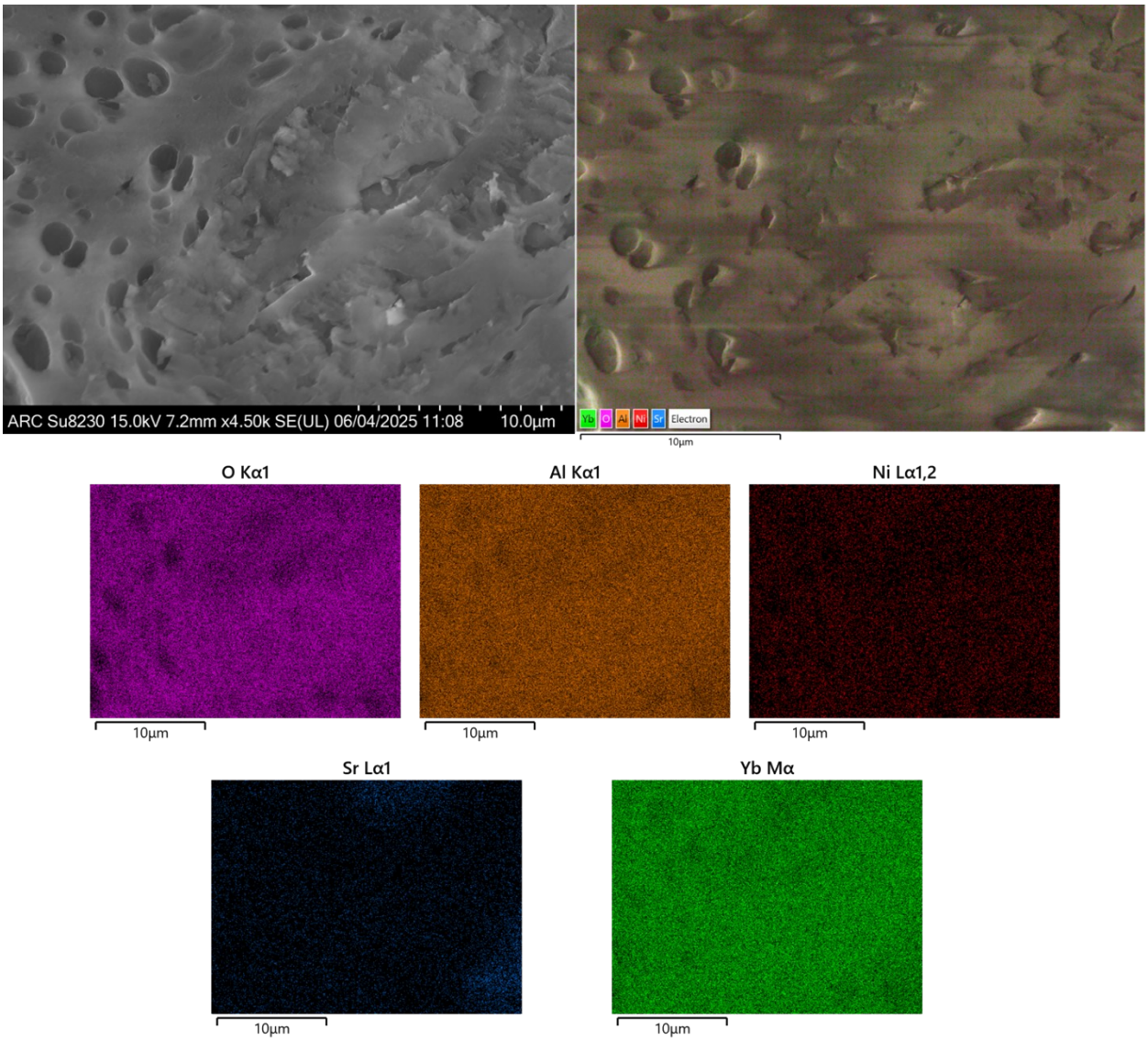

Figure S 109. SEM of the NiYbSr catalyst cross section after reaction.

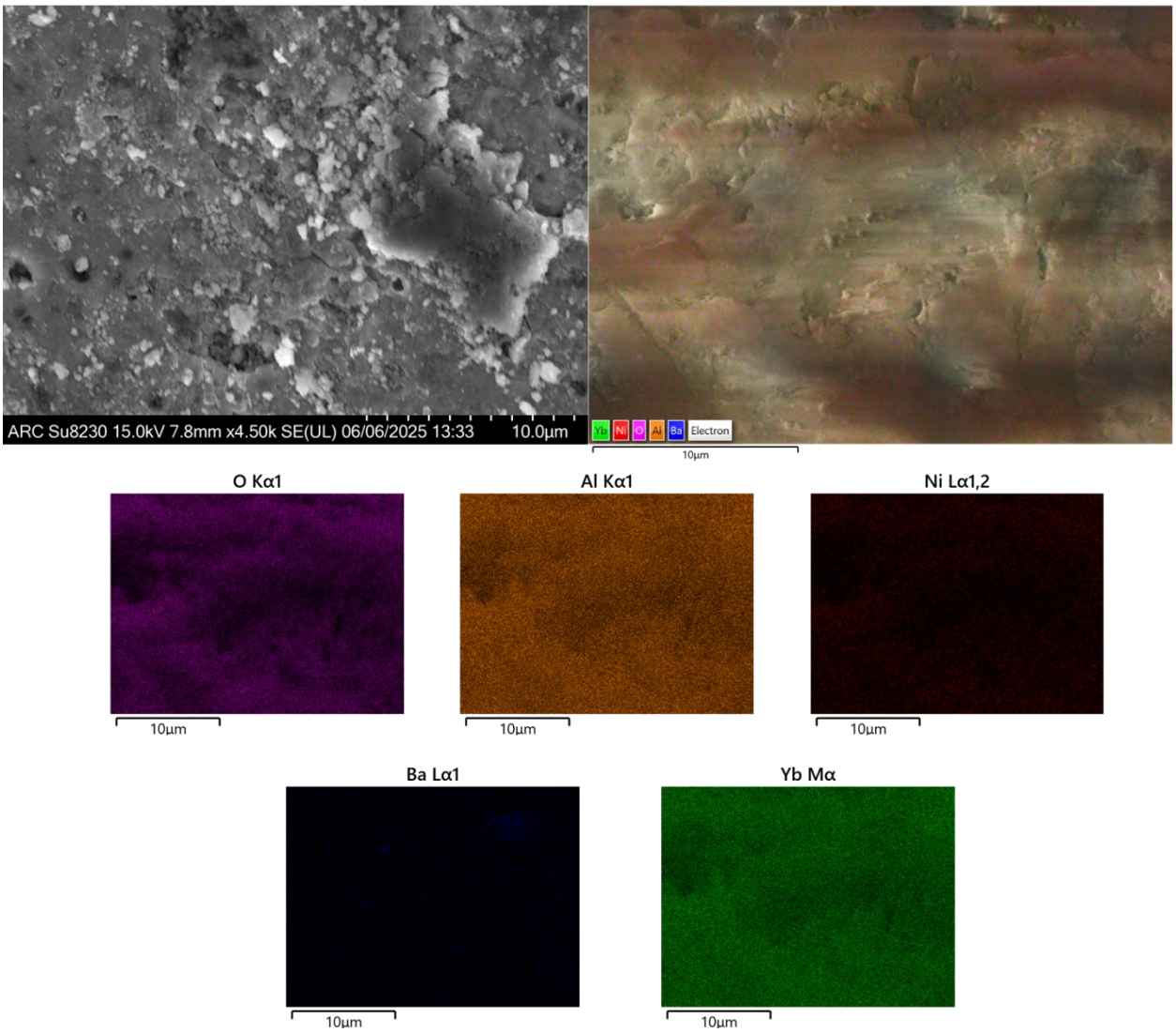

Figure S 110. SEM of the NiYbBa catalyst outer shell before reaction.

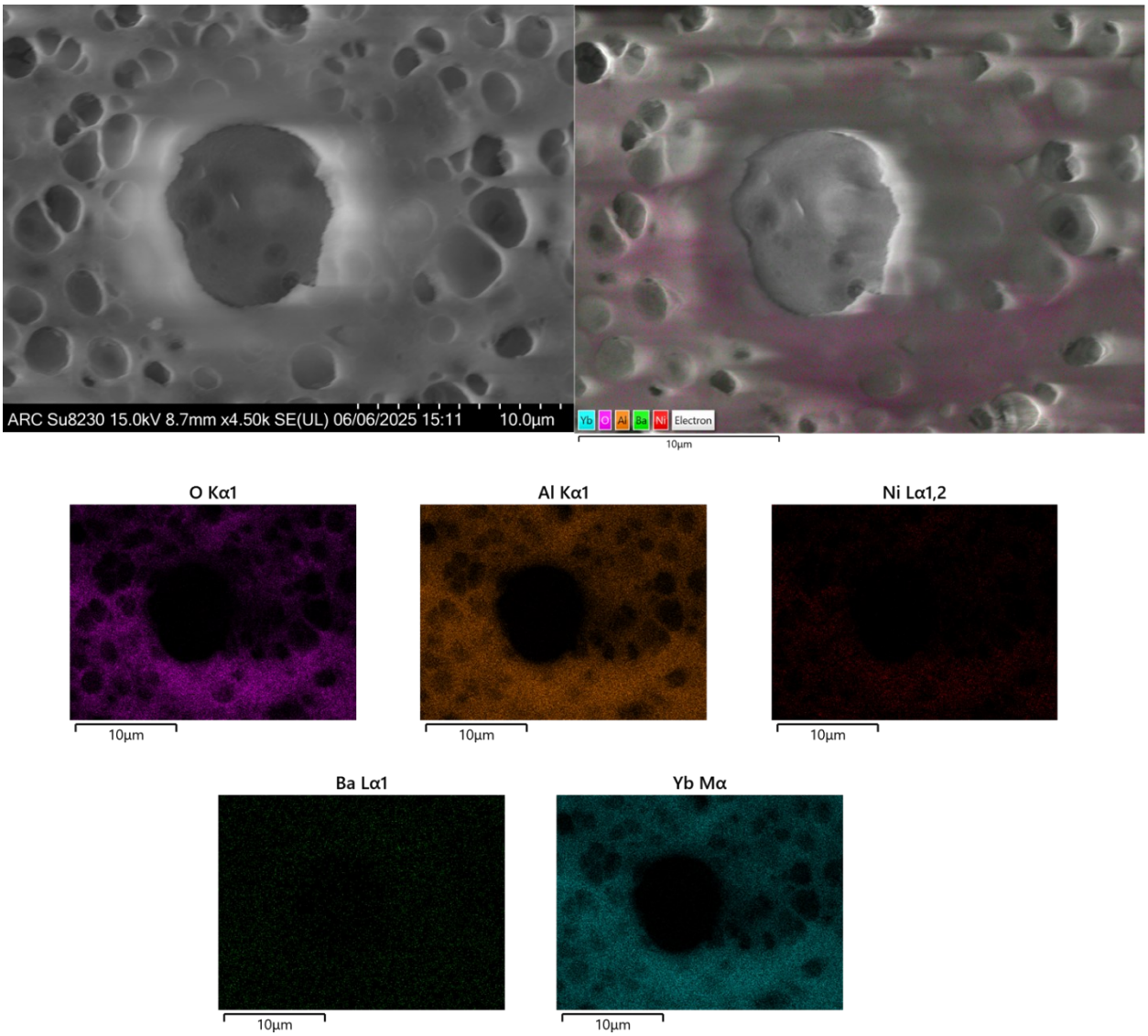

Figure S 111. SEM of the NiYbBa catalyst cross section before reaction.

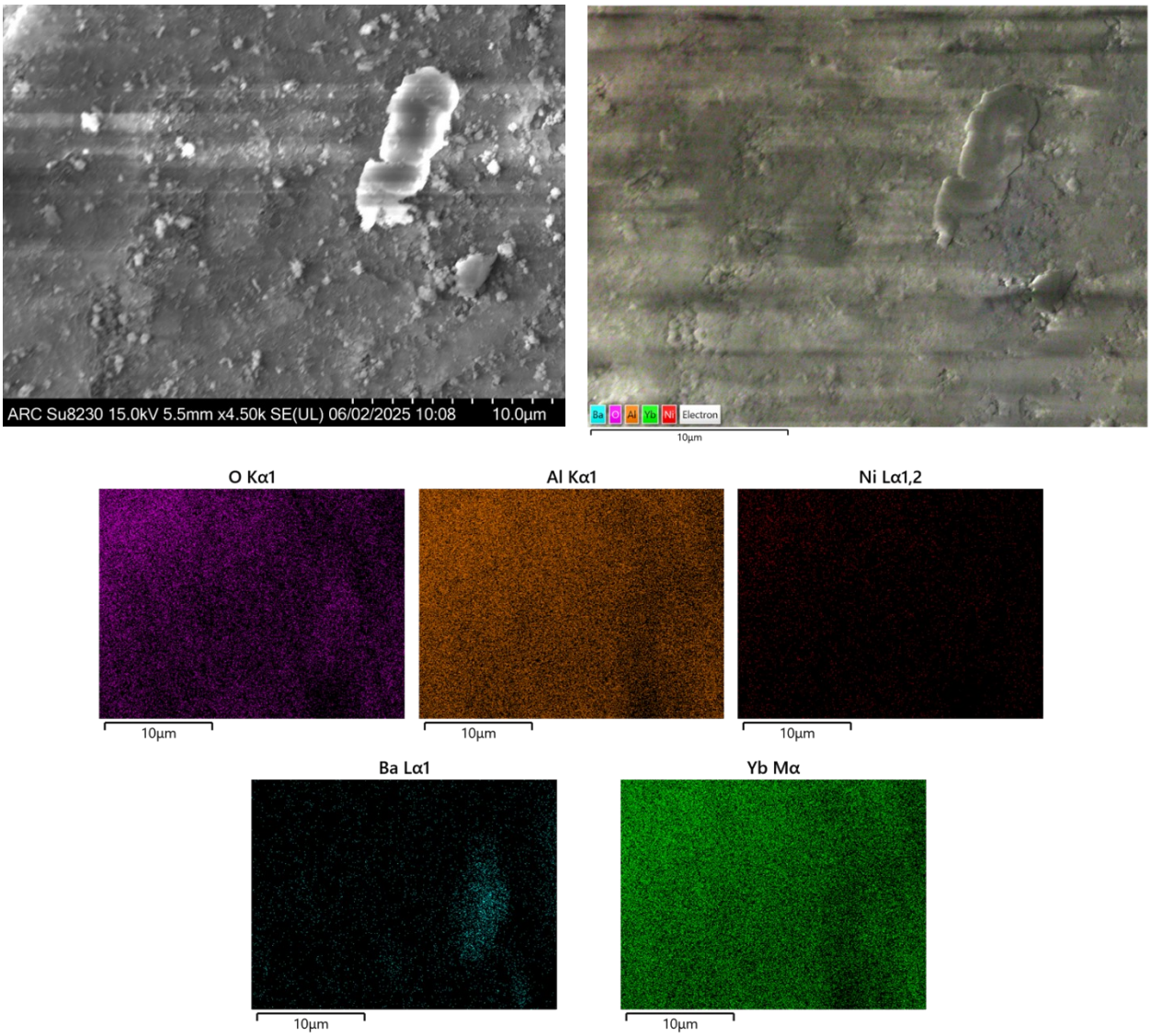

Figure S 112. SEM of the NiYbBa catalyst outer shell after reaction.

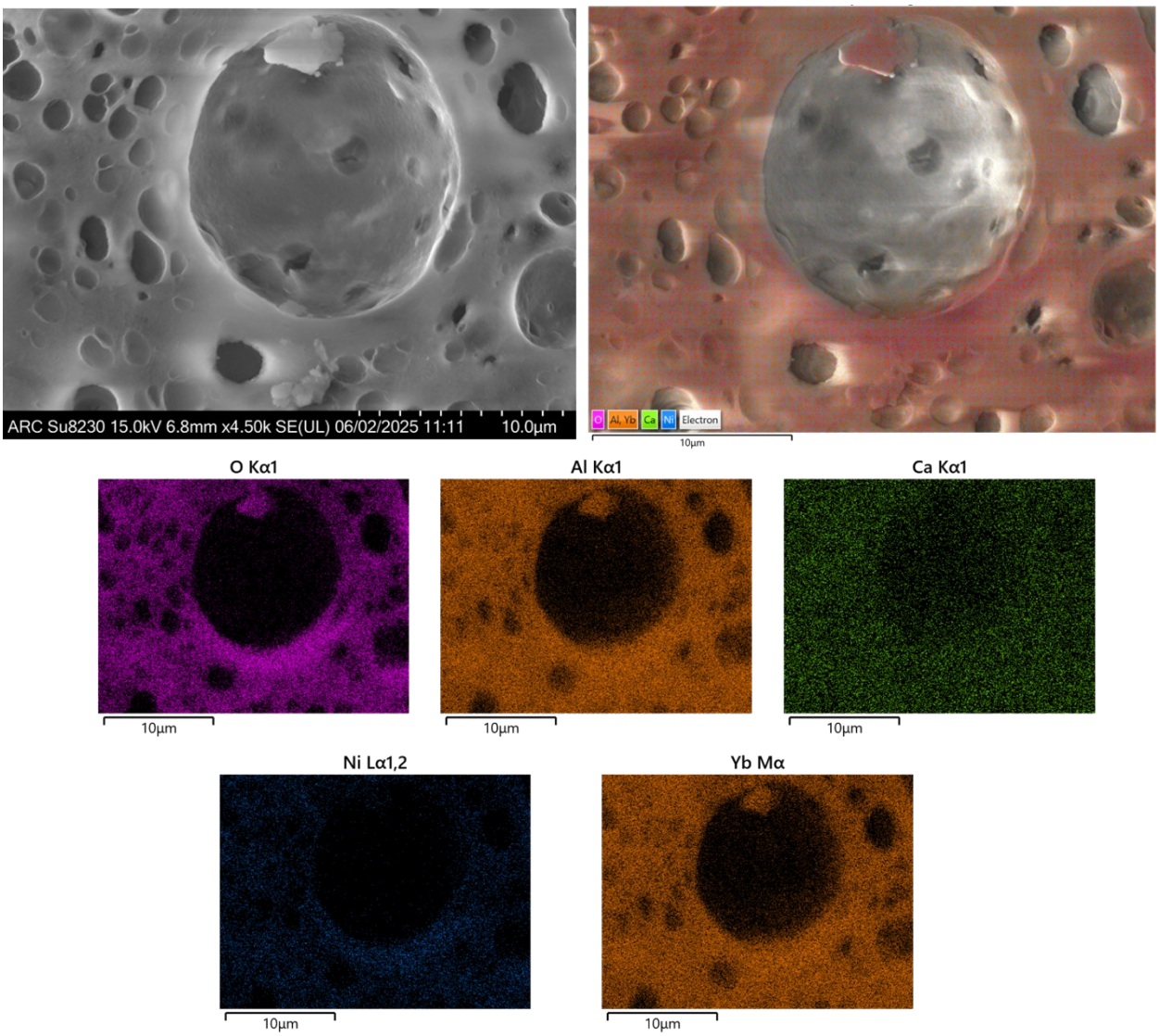

Figure S113. SEM of the NiYbBa catalyst cross section after reaction.

Higher Magnification SEM of crushed samples

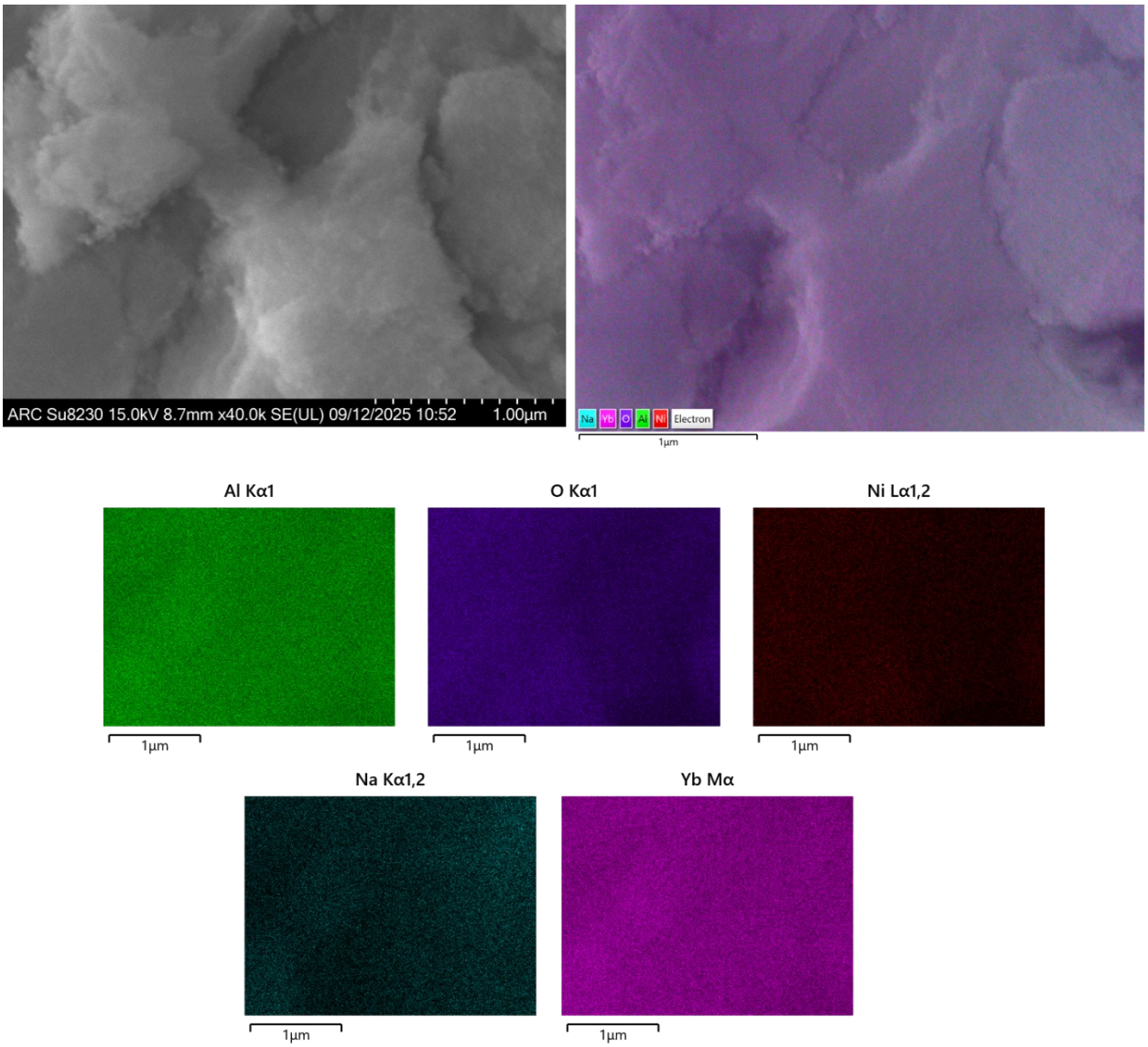

Figure S114. SEM of the crushed NiYbNa catalyst at higher magnification.

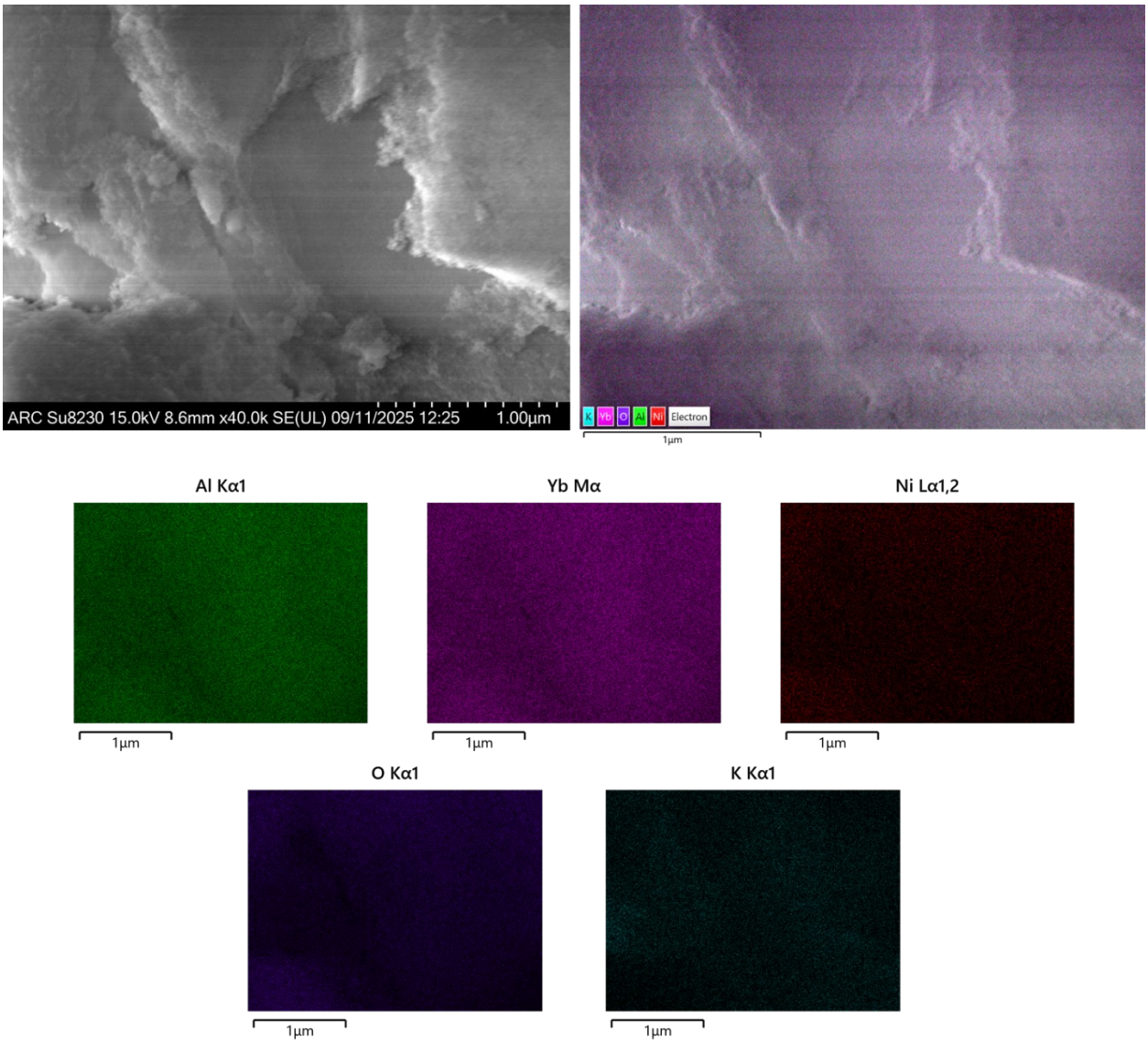

Figure S115. SEM of the crushed NiYbK catalyst at higher magnification.

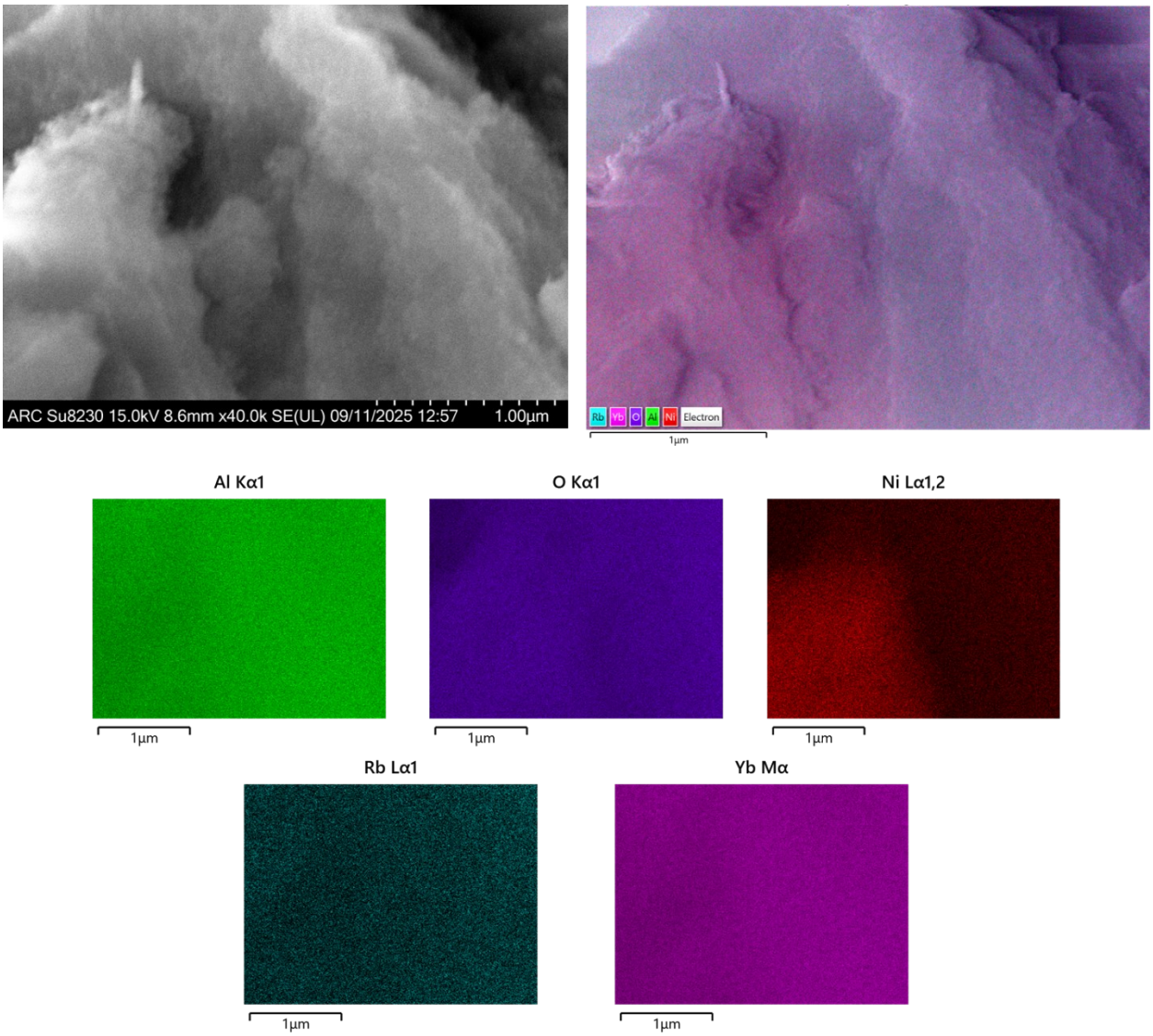

Figure S116. SEM of the crushed NiYbRb catalyst at higher magnification.

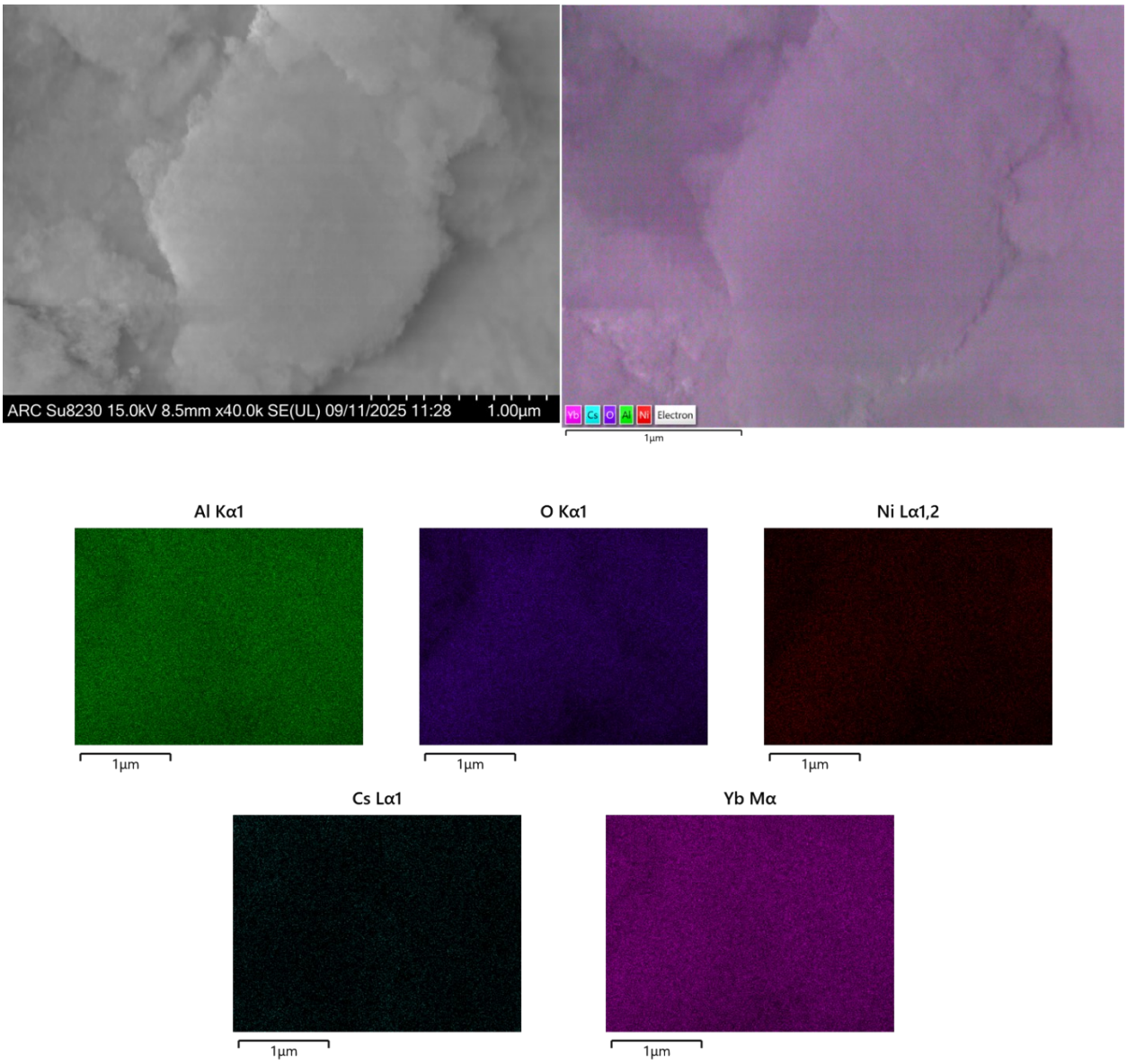

Figure S117. SEM of the crushed NiYbCs catalyst at higher magnification.

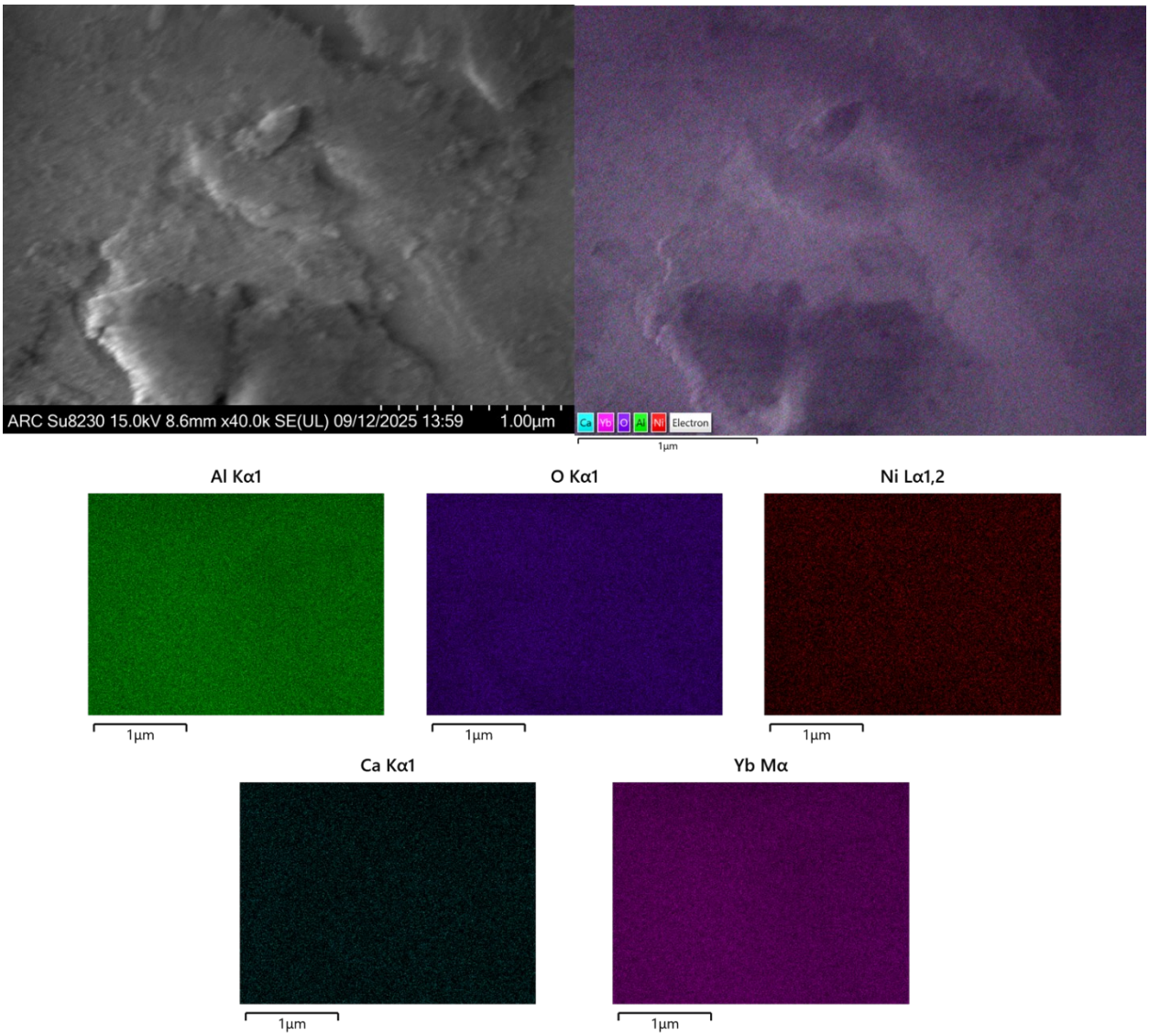

Figure S118. SEM of the crushed NiYbCa catalyst at higher magnification.

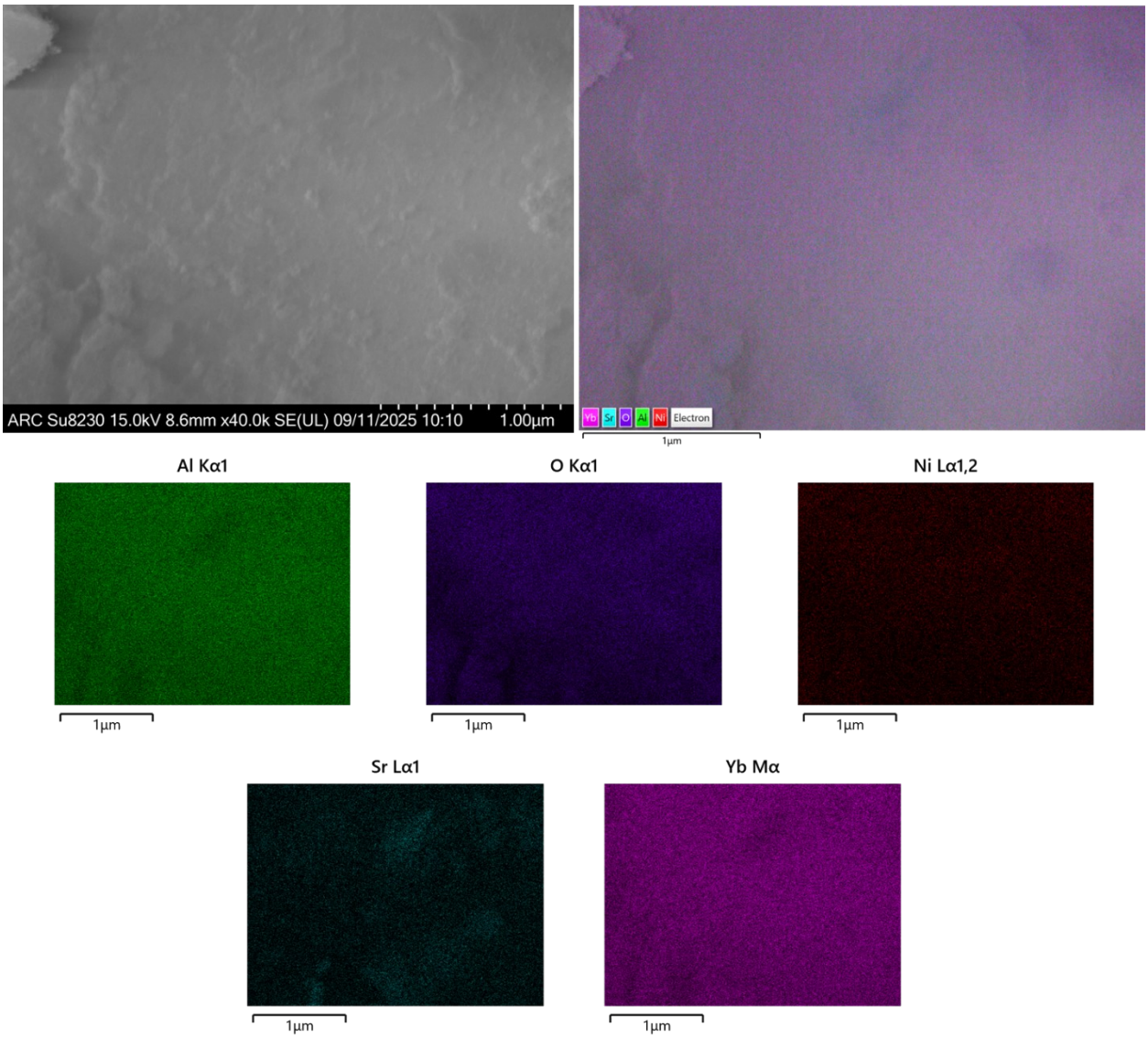

Figure S119. SEM of the crushed NiYbSr catalyst at higher magnification.

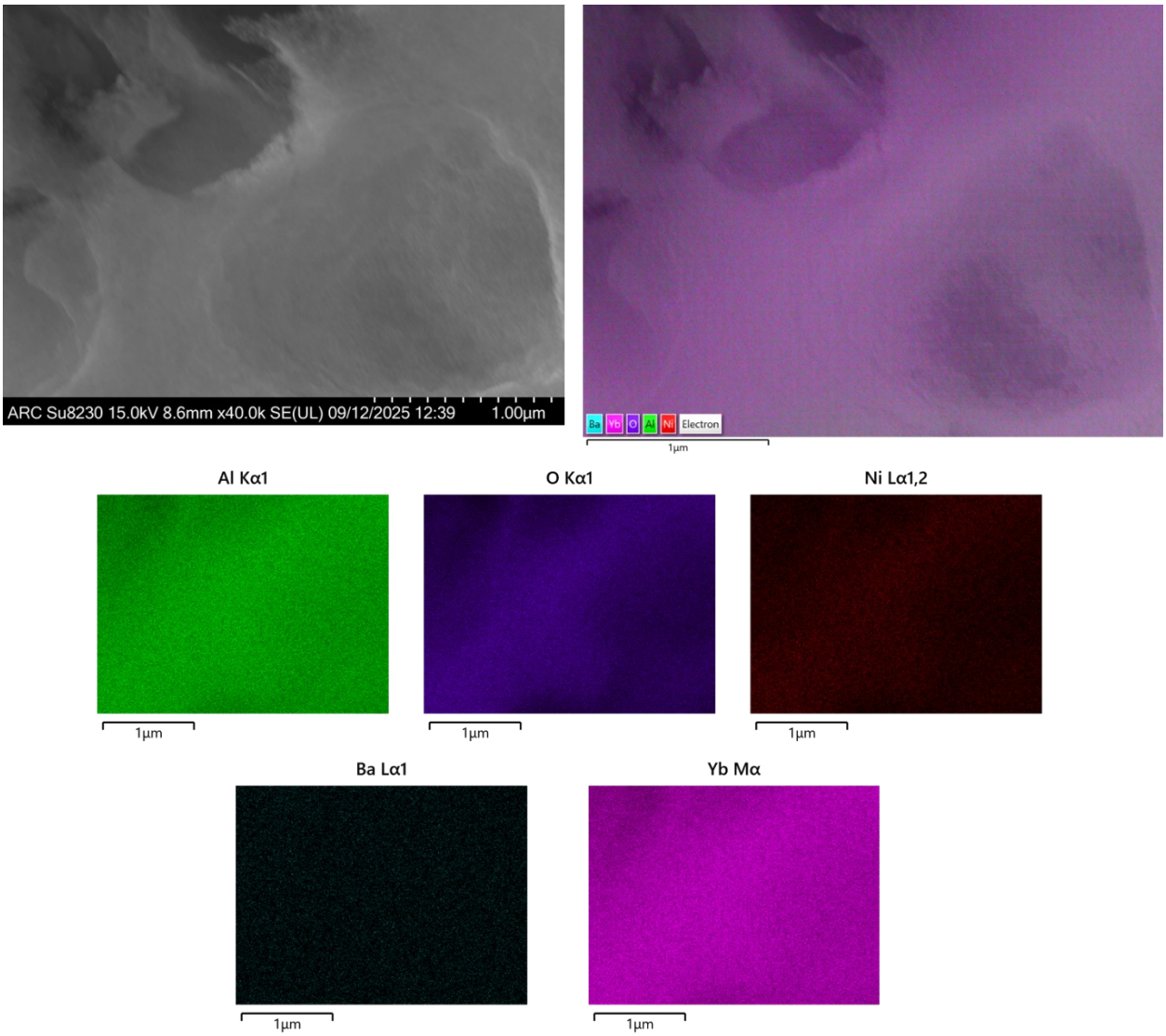

Figure S120. SEM of the crushed NiYbBa catalyst at higher magnification.

Wide Angle X-Ray Diffraction

The wide angle X-Ray Scattering Spectroscopy (WAXS) is shown in Figure S121 to Figure S127 for the NiYbM catalysts. The WAXS spectra were converted to 2Θ with a copper laser source from the original measurements conducted in d-spacing.

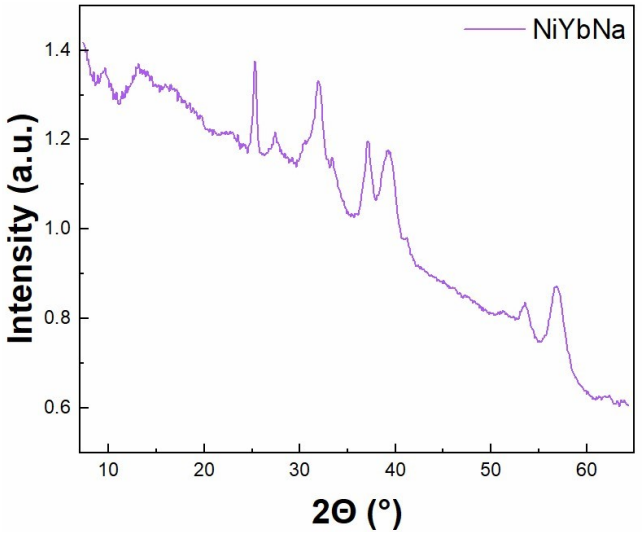

Figure S121. Wide Angle X-Ray Scatttering Spectroscopy for the 12%Ni/4%Yb/12%Na/Al_2O_3 catalyst before reaction.

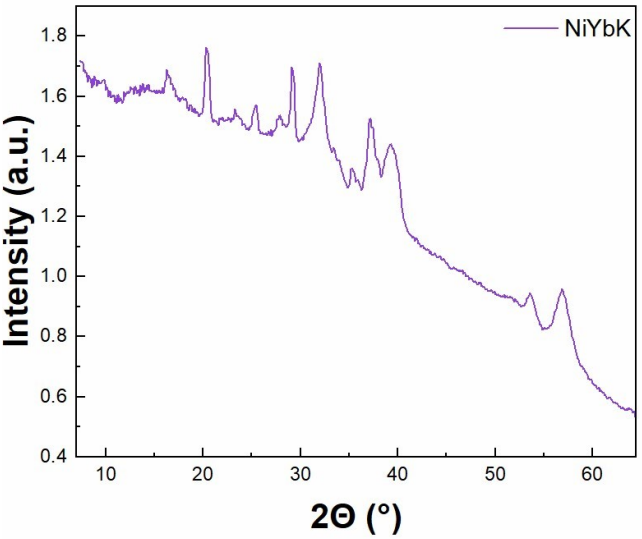

Figure S122. Wide Angle X-Ray Scatttering Spectroscopy for the 12%Ni/4%Yb/12%K/Al_2O_3 catalyst before reaction.

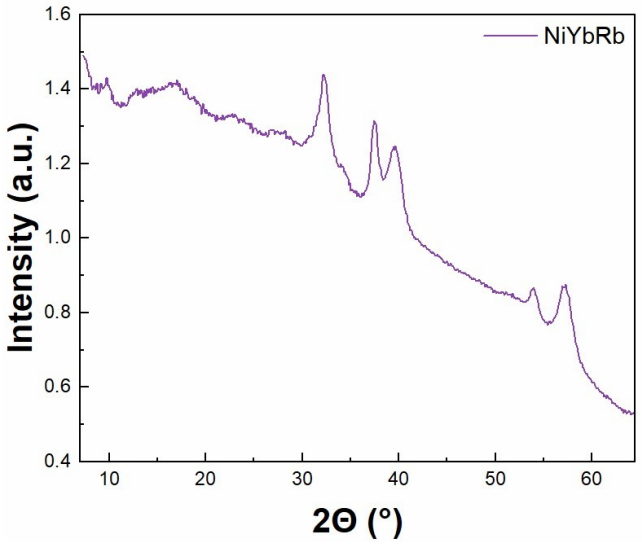

Figure S123. Wide Angle X-Ray Scatttering Spectroscopy for the 12%Ni/4%Yb/12%Rb/Al_2O_3 catalyst before reaction.

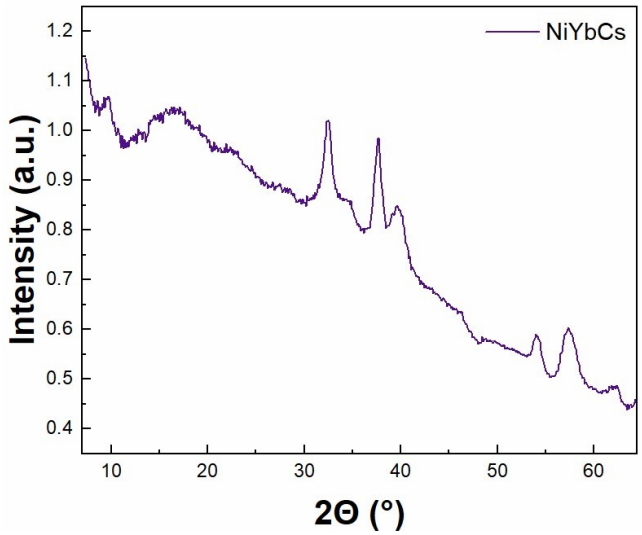

Figure S124. Wide Angle X-Ray Scatttering Spectroscopy for the 12%Ni/4%Yb/12%Cs/Al_2O_3 catalyst before reaction.

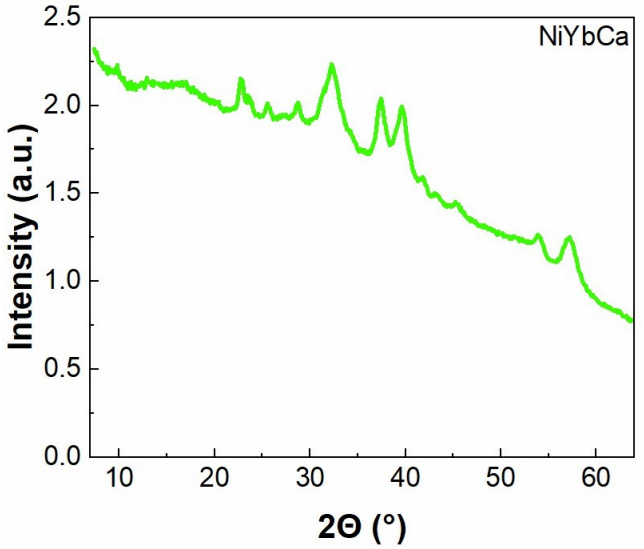

Figure S 125. Wide Angle X-Ray Scatttering Spectroscopy for the 12%Ni/4%Yb/12%Ca/Al_2O_3 catalyst before reaction.

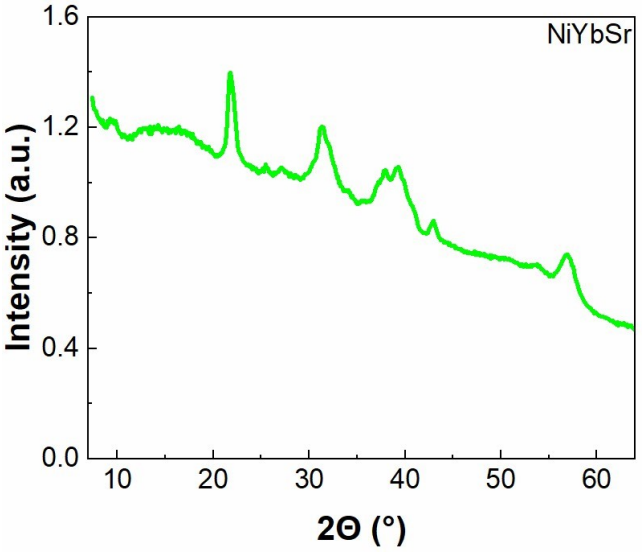

Figure S126. Wide Angle X-Ray Scatttering Spectroscopy for the 12%Ni/4%Yb/12%Sr/Al_2O_3 catalyst before reaction.

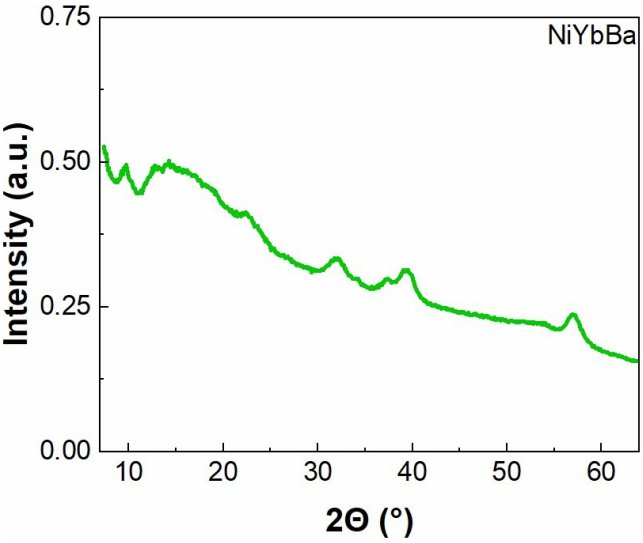

Figure S127. Wide Angle X-Ray Scatttering Spectroscopy for the 12%Ni/4%Yb/12%Ba/Al_2O_3 catalyst before reaction.

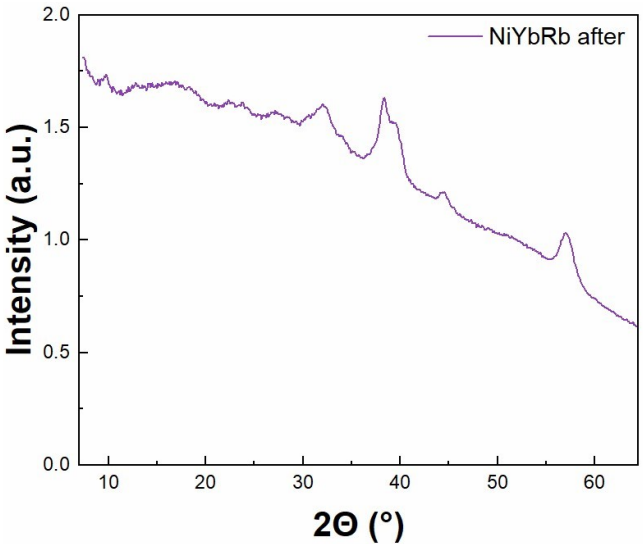

Figure S128. Wide Angle X-Ray Scatttering Spectroscopy for the 12%Ni/4%Yb/12%Rb/Al_2O_3 catalyst after reaction.

Additional Information on the catalyst cost calculations

Tables S17-S20 contain additional information about the catalyst cost analysis performed in Table 1 of the manuscript. Table S17 has additional information of the metal precursors utilized in the calculations and Table S18 contains price information for the metals. Potassium metal was not included due to potassium chloride spot prices being more industrially prevalent.

Table S17. Cost of the base components for the catalysts utilized in the catalyst cost study.

Catalyst	Material	Manufacturer	Quantity	Price (USD)
5% Ru on alumina	5% Ruthenium on alumina	Millipore Sigma	25 g	$248.00
12%Ni4%Yb12% Rb				
	Gamma alumina	Millipore Sigma	2000 g	$132.00
	Nickel nitrate hexahydrate	ThermoFisher	1000 g	$106.00
	Rubidium Nitrate	ThermoFisher	100 g	$433.00
	Ytterbium (III) nitrate hexahydrate	GFS chemicals	500 g	$538.22
3%Ru1%Y12%K				
	Gamma alumina	Millipore Sigma	2000 g	$132.00
	Ruthenium(III) nitrosylnitrate, Ru 31.3% min	ThermoFisher	25 g	$1,689.00
	Yttrium nitrate hexahydrate	Thermofisher	100 g	$102.00
	Potassium nitrate	Millipore Sigma	2500 g	$220.80

Table S18. Spot prices of the metals utilized.

Metal	**Spot Price ($USD/kg)**
Nickel	15.20
Ruthenium	25,0000
Ytterbium	584.95
Yttrium	29.08
Rubidium	36,000

The catalyst cost analysis was done in three ways. The manuscript shows the catalyst cost with the cheapest combination of the precursor and spot prices. Table S19 shows the price with just metal precursors being bought. Table S20 shows the cost of the catalyst with the metal spot prices being utilized.

Table S19. Catalyst Cost analysis with only commercial precursors utilized.

Catalyst	Conversion (%)	CatCost ($USD/$kg_{cat}$)	Conditions
5%Ru/Al_2O_3[a]	53.7	$9920	0.5 g catalyst
12%Ni/4%Yb/12%Rb/γ-Al_2O_3	10.9	$674	0.5 g catalyst
3%Ru/1%Y/12%K/γ-Al_2O_3	65.9	$2275	0.5 g catalyst
12%Ni/4%Yb/12%Rb/γ-Al_2O_3[b]	51.0	$674	PMR 2.5 g catalyst
3%Ru/1%Y/12%K/γ-Al_2O_3[b]	99.9	$2275	PMR 4.5 g catalyst
12%Ni/4%Yb/12%Rb/γ-Al_2O_3[c]	99.9	$674	PMR 2.5 g catalyst

Conditions: TOF and CatCost were done with the following conditions: 450°C, 60 mL/min ammonia flow rate in a fixed bed reactor [a] based on a literature report utilizing a commercial 5%Ru/Al_2O_3 catalyst,[1] [b] in a permeation membrane reactor, [c] at 500°C in a permeation membrane reactor.

Table S20. Catalyst Cost analysis with only metal spot prices utilized.

Catalyst	Conversion (%)	CatCost ($USD/$kg_{cat}$)	Conditions
5%Ru/Al_2O_3[a]	53.7	$9920	0.5 g catalyst
12%Ni/4%Yb/12%Rb/γ-Al_2O_3	10.9	$4525	0.5 g catalyst
3%Ru/1%Y/12%K/γ-Al_2O_3	65.9	$830	0.5 g catalyst
12%Ni/4%Yb/12%Rb/γ-Al_2O_3[b]	51.0	$4525	PMR 2.5 g catalyst
3%Ru/1%Y/12%K/γ-Al_2O_3[b]	99.9	$830	PMR 4.5 g catalyst
12%Ni/4%Yb/12%Rb/γ-Al_2O_3[c]	99.9	$4525	PMR 2.5 g catalyst

Conditions: TOF and CatCost were done with the following conditions: 450°C, 60 mL/min ammonia flow rate in a fixed bed reactor [a] based on a literature report utilizing a commercial 5%Ru/Al_2O_3 catalyst,[1] [b] in a permeation membrane reactor, [c] at 500°C in a permeation membrane reactor.

References

1. J. W. Makepeace, T. J. Wood, H. M. A. Hunter, M. O. Jones and W. I. F. David, *Chemical Science*, 2015, **6**, 3805-3815.